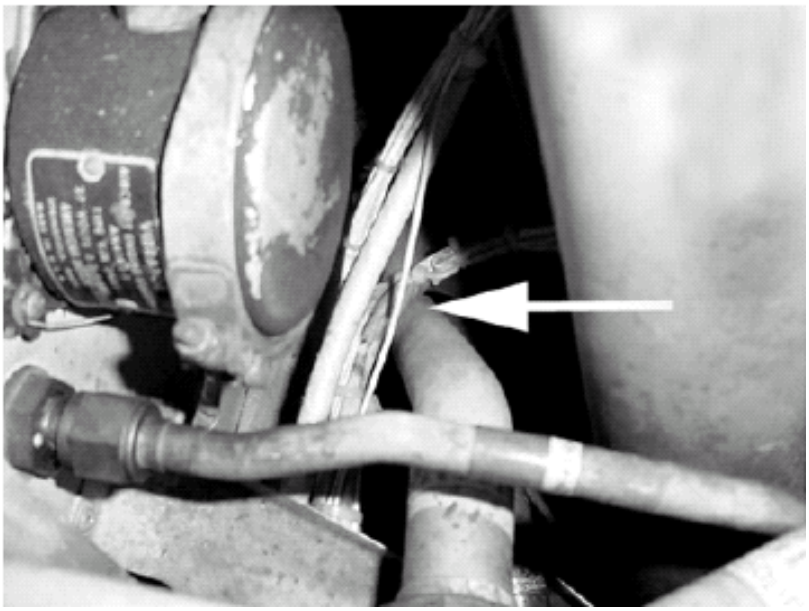

Mathematical model based fault generation and classification for a hydraulic cylinder drive

Customer: VTT

VTT TECHNICAL RESEARCH CENTRE OF FINLAND

VTT INDUSTRIAL SYSTEMS

Public	X	Registered in VTT publications register JURE	X
Confidential until / permanently			
Internal use only			

Title Mathematical model based fault generation and classification in hydraulic cylinder drive	
Customer or financing body and order date/No. VTT	Research report No. BTUO43-051389
Project T4Liikkudia	Project No. G3SU00053
Author Ville Vidqvist	No. of pages/appendices 22 /31
Keywords hydraulics, fluid power, fault, model, classifier, bayes theory, parzen window, neural network	

Summary

Computer based modeling and simulation is becoming a regularly used tool in the design of hydraulic machinery. Once built the computer model can be used to design appropriate means for machine condition monitoring. The model can also be used to simulate failures. The simulation will help in designing measurements for fault detection and in the development of diagnostic tools. Sometimes simulation is the only feasible approach since testing is dangerous or expensive. Two simulation models were used to examine the efficiency of different classifiers in electrical signal-, control valve sticking-, and different leaking faults in a position feedback valve-controlled hydraulic cylinder. 100 modified simulation runs were performed for each fault and different statistical windows were used for feature extraction. Linear, quadratic, Parzen and neural network based classifiers were trained, tested and evaluated using the windowed data.

Date Espoo 7 November, 2005

Helena Kortelainen	Ville Vidqvist	
Research Manager	Research Scientist	Checked

Distribution (customers and VTT):

VTT TECHNICAL RESEARCH CENTRE OF FINLAND
VTT INDUSTRIAL SYSTEMS
Metallimiehenkuja 6, Espoo
P.O. Box 1702, FIN-02044 VTT
FINLAND
Tel. +358 9 4561
Fax +358 9 460 627
name.surname@vtt.fi
www.vtt.fi/tuo
Business ID 0244679-4

Foreword

This report was prepared as part of the project Monitoring and Diagnostics - Lifetime Management of Mobile Machinery (Liikkudia). The project is part of VTT' activities focused on safety and reliability. The author would like to thank VTT for providing funding for this research.

Espoo

Author

Table of contents

1 Introduction

In the design phase of machines operating with hydraulics, virtual testing is coming more common [1]. The system is modeled with a computer and design parameters can be defined without the use of real world prototypes. Especially elasticity related dynamical properties can be accessed. Modeling can also be used to design condition monitoring methods for machinery. Models can be used to simulate faults and measurement information can be accessed cost-efficiently using virtual measurement instead of real sensors in real machines. This information can be used to design automatic fault diagnostic algorithms or fault classifiers [2]. Sometimes this might be the only way to design fault classifiers, since faults have a low probability of occurrence. It may take several years for critical faults to emerge. A common problem in process industry (e.g. energy production, paper production and steel production) is that machinery has been updated or modified which makes the measured history data at least partially outdated.

Pattern recognition and hydraulic servo controls are widely researched fields. Mathematical methods used in both are basically the same. The control theory tries to diminish step response vibration while pattern recognition tries to find optimal method for extracting overlapping signal information. Not much has been done upon pattern recognition in fault diagnostics of hydraulics. Automotive industry is being active in analyzing electro-hydraulic steering and breaking components [3, 4]. Parameter variation has been examined in the case of simple hydraulic motor drive model [5]. Models related to leakage have recently raised interest. The use of Kalman filtering in hydraulic leakage detection [6] and QFT (Quantitative Feedback Theory) fault tolerant control under leakage [7] has also been studied. Supply pressure and sensor faults as well as fluid contamination have been studied in relation to QFT-fault tolerant control [8] and by using Volterra nonlinear models [9].

The measurement of pressure over filter is the usual method for hydraulic system monitoring. Fluid condition is usually monitored by laboratory analysis, since development of on-line oil quality measuring sensors is relatively slow and difficult [10, 11]. Major improvements have been made in the fields of moisture sensors and dielectric constant measuring sensors. Marine-, off-shore- and paper-industries have an increasing interest towards low cost humidity (or water content) in oil measurement devices.

The viewpoint of this report is that the direct on-line measurements available are not enough to monitor hydraulic fluid powered machinery. More information is needed for early fault detection and reliable fault diagnostics. The viewpoint includes also fewer sensors with increased intelligence. Intelligence is based on modeling.

2 Goals

The goal of the work was to study the possibility to use mathematical simulation in the design of fault classifier in hydraulic servo proportional system. The present report concentrates on fault simulation, as well as classification of the simulated faults. The root causes of the faults have not been analyzed fundamentally.

3 Description of the target

The analyses were carried with two feedback servo-proportional controlled cylinder drive simulation models using semi-empirical parameters. The first model was constructed earlier [12]. The second model was developed from the first model by adding a pressure relief valve and more advanced friction model. The models were created using Matlab R11 Simulink building blocks.

3.1 Simulation model 1

The model applies the principle of centralized pressures. The hydraulic circuit is divided into volumes in which the pressure is assumed to be uniform. Valves and pipelines are assumed to be flow limiters. The flows passing limiters can be calculated, since the pressures are known from volumes and effective bulk modulus values. The main parameters of simulation model are shown in Figure 1.

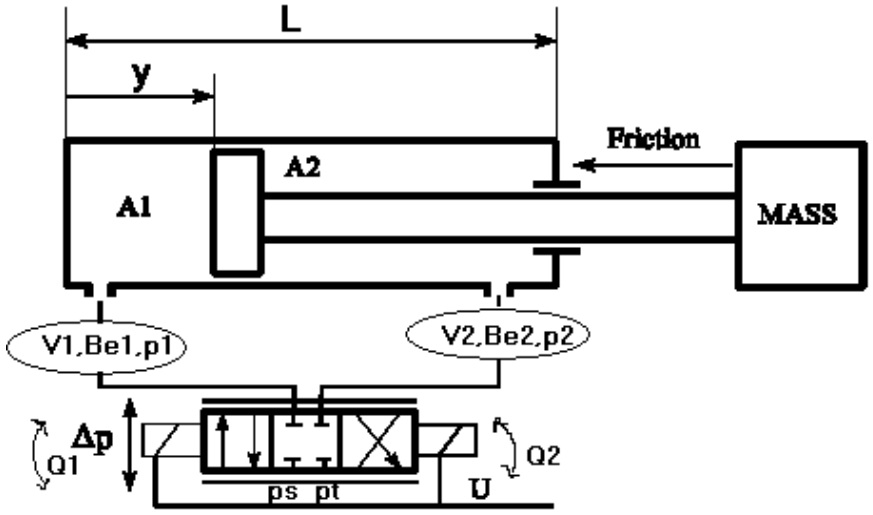

Figure 1. The main parameters of simulation model [12].

Shown parameters of Figure 1 are:

p_s = supply-side pressure [Pa]
p_t = tank pressure [Pa]
p_1 = cylinder-side pressure [Pa]
p_2 = piston-side pressure [Pa]
Q_1 = cylinder-side flow [m^3/s]
Q_2 = piston-side flow [m^3/s]
B_{e1} = effective bulk modulus of cylinder side [Pa]
B_{e2} = effective bulk modulus of piston side [Pa]
V_1 = volume of cylinder side [m^3]
V_2 = volume of piston side [m^3]
A_1 = cylinder-side area of piston [m^2]
A_2 = piston-side area of piston [m^2]
y = position [m]
L = length of cylinder [m]
U = voltage input [V]
Δp = pressure difference [Pa]

Feedback sensor, controller, valve dead zone, valve hysteresis, A/D conversion (digital control), and control delay factors are also included in the model. The characteristics of mechanical components were modeled simply with one rigid component. The model has been described in detail previously [12].

3.2 Simulation model 2

Model generation and parameter function rules are basically the same as in Model 1 with some additions and changes to the model. The main parameters of simulation model 2 are shown in Figure 2:

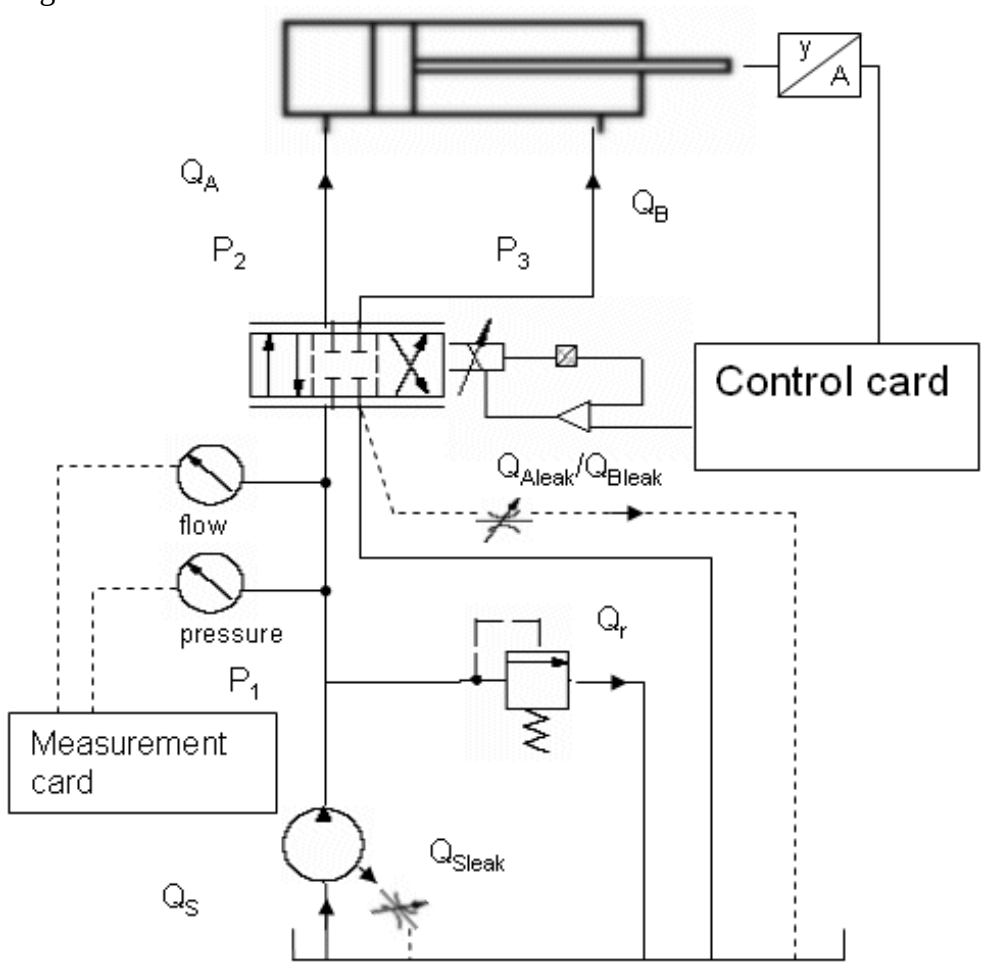

Figure 2. The main parameters of simulation model 2.

The parameters in Figure 2 are as follows:

y = piston position [m]
p_1 = pressure before control valve [Pa]
p_2 = cylinder-side pressure [Pa]
p_3 = piston-side pressure [Pa]
Q_S = flow from pump [m^3/s]
Q_{Sleak} = leak flow from pump [m^3/s]
Q_r = flow from relief valve to tank [m^3/s]
Q_{Aleak}, Q_{Bleak} = leak flow from valve to tank [m^3/s]
Q_A = cylinder-side flow [m^3/s]
Q_B = piston-side flow [m^3/s]

The friction in the cylinder was modeled in simulation Model 1 by adding extra load to the system. This does not represent well the real situation as there is no differentiation between static and slip friction. Simulation model 2 uses friction model that was generated originally for sliding pair contact [13,14]:

$$\begin{cases} F_\mu = \sigma_0 z + \sigma_1 \dot{z} + b\dot{y} \\ \sigma_0 = F_{St} / z_{\max} \\ \sigma_1 = \sqrt{m\sigma_0} \end{cases} \quad (1)$$

where,
F_μ = friction force [N]
σ_0 = spring coefficient of piston seal [N/m]
z = seal deflection [m]
$\dot{z}$ = speed of deflection change [m/s]
σ_1 = damping coefficient of piston seal [Ns/m]
b = coefficient of viscous friction [Ns/m]
$\dot{y}$ = piston velocity [m/s]

The supply force produced by the cylinder [26]:

$$F_{Su} = A_C p_2 - A_P p_3 - F_\mu \quad (2)$$

where,
F_{su} = supply force [N]
A_C= cylinder-side area of piston [m^2]
A_P= piston-side area of piston [m^2]

The cylinder is placed vertically towards ground, which leads to the following mechanism equation:

$$F_{Su} = mg \quad (3)$$

where,
m = combined mass of piston and load [kg]
g = gravitational coefficient [m/s^2]

A pressure relief valve was added to Model 2. The pressure relief valve was planned originally to Model 1, but the stability of the model was not achieved. The relief valve changes the pressure-equations into following [25]:

$$\begin{cases} \dot{p}_1 = \dfrac{B_{e1}}{V_{10}}(Q_S - Q_r - Q_A - Q_B) \\ \dot{p}_2 = \dfrac{B_{e2}}{V_{20} + A_C y}(Q_A - Q_{Aleak} - A_C \dot{y}) \\ \dot{p}_3 = \dfrac{B_{e3}}{V_{30} + A_P (L - y)}(Q_B - Q_{Bleak} + A_P \dot{y}) \end{cases} \quad (4)$$

where
$\dot{p}_1, \dot{p}_2, \dot{p}_3$ = pressure differentials [Pa/s]
V_{10}, $V_{20,}$ V_{30} = constant volumes related to different pressure [m^3]
B_{e1}, B_{e2}, B_{e3} = effective bulk modulus values related to different pressure [Pa]
L = stroke of piston [m]

The bulk modulus of casing prior to the control valve is assumed to be infinitely high (rigid), which leads to the following effective bulk modulus:

$$B_{e1} = B_o \,, \tag{5}$$

where
B_o = bulk modulus of oil [Pa]

Pipes are used after the control valve. For the calculation of cylinder and piston side effective bulk modulus values, the piston is positioned to L/2. The bulk modulus values are then [16]:

$$\begin{cases} \dfrac{1}{B_{e2}} = \dfrac{1}{B_o} + \dfrac{1}{B_p}\dfrac{V_{20}}{V_{t2}} \\ \dfrac{1}{B_{e3}} = \dfrac{1}{B_o} + \dfrac{1}{B_p}\dfrac{V_{30}}{V_{t3}} \end{cases}, \tag{6}$$

where
B_p = bulk modulus of pipe [Pa]
V_{t2}, V_{t3} = total volume for effective bulk model calculation (y =L/2) [m^3]

The dynamics of control valve is expressed as a second-order system between the spool displacement and the input voltage [25]:

$$\begin{cases} \ddot{x} = U(t)\omega_v^{\,2} - x\omega_v^{\,2} - 2\dot{x}\delta_v\omega \\ \omega_v = \dfrac{1}{\tau_2} \\ \tau_1 = \dfrac{\tau_2}{|G|_{\omega-90°}} \\ \delta_v = \dfrac{\tau_1}{2\tau_2} \end{cases} \tag{7}$$

where
x = spool position [m]
$\dot{x}$ = spool velocity [m/s]
$\ddot{x}$ = spool acceleration [m/s^2]
U(t)= voltage input to servo solenoid valve [V]
ω_v = nominal angular velocity (frequency) in valve dynamics [rad/s]
δ_v = cancellation ratio of valve dynamics
$|G|_{\omega-45°(5\%)}, \tau_1, \tau_2$ = valve coefficients

The cylinder side flow and the leak flow are defined as follows [25]:

$$\begin{cases} Q_A = C_v \cdot U \cdot sign(p_1 - p_2) \cdot \sqrt{|p_1 - p_2|} & U > 0 \\ Q_A = C_v \cdot U \cdot sign(p_2 - p_T) \cdot \sqrt{|p_2 - p_T|} & U \le 0 \\ Q_{Aleak} = \dfrac{v_{alle}}{2} \dfrac{Q_N}{P_{Ns}} (p_2 - p_t) & U > 0 \\ Q_{Aleak} = 0 & U \le 0 \end{cases} \quad (8)$$

where
C_v = valve semi-empiric flow coefficient [$m^3/(sV(Pa)^{0.5})$]
p_T = tank pressure [Pa]
v_{alle}= total leak flow relative to maximal flow [%]
Q_N=nominal flow through valve [m^3/s]
p_{Ns}=nominal input pressure of valve [Pa]
U = control valve voltage [V]

The piston side flow is defined correspondingly as follows [25]:

$$\begin{cases} Q_B = C_v \cdot U \cdot sign(p_T - p_3) \cdot \sqrt{|p_T - p_3|} & U > 0 \\ Q_B = C_v \cdot U \cdot sign(p_3 - p_1) \cdot \sqrt{|p_3 - p_1|} & U \le 0 \\ Q_{Aleak} = 0 & U > 0 \\ Q_{Aleak} = \dfrac{v_{alle}}{2} \dfrac{Q_N}{P_{Ns}} (p_3 - p_t) & U \le 0 \end{cases} \quad (9)$$

The flow from pump is as follows [27]:

$$Q_S = \eta_S \cdot V_{Srev} \cdot n_S \quad (10)$$

where
η_S= overal efficiency of pump
V_{Srev}= pump displacement [m^3/rev]
n_s=pump speed [rev/s]

The flow through relief valve follows normal valve flow equation and is [27]:

$$Q_r = k_r \cdot sign(p_1 - p_T) \cdot \sqrt{|p_1 - p_T|} \quad (11)$$

where
k_r = amplification coefficient of pressure relief valve []

The dynamics of the relief valve is expressed through relief valve amplification coefficient as a first order system as follows [27]:

$$\dot{k}_r = \frac{(p_1 - p_{ref}) - (C_1 + C_2 p_1) \cdot k_r}{C_{dyna}} \quad (12)$$

where
p_{ref} = reference pressure of relief valve [Pa]
C_1,C_2,C_{dyna} = semi-empirical coefficients of relief valve

The A/D-conversion properties were not included in Model 2 (analog control instead of digital control). PI-controller was used in Model 2. Model 1 uses look-up table based controller

3.3 Fault modeling

The same faults were included in Model 2 that were present in Model 1. The Following faults were included:

- Electrical signal failure
- Leak from cylinder side to outside system
- Leak from piston side to outside system
- Cylinder inside leak
- Valve spool sticking (jamming)

The electrical signal was modeled by setting the input voltage to zero for predefined time:

$$U(t) = 0, \quad t_{0Vstart} \le t \le t_{0Vend} \quad (13)$$

where
$t_{0Vstart}$ = start time of electrical signal failure [s]
t_{0Vend} = end time of electrical signal failure [s]

Valve spool sticking was modeled through voltage. The voltage value was kept constant for predefined time:

$$U(t) = U(t_{jamstart}), \quad t_{jamstart} \le t \le t_{jamend} \quad (14)$$

where
$t_{jamstart}$ = start time of spool sticking [s]
t_{jamend} = end time of spool sticking [s]

Cylinder side leak was modeled using a circle as flow orifice outside the system:

$$Q_{Aof} = Q_A - Q_{hole}(p_x = p_2, p_y = p_{air}) \quad (15)$$

where
Q_{Aof} = valve flow under cylinder side leak [m^3/s]
Q_{hole} = leak flow through hole [m^3/s]
p_{air} = atmospheric pressure [Pa]

Piston side leak was modeled correspondingly:

$$Q_{Bof} = Q_B - Q_{hole}(p_x = p_3, p_y = p_{air}) \tag{16}$$

where
Q_{Bof} = valve flow under piston side leak [m^3/s]

A leak inside affects both flows as follows:

$$\begin{cases} Q_{Aif} = Q_A + Q_{hole}(p_x = p_2, p_y = p_3) \\ Q_{Bif} = Q_B - Q_{hole}(p_x = p_2, p_y = p_3) \end{cases} \tag{17}$$

where
Q_{Aif}, Q_{Bif} = valve flow under inside leak [m^3/s]

The flow through the hole during leaking is calculated in the following way (both laminar and turbulent flows included) [15, 16]:

$$\begin{cases} Q_{hole}(p_x, p_y) = sign(p_x - p_y)\dfrac{-K_L\dfrac{128\nu\rho}{\pi} + \sqrt{\left|\left(K_L\dfrac{128\nu\rho}{\pi}\right)^2 + 4\left(K_T\dfrac{8\rho}{\pi^2}(p_x - p_y)\right)\right|}}{2K_T\dfrac{8\rho}{\pi^2}} \\ K_L = \dfrac{l_{hole}}{d_{hole}^4} \\ K_T = \dfrac{\zeta_{hole}}{d_{hole}^4} \end{cases} \tag{18}$$

where
l_{hole} = length of the hole [m]
d_{hole} = diameter of the hole [m]
ξ_{hole} = flow resistance coefficient of the hole

4 Methods

Signals generated with Simulink were analyzed using Matlab and its toolboxes. Pattern recognition toolbox (Prtools 3.16) was used to generate and test various classifiers [17]. Feature extraction was performed using statistical windows reduced simulation data. Four classifiers were chosen to analyze data with different window sizes.

4.1 Generation of simulated signals

Simulink used variable step size for simulation runs. The Duration in Model 1 was 20 s and in Model 2 3.5 s. Model 1 signals were linearized to 38500 points and Model 2 signals to 20000 points. Noise signal was added to the position feedback signal. Model 1 used a random signal generator with random wave generation and sample time of 0 seconds. Model 2 used a

random number generator with 0.15 s sample time. Noise signal was set to about +/- 1 mm. Figure 3 presents 2 examples of the modeled noise signals.

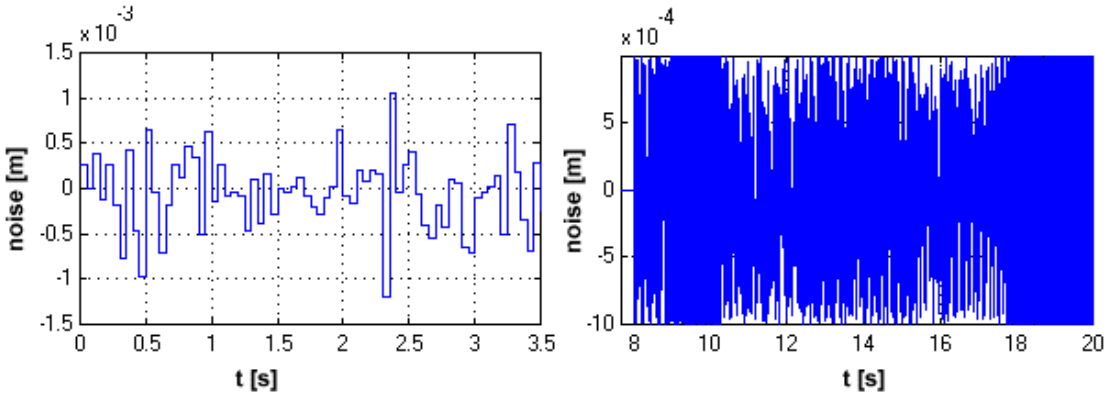

Figure 3. An example of Model 2 noise signal (left) and an example of Model 1 noise signal (right).

Gaussian distribution is used in both cases to generate the random signal. 100 simulation runs were performed for each fault in addition to 'no fault'-case. Faults were modified using random number generator for each simulation run according to Table 1.

Table 1. Fault variation in simulation runs.

	Model 1 (9-20s)	**Model 2 (0-3.5 s)**
leaks	t_{start}: 9+0...1*9 [s] t_{stop}: t_{start}+0...1*2 [s] d_{hole}: 5e-5 [m]	t_{start}: whole simulation [s] t_{stop}: whole simulation [s] d_{hole}: 5e-5+0...1*5e-4 [m]
sticking faults	t_{start}:9+0...1*9 [s] t_{stop}:t_{start}+0...1*1 [s]	t_{start}: round(0...1)*2+0.4+0...1*0.85 [s] t_{stop}: t_{start}+0.1+0...1*0.1 [s]
zero volt faults	t_{start}:9+0...1*9 [s] t_{stop}:t_{start}+0...1*1 [s]	t_{start}: round(0...1*3)+0.3+0..1*0.15 [s] $t_{stop:}$ t_{start}+0.1+0...1*0.1 [s]

Model 1 had an additional fault simulation drive that had both outside leaks on (total was then 7 faults x 100 simulations x 38500 points). This fault situation was not used in simulation with Model 2. Model 1 used two position step signals as input signal. In the case of Model 2, the steps were changed to ramp signals. Signal vectors presented in Table 2 were stored in binary format.

Table 2. Stored signals from simulations (rows were 20000 or 38500 point vectors).

	Model 1 matrix-file column (9-20 s)	**Model 2 matrix-file column (0-3.5 s)**
1	t = time [s]	t = time [s]
2	y_{in} = wanted position/input [m]	y = actual position [m]
3	y = actual position [m]	p_1 = pressure before control valve [m]
4	$\dot{y}$ = piston velocity [m/s]	p_2 = cylinder side pressure [Pa]
5	F_{su} = piston generated force [N]	p_3 = piston side pressure [Pa]
6	Q_1 = cylinder side flow [m^3/s]	Q_A = cylinder side flow [m^3/s]
7	Q_2 = piston side flow [m^3/s]	Q_B = piston side flow [m^3/s]
8	p_1 = cylinder side pressure [Pa]	F_{su} = piston generated force [N]
9	p_2 = piston side pressure [Pa]	U = Control valve voltage [V]
10		Q_{re} = flow from relief valve [m^3/s]

The characteristic Model 1 output signals for all simulated faults are shown in Appendix 1. Leak faults are plotted for the whole simulation. The characteristic output signals of Model 2 for all faults are shown in Appendix 2.

4.2 Feature extraction

Statistical windows were chosen for feature extraction method. The calculation is visualized in Appendix 3. The statistical parameters used for windows are explained in Table 3.

Table 3. Explanation of statistical parameters for windows [18].

Parameter	Calculation	Explanation
iqr	$median(x_{i75\%})$ - $median(x_{i25\%})$	Iqr computes the difference between the 75th and the 25th percentiles of the sample. The iqr is a robust estimate of the spread of the data, since changes in the upper and the lower 25% of the data do not affect it.
kurtosis	$k = \frac{E(x-\mu)^4}{\sigma^4}$	Kurtosis is a measure of how outlier-prone a distribution is. The kurtosis value of the normal distribution is 3. Distributions that are more outlier-prone than the normal distribution have kurtosis greater than 3; distributions that are less outlier-prone have kurtosis less than 3.
skewness	$k = \frac{E(x-\mu)^3}{\sigma^3}$	Skewness is a measure of the asymmetry of the data around the sample mean. If skewness is negative, the data are spread out more to the left of the mean than to the right. If skewness is positive, the data are spread out more to the right. The skewness of the normal distribution (or any perfectly symmetric distribution) is zero.
mean	$\bar{x}_j = \frac{1}{n}\sum_{i=1}^{n} x_{ij}$	Mean is the average value of the samples.
rms	$rms = \sqrt{\frac{\sum_i x_i^2}{n}}$	The root mean square value (rms) of a sample is a scalar that gives some measure of its magnitude.
max	$\max(x_i)$	Returns the largest elements along of an array.
slope	$k = \frac{f(x_i)-b}{x_i}$	Slope defines if the values of a sample are increasing or decreasing

Cylinder side pressure (p_1) was chosen for feature extraction measurement quantity in Model 1. In the case of Model 2, feature vectors (feature vector = total amount of points in linearized simulation vector divided with window size) were calculated for the cylinder side pressure (p_2), the piston side pressure (p_3) and the valve control voltage (U). For Model 1 feature vector sizes of p_1 were defined as 20, 15, 10 and 5 points. In addition to these four vectors 100, 75, 50, 25 were defined for Model 2 voltage measurement quantity. Also 20, 15, 10, 5 size vectors were calculated for p_2 and p_3 of Model 2. The feature extraction algorithm calculated windows with remainders by leaving the last signal points out (eg. in the calculation of 15 size feature vector for Model 2, 19995 first signal points are used as

1333*15=19995 and 1334*15=20010). Some examples of feature vectors are plotted in Appendix 4.

4.3 Classification

Bayesian classifiers were tested in the classification of feature vectors **x** generated with statistical windows using different parameters. The likelihood functions of classes' ω_i (here 5+1 or 6+1) with respect to **x** in the *l*-dimensional feature space (here 5...100) follow the general multivariate normal density [19]

$$p(\mathbf{x}|\omega_i) = \frac{1}{(2\pi)^{l/2}|\Sigma_i|^{1/2}} \exp\left(-\frac{1}{2}(\mathbf{x}-\boldsymbol{\mu}_i)^T \Sigma_i^{-1}(\mathbf{x}-\boldsymbol{\mu}_i)\right), \quad i = 1,\ldots,M \tag{19}$$

where $\boldsymbol{\mu}_i = E[\mathbf{x}]$ is the mean value of the ω_i class and Σ_i the $l \times l$ covariance matrix defined as [20]

$$\Sigma_i = E\left[(\mathbf{x}-\boldsymbol{\mu}_i)(\mathbf{x}-\boldsymbol{\mu}_i)^T\right] \tag{20}$$

$|\Sigma_i|$ denotes the determinant of Σ_i and E[$\bullet$] the mean (or average or expected) value of random variable. Equation 19 is preferable to work with logarithmic functions due to its exponential form. This result [19]

$$g_i(\mathbf{x}) = \ln\left(p(\mathbf{x}|\omega_i)P(\omega_i)\right) = \ln p(\mathbf{x}|\omega_i) + \ln P(\omega_i) \tag{21}$$

or [19]

$$g_i(\mathbf{x}) = -\frac{1}{2}(\mathbf{x}-\boldsymbol{\mu}_i)^T \Sigma_i^{-1}(\mathbf{x}-\boldsymbol{\mu}_i) + \ln P(\omega_i) + c_i \tag{22}$$

where c_i is a constant equal to $-(l/2)\ln 2\pi - (1/2)\ln|\Sigma_i|$. This can be expanded to [19]

$$g_i(\mathbf{x}) = -\frac{1}{2}\mathbf{x}^T\Sigma_i^{-1}\mathbf{x} + \frac{1}{2}\mathbf{x}^T\Sigma_i^{-1}\boldsymbol{\mu}_i - \frac{1}{2}\boldsymbol{\mu}_i{}^T\Sigma_i^{-1}\boldsymbol{\mu}_i + \frac{1}{2}\boldsymbol{\mu}_i{}^T\Sigma_i^{-1}\mathbf{x} + \ln P(\omega_i) + c_i \tag{23}$$

term $\mathbf{x}^T\Sigma_i^{-1}\mathbf{x}$ indicates that the decision curves are quadratic (e.g., ellipsoids, parabolas, hyperbolas, pairs of lines). For l>2 the decision surfaces become hyperquadratic. This classification is referred here as *quadratic classifier (*qdc is the used Prtools function*)*. If the covariance matrix is the same in all classes, that is, $\Sigma_i = \Sigma$, the quadratic term and c_i will be same in all discriminant functions. *g(***x***)* can be redefined to the following form [19]

$$g_i(\mathbf{x}) = \boldsymbol{\mu}_i^T\Sigma^{-1}\mathbf{x} - \frac{1}{2}\boldsymbol{\mu}_i^T\Sigma\boldsymbol{\mu}_i + \ln P(\omega_i) \tag{24}$$

Hence $g_i(\mathbf{x})$ is a linear function of x, the decision surfaces become hyperplanes. This type of classification is referred here as *linear classifier* (ldc in prtools).

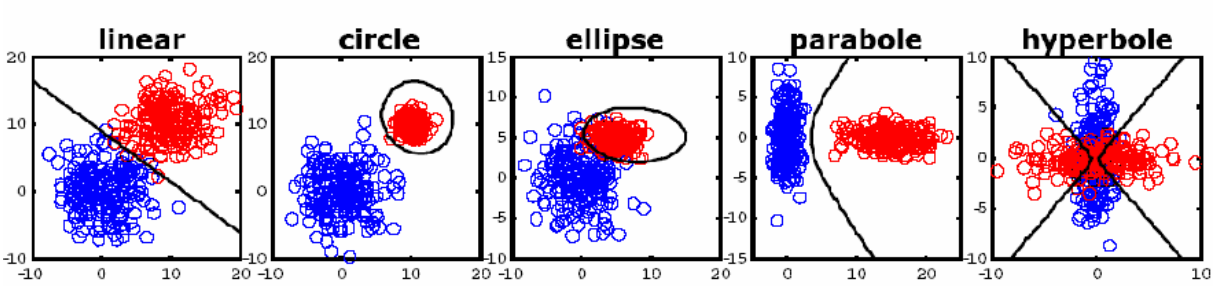

Figure 4. Linear and quadratic classification in the case of two class two feature space. [17]

In addition to Bayesian based classifiers, *Parzen classifier* was tested for all feature vectors (parzenc). The density estimate is modified from eq. 19 [20, 21]

$$p(\mathbf{x}|\omega_k) = \frac{1}{(2\pi)^{l/2} h_k |\Sigma_k|^{1/2}} \exp\left(-\frac{1}{2h_k^2} (\mathbf{x} - \boldsymbol{\mu}_k)^T \Sigma_k^{-1} (\mathbf{x} - \boldsymbol{\mu}_k) \right), \quad k = 1,...,M \tag{24}$$

h_k is the parzen window size of class ω_k. Prtools use Lissack & Fu error estimate for the calculation of optimal window size [22].

The last classifier tested was *neural net classifier* (bpxnc in prtool). The tested classifier is a feedforward network with two hidden layers and with batch mode updating using traditional sigmoid transfer function [21, 24]. Initialization is performed using Nguyen-Widrow method [23, 24].

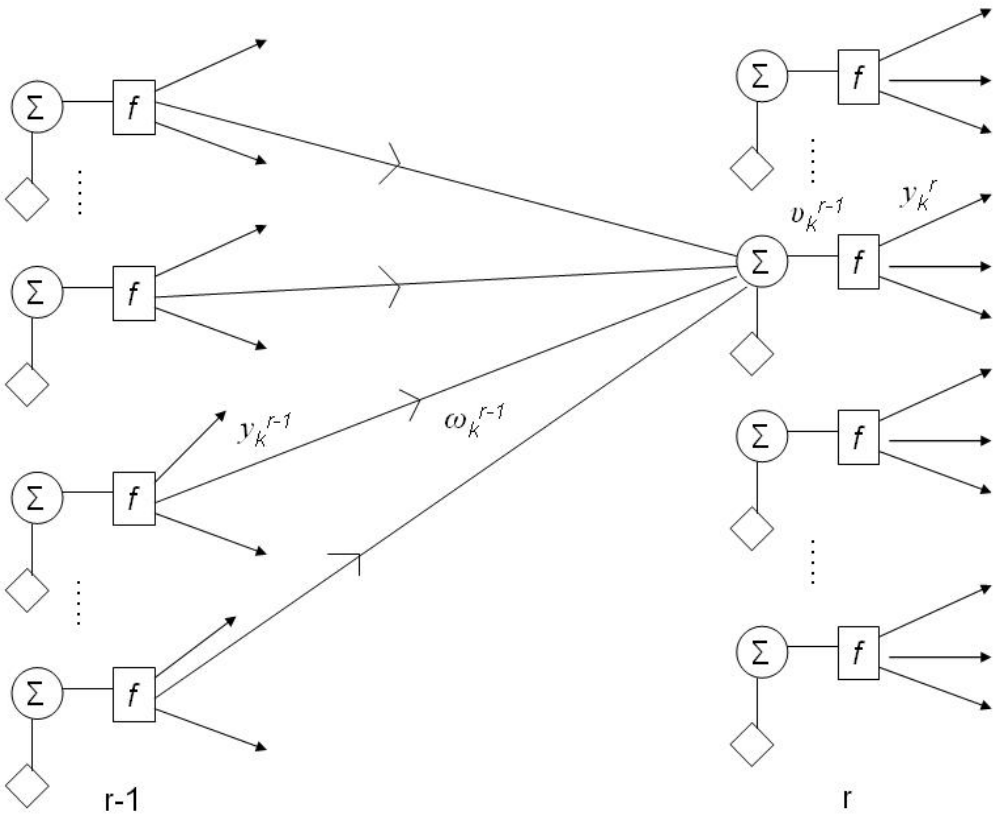

Figure 5. The definition of variables involved in the backpropagation algorithm [19].

The calculations are based on the use of backpropagation algorithm. Forward computations are calculated after initialization for each training vector **x***(i)*, i=1,2...,N (Fig. 5) [19]

$$v_j^r(i) = \sum_{k=1}^{k_{r-1}} \omega_{jk}^r y_k^{r-1}(i) + \omega_{j0}^r \equiv \sum_{k=1}^{k_{r-1}} \omega_{jk}^r y_k^{r-1}(i) \quad r = 1,2,...,L \;\; j = 1,2,...,k_r \tag{25}$$

The cost function J is then updated [19]

$$\begin{cases} J = \sum_{i=1}^{N} \varepsilon(i) \\ \varepsilon(i) \equiv \frac{1}{2} \sum_{m=1}^{k_L} e_m^2(i) \equiv \frac{1}{2} \sum_{m=1}^{k_L} \left(f(v_m^L(i) - y_m(i)) \right)^2 \end{cases} \tag{26}$$

after this backward computations are calculated [19]

$$\delta_j^L(i) = e_j(i) f'(v_m^L(i) - y_m(i)) \quad i = 1,2,...,N \;\; j = 1,2,...,k_L \tag{27}$$

and in the sequel [19]

$$\begin{cases} \delta_j^{r-1}(i) = e_j^{r-1}(i) f'(v_j^{r-1}(i) \quad r = L, L-1,...,2 \;\; j = 1,2,...,k_r \\ e_j^{r-1}(i) = \sum_{k=1}^{k_r} \delta_k^r(i) \omega_{kj}^r \end{cases} \tag{28}$$

finally weights are updated [19]

$$\begin{cases} \mathbf{w}_j^r(new) = \mathbf{w}_j^r(old) + \Delta \mathbf{w}_j^r \;\; r = 1,2,...,L \quad j = 1,2,...,k_r \\ \Delta \mathbf{w}_j^r = -\mu \sum_{i=1}^{N} \delta_j^r(i) \mathbf{y}^{r-1}(i) \end{cases} \tag{29}$$

where $\mathbf{w}_j^r = \left[\omega_{j0}^r, \omega_{j1}^r, ..., \omega_{jk_{r-1}}^r \right]$. The training is stopped by prtool when iteration epochs are twice that of the best classification result. The number of output neurons equals the number of classes (here 5+1 or 6+1) and the input neurons the size of feature vectors (5...100).

5 Restrictions of the study

Major assumptions have been made in the modeling of hydraulic components. The most important assumptions made in this work are as follows [27]:

- The viscosity of oil, the bulk modulus of oil, the discharge coefficients and flow angles of valve orifices are constants
- Pressure is distributed evenly
- Pressure does not saturate or cavitate
- The inlet pressure of each valve is greater than or equal to outlet pressure and the tank pressure is zero

- the compressibility of oil in the damping chambers as well as the Coulomb and the viscous friction force between the valve spool or poppet and the valve housing can be neglected

The simulated parameters have not been verified by measurements. Although the values of the parameters do lack realism, it is expected that they have been estimated “close enough”. As the classifiers function correctly with relatively noisy data, the exact values are not necessarily needed. Similar hydraulic system models without faults have been verified previously [16, 25, 26, 27]. The bulk modulus values of the model are not compensated by piston movement. The modulus values are calculated when the piston is in the middle position of the stroke. This is due to technical problems in the calculation. Also the pressure relief valve model was reduced to a first order model.

6 Results

From 100 simulations (6 or 7 cases in each simulation) 80 were used for training (6*80=480 or 7*80=560) and 20 were used for testing. The selection of training and testing vectors were random. 112 classifiers were trained and tested for model 1 (pressure measurement quantity * 4 different feature vector sizes * 4 different classifiers * 7 different parameters for feature vectors). 448 classifiers were trained and tested for model 2 (voltage measurement quantity * 8 different feature vector sizes * 4 different classifiers * 7 different parameters for feature vectors + 2 pressure quantities * 4 different feature vector sizes * 4 different classifiers * 7 different parameters for feature vectors). The results are presented in Appendix 5. The Tables in the Appendix show the fraction of incorrectly classified cases for each method applied. Thus, a small value indicates good result. The tables present some classifier result averages of fractions of incorrectly classified tests as well, which help to compare different classifiers irrespective of window size.

7 Discussion

A large amount of oil leaking out of the system is usually easily visible as fluid puddles under the machinery. This is especially the case when the hose is leaking. The situation is different in the case of pipe breakage or seal damage. The leak may be small enough to remain unnoticed. The oil consumption increases slightly, but not necessarily enough to arise any concerns. Even if the correct conclusions are made, finding the leak may be a tedious task.

Extra load was used in Model 1 for cylinder friction modeling. De-Wit model was used in Model 2 (eq. 1). A common model invented by Karnopp was used in the work by Tan and Sepehri [9]:

$$\begin{cases} F_c(\dot{x}) = f_{sl} + (f_{st} - f_{sl}) \cdot e^{\frac{|\dot{x}|}{a}} \cdot \operatorname{sgn}(\dot{x}) + d\dot{x} & |\dot{x}| > v_0 \\ F_c(\dot{x}) = f_{st} \cdot \operatorname{sgn}(\dot{x}) & |\dot{x}| \le v_0 \end{cases} \tag{30}$$

There are several reasons for using of the Karnopp model. It is quite simple, easy to understand and it is numerically efficient. Disadvantages include that the actuator is drifting when the outside load and the friction load are in balance. In reality as well as in De-Wit

model, the position is not affected. Complexity and the definition of parameter σ_1 are the disadvantages of De-Witt model.

In Model 1 the controller operation is relatively slow. The difference between the target position and the actual position is quite large (see App. 1., Fig. 6). The main reason for the slow motion is that the model had restrictions on the maximum piston speed. The slow piston speed reduces pressure peaks. Another way is to use a ramp function, as has been done in Model 2.

The pressure signals become negative in the case of inside leak (see green curves of App. 1. and App 2.). This is due to the limitations of the model, which does not compensate the rapid pressure fluctuations fast enough. Also in Model 2 the pressure relief valve flow (see App. 2., Fig. 8) was set so that negative flow is not possible (i.e. flow from tank to system). The sudden pressure increase (see blue curves of App. 2., Fig. 3 and 4 at 1.5 s) in the piston side leak fault is due to the elimination of negative flow.

The zero-volt control signal changes the spool position very rapidly. This can be seen directly from the flow and pressure changes (see blue curves of App. 1. at 11 s. and yellow curves of App. 2. at 3 s). The piston position is also heavily affected and the work cycle is delayed. The effect is basically same in both models. The amplitude of pressure vibration is higher in Model 2 as there is no velocity threshold. The fluid leak to air (atmospheric pressure) produces some visible changes to the position signal. The position is slightly over steered during the cylinder side leak and under steered during the piston side leak in both models (see pink or cyan curve of App. 1., Fig. 1 and pink or blue curve of App. 2., Fig. 2). The reason for excessive over steering in Model 2 as compared to Model 1 is the negative flow aspect of the pressure relief valve mentioned before. The pressure increases as the closed loop system seeks balance between pressure and flow at near piston stroke (1 or 0.4 m) position by adjusting the valve opening (see e.g. cyan and pink curves of App. 1., Fig. 2 at 12-15 s or pink and blue curves of App. 2., Fig. 3 at 1.5-2.5 s). A Larger hole size should produce pressure drop. The vibration amplitudes are smaller during outside leaking near the piston stroke position. Leaking inside the cylinder produces serious pressure vibration (see e.g. green curves of App. 1., Fig 2. at 13-15 s and App 2., Fig. 3 at 1.5-2.5 s). The pressure vibration was so extensive that it induced vibration to the position signal in both models. This kind of a variation in hydraulic system pressure is undesirable since it produces wear. In Model 1, the sudden stop of the valve spool in the valve sticking fault produces first a steady flow and a high flow peak after the spool is released. This is also indicated as vibrating pressure. The piston movement response is decreased with better friction model in Model 2 and this filters the flow peak. Otherwise the effect is the same. There is only a negligible visible effect on pressure if sticking or jamming takes place while the spool is not moving. Also in the case of zero volt-fault, the effect is minimal if the control voltage (flow) is already zero. Fault phenomena modeling were changed in Model 2 to represent amplified effect to output signals. The zero volt fault was run so that the control voltage was either high or low. The sticking failure was run during the spool movement. The leak duration was set for the whole simulation and the leak size was increased (see table 1).

The general requirement to keep the measurement costs low was the reason for measurement quantity selection for windows and classifiers. Flow sensors are expensive and flow information can be accessed more easily by measuring the control voltage. Pressure measurement is moderately expensive, but it is less costly than flow measurement. As sensors are not needed in voltage measurement, it is the most preferable choice for monitoring

purposes. Sensor prices may be irrelevant as the signal processing unit represents the highest cost in the system.

Classification error probability in Model 1 is too high. The acceptable level is lower than 20 % (or 0.2). Simulated signals do not show clear difference between the fault situation and the normal operation. The short duration of the leak is the main reason. Also the mentioned zero volt fault when the control voltage is already zero and the spool sticking fault when the spool is not moving are reasons for the lack of difference in the signal. In other words short leaks are extremely hard to find in the system using these techniques. The probability of short leak to take place is quite low. If the pipe or seal breaks, it is seldom a temporary fault. Although it is possible that seal leak is effective only in some high or low pressure range.

Model 2 was used to simulate faults in places where substantial effect can be seen. The error probability in almost all cases decreases to acceptable level. Even zero error can be seen using voltage, 2000 point window (10 point feature vector) and the maximum value of feature vector (Appendix 5 page 2). Small windows (or large feature vector) were not tested for pressure signals. The feature matrices were singular, which stopped teaching of the classifier algorithm. This is a common problem for classifiers [27]. The comparison of voltage (Appendix 5 p. 2) and pressure signals (Appendix 5 p. 3-4) does not show much difference in classification. Best window sizes seem to be 2000 points (10 point feature vector) or 1333 points (15 point feature vector) wide. The averages on the right side of Tables (Appendix 5) tell that the best results can be achieved using parameters like the root mean square (RMS) or the maximum value of the feature vector (max). These parameters are the most used also for elements of rotating machines in vibration condition monitoring (e.g. rolling bearings, gears) [28]. The Parzen classifier produced the smallest error in classifying voltage and cylinder side pressure data. The quadratic classifier was the best in classifying the data of piston side pressure signal. The results depend more on the feature extraction method than on the classifier type. In this work the linear and neural net classifiers performed worse than the quadratic or Parzen classifiers. The linear classifier does not seem to be adequate for the present nonlinear problem. The neural network had two hidden layers. The number of training vectors was 80. The network can have 75 or 100 input neurons (the size of feature vector). The number of training vectors should be ten times more with these sizes of networks. The idea was to test the classifier with a small number of training vectors. Also the neural networks have the tendency to find local optimum [6].

The feature vectors are plotted in Appendix 4. The first series (p. 1-8) visualizes the effect of window size reduction to the signal. The RMS-feature vectors are plotted for no fault- and sticking fault. The work sequence is not recognizable in the 5 point vector (p. 8), since too much signal information is lost. The effect is visible also in the classifier results (Appendix 5) as the 5 point vector performs worse than the 10 or 15 point vectors. Excessive information like 100 or 75 point vectors also reduce the classifier efficiency.

The second series visualizes (p. 9-15, appendix 4) the effect of the change of the windows parameters. The inter quartile range (iqr) parameter values are different if compared to the RMS or the average (mean). This means that most of the values are not in the 25% range from the median. The high sensitivity of kurtosis (p.10) and skewness (p.14) can be noticed as large variation in the fault cases. The sensitivity of parameter decreases classifier efficiency [29]. In general, the average efficiency of kurtosis and skewness (appendix 5 two columns on right) was worse than that of robust parameters like mean or rms. The differences between classifier efficiencies in Model 1 were smaller than in Model 2, since the quality of training data was

inadequate in Model 1. The differences in Model 1 were few percentages, but over ten percentage in Model 2.

The third set of Figures (p.16-18, Appendix 4) visualizes the effects of different faults to 20 points max feature vector. The clear difference between the figures shows why the max parameter performed best in the classification.

8 Conclusions

It has been demonstrated that statistical windows based data classification can be used for analyzing a hydraulic cylinder drive, which is essentially a nonlinear system. The modeled fault phenomena were not verified experimentally. The tested classification methods worked well with simulated faults like electrical signal failure, control valve sticking, and leaking in feedback valve-controlled hydraulic cylinder. The used hydraulic component models have been verified in various previous research papers [16, 25, 26, 27]. The smallest classification error was reached with Model 2 when using the Parzen classifier. The analyzed parameter was the maximum value of control valve voltage signal, with window size of 2000 points (from 20000 points). In general the root mean square (RMS) and the maximum value of window (max) parameters functioned best with window sizes of 1333 points (15 points size feature vector) and 2000 points (10 points size feature vector). The Parzen and quadratic classifiers performed better than the linear and neural network based classifiers. There was no significant difference in results, if the used measurement quantity was voltage or pressure. Classification of Model 1 data did not produce acceptable results. There was not enough difference in the faulty and normal signals for feature extraction. The problem was solved by developing enhanced failure models for Model 2.

References

[1] Adams Hydraulics datasheet
http://www.mscsoftware.com/assets/1704_ADM6_02_DAT_HYD_EE_R4.pdf

[2] Leonhardt, S. Ayoubi, M., Methods of fault diagnosis, Control Engineering Practice, v 5, n 5, May, 1997, p 683-692

[3] Börner M., Straky, H., Weispfenning, T., Isermann, R. Model based fault detection of vehicle suspension and hydraulic brake systems Mechatronics, Volume 12, Issue 8, October 2002, Pages 999-1010

[4] Hahn, J-O., Hur, J-W., Cho, Y.M., Lee K.I. Robust observer-based monitoring of a hydraulic actuator in a vehicle power transmission control system. Control Engineering Practice, Volume 10, Issue 3, March 2002, Pages 327-335

[5] Yu, D. Fault diagnosis for a hydraulic drive system using a parameter-estimation method Control Engineering Practice, Volume 5, Issue 9, September 1997, Pages 1283-1291

[6] An, L., Sepehri, N. Leakage fault identification in a hydraulic positioning system using extended Kalman filter. American Control Conference, 2004. Proceedings of the 2004 Volume 4, 30 June-2 July 2004 Page(s):3088 - 3093 vol.4

[7] Karpenko, M.,. Sepehri, N. Fault-tolerant control of a servohydraulic positioning system with crossport leakage. Control Systems Technology, IEEE Transactions on Volume 13, Issue 1, Jan. 2005 Page(s):155 - 161

[8] Niksefat, N., Sepehri, N. A QFT fault-tolerant control for electrohydraulic positioning systems. Control Systems Technology, IEEE Transactions on Volume 10, Issue 4, July 2002 Page(s):626 - 632

[9] Hong-Zhou Tan, Sepehri, N. Parametric fault diagnosis for electrohydraulic cylinder drive units. Industrial Electronics, IEEE Transactions on Volume 49, Issue 1, Feb. 2002 Page(s):96 - 106

[10] Parikka, R., Vidqvist V., Vaajoensuu, E. Low-cost analysers based on light transmittance for oil condition monitoring. 2004 AIMETA International Tribology Conference, 14-17 Sept. 2004, Rome. AITC. Rooma (2004), 725 - 734

[11] Parikka, R., Tervo, Jyrki. Condition monitoring of oil in mobile machinery Condition monitoring 2003. Oxford, 2 - 4 July 2003. Coxmoor Publishing. Oxford (2003), 400 - 407

[12] Vidqvist, V. Fault Simulation for Hydraulic Cylinder Drive, 2004. VTT Industrial Systems, Espoo. 13 s. BTUO: 43-041229

[13] Canudas de Wit, C., Olsson, H., Åström, K.J. & Lischinsky. P. 1995. A New Model for Control of Systems with Friction. IEEE Transactions on Automatic Control, Vol. 40, No. 3, pp. 419-425.

[14] Canudas-de-Wit, C. Comments on “A new model for control of systems with friction” Automatic Control, IEEE Transactions on olume 43, Issue 8, Aug. 1998 Page(s):1189 - 1190 Digital Object Identifier 10.1109/9.704999

[15] Backé, W. Grundlagen der Ölhydraulic, Institut für hydraulische und pneumatische Antriebe und Steurungen der RWTH Aachen, 6. Auflache, 1986.

[16] Merrit, H. Hydraulic Control Systems, USA, John Wiley & Sons Inc., 1967, 354 pp., ISBN 0-471-59617-5.

[17] Duin, R.P.W. PRTools_3, A Matlab Toolbox for Pattern Recognition, Delft University of Technology, January 2000

[18] Statistics toolbox for use with Matlab, users guide version 2. Mathsoft inc. 1999. 420 p.

[19] Theodoridis, S., Koutroumbas, K. Pattern recognition Academic Press, San Diego, CA. 1999 . - 625 s. ISBN: 0-12-686140-4

[20] Jain A. K., Ramaswami, M., D. Classifier design with Parzen windows, Pattern Recognition and Artificial Intelligence, E. S. Gelsema and L. N. Kanal (Eds), pp. 211- 228. Elsevier, Amsterdam (1988).

[21] Hamamoto, Y., Fujimoto, Y, Tomita, S. On the estimation of a covariance matrix in designing Parzen classifiers. Pattern Recognition 29(10): 1751-1759 (1996)

[22] Lissack, T., Fu, K.S.: Error estimation in pattern recognition via L^{α} − distance between posterior density functions. IEEE Transitions on Information Theory 22 (1976) 34–45

[23] Demuth, H., Beale, M. Neural Network Toolbox for use with Matlab User's Guide Version 3.0. Mathsoft inc. 1998. 742 pp.

[24] Nguyen, D., and B. Widrow, “Improving the learning speed of 2-layer neural networks by choosing initial values of the adaptive weights,” Proceedings of the International Joint Conference on Neural Networks, vol 3, pp. 21-26, 1990.

[25] Virvalo,T. Nonlinear model of analog valve. In the 5th Scandinavian International Conference on Fluid Power, Linköping, May 1997, pp 199-214.

[26] Virvalo, T. On the Damping of a Hydraulic Cylinder Drive, Sixth Scandinavian International Conference on Fluid Power, SICFP'99, May 26-28, 1999, Tampere, Finland.

[27] Handroos, H. Methods for combining a theoretical and an empirical approach in modelling pressure and flow control valves for CAE-programs for fluid power circuits. Helsinki, Finnish Academy of Technology, 1990. 53 p.

[28] Vidqvist, V. Development of vibration based condition monitoring in rolling bearing of roll (in finnish) MSc Thesis, Lappeenranta University of technology/Department of mechanical engineering, 2001.

[29] Hyötyniemi, H. Multivariate regression - Techniques and tools. Helsinki, Finland: Helsinki University of Technology, Control Engineering Laboratory, 2001. 207 p. (Helsinki University of Technology, Control Engineering Laboratory Report 125).

[30] (Cover Picture) Transport Canada, Bombardier Canadair CL-215 1A10 Chafed Wiring, http://www.tc.gc.ca/CivilAviation/certification/continuing/Alert/2004-09.htm

Model 1 simulations with 5 fault cases and 1 no fault case.

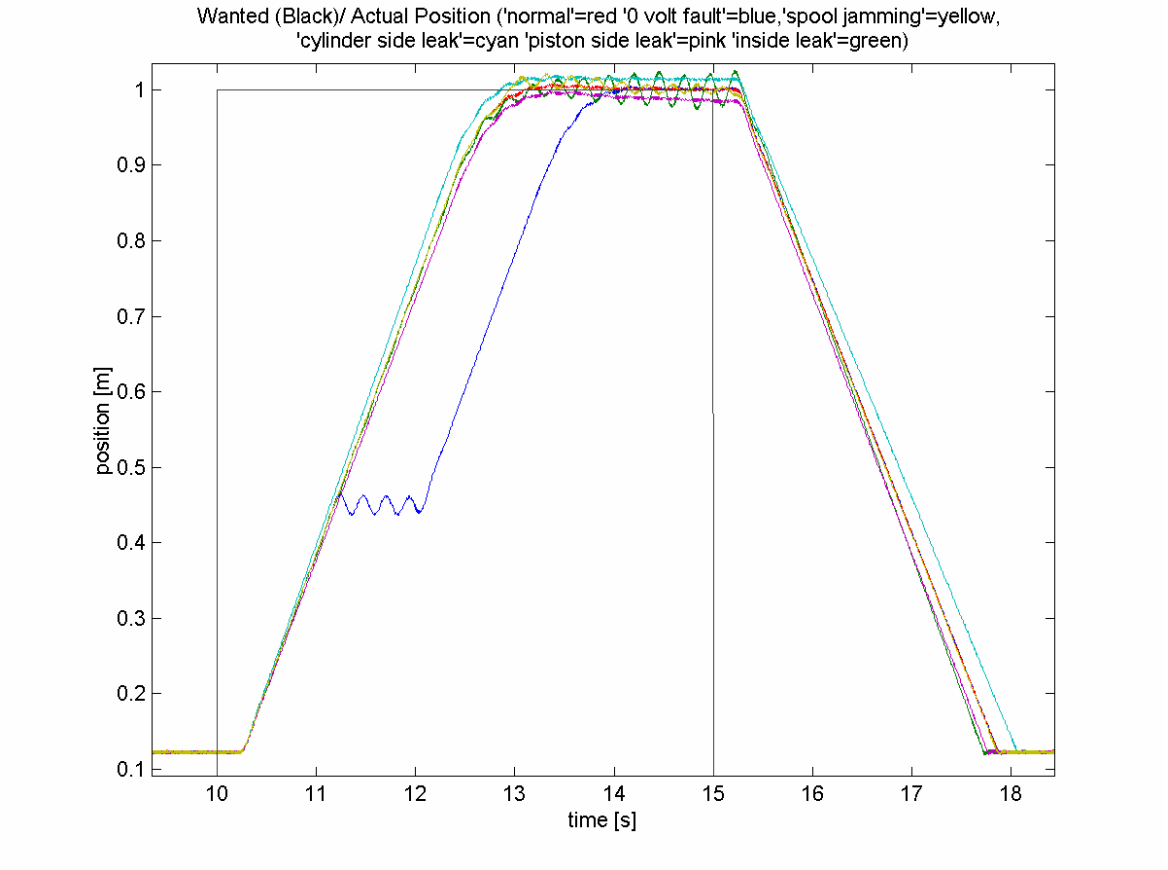

Figure 1. Position output(y) and input with different faults.

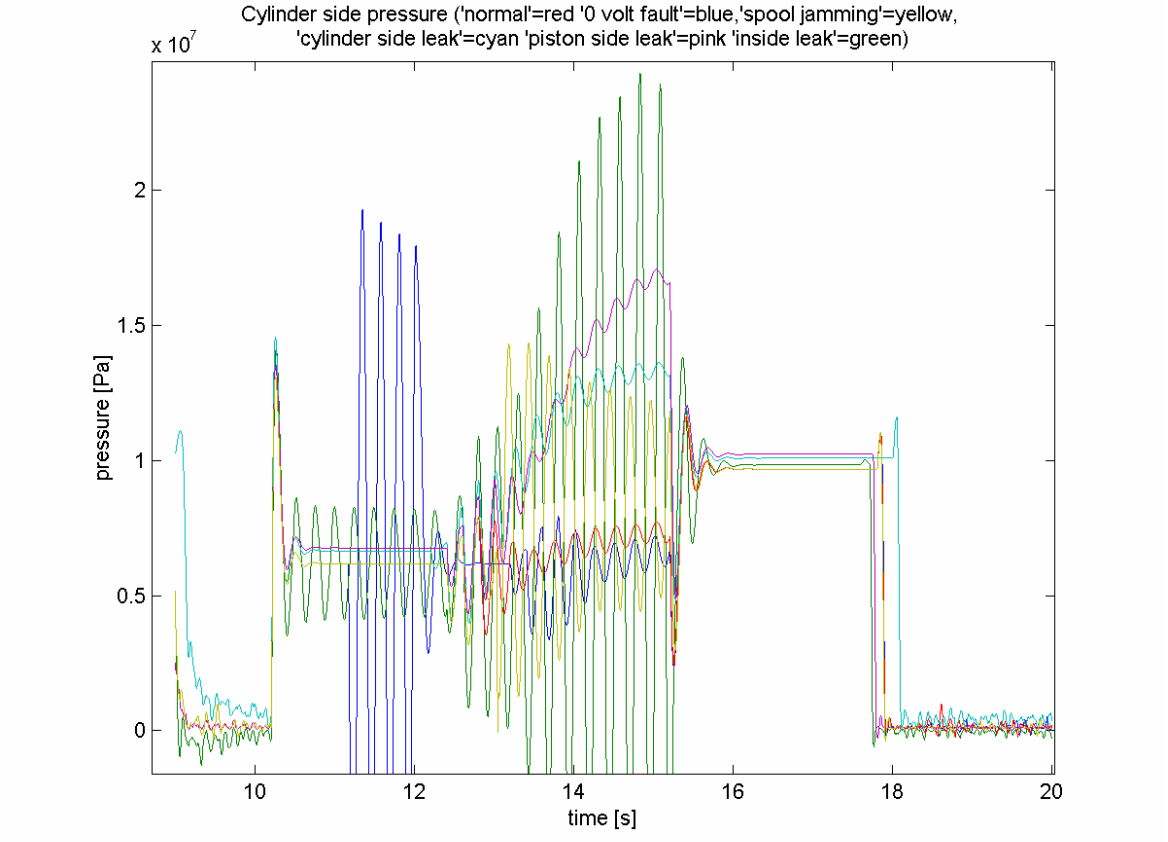

Figure 2. Cylinder side pressure output (p_1) with different faults.

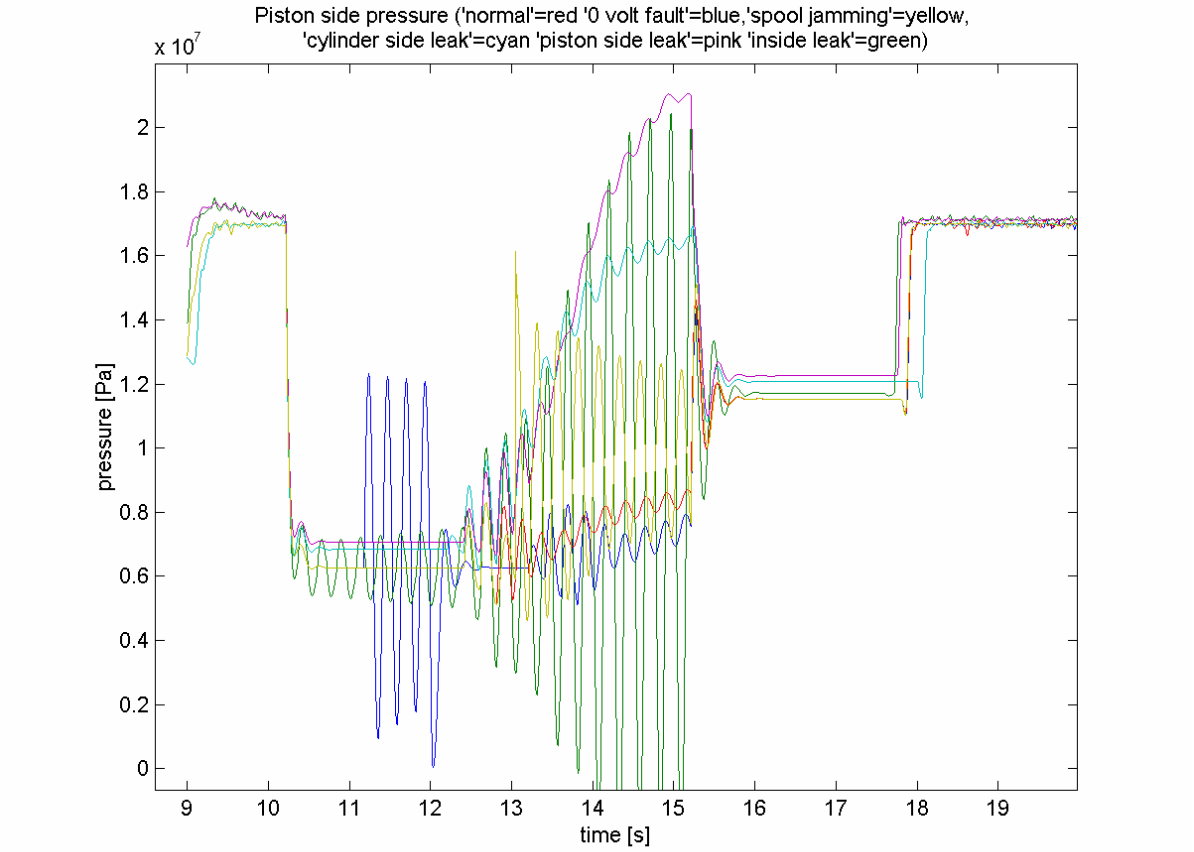

Figure 3. Piston side pressure output (p_2) with different faults.

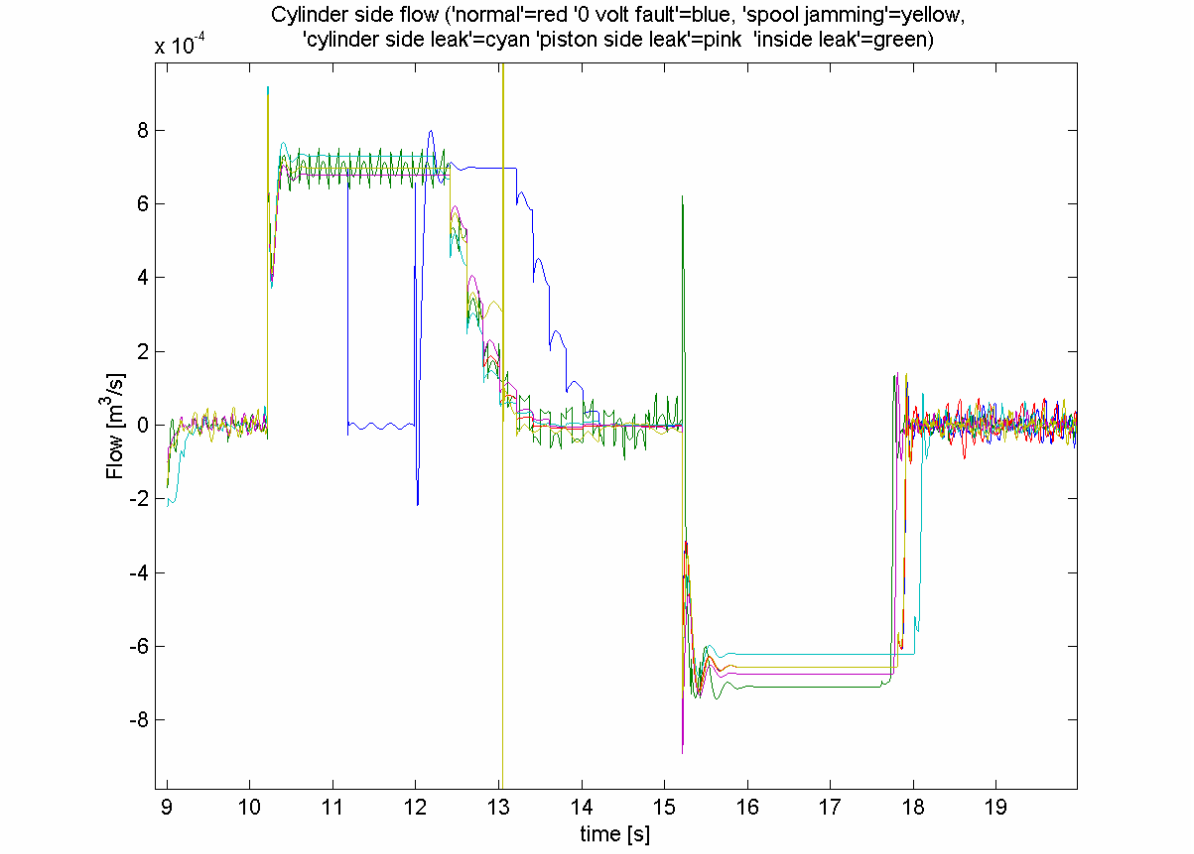

Figure 4. Cylinder side flow output (Q_1) with different faults.

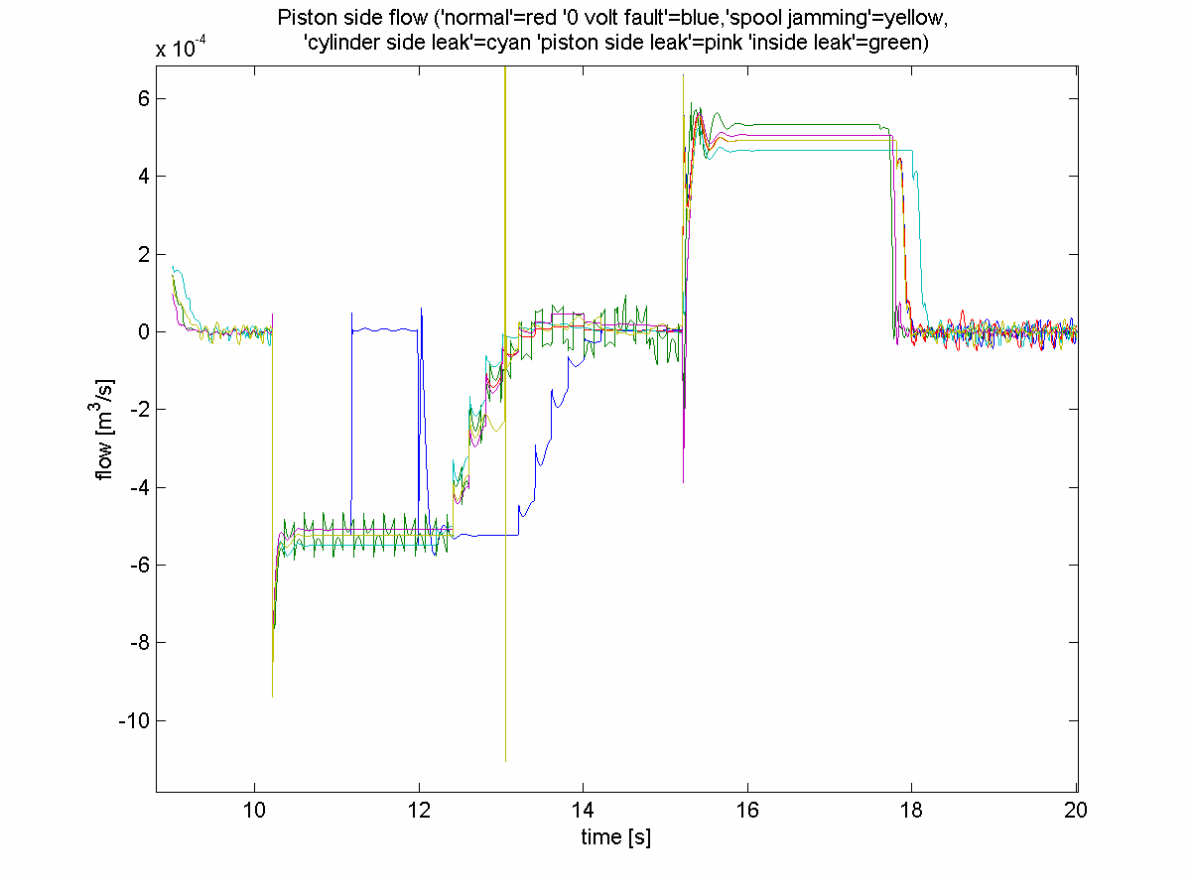

Figure 5. Piston side flow output (Q_1) with different faults.

Model 2 simulations with 5 fault cases and 1 no fault case.

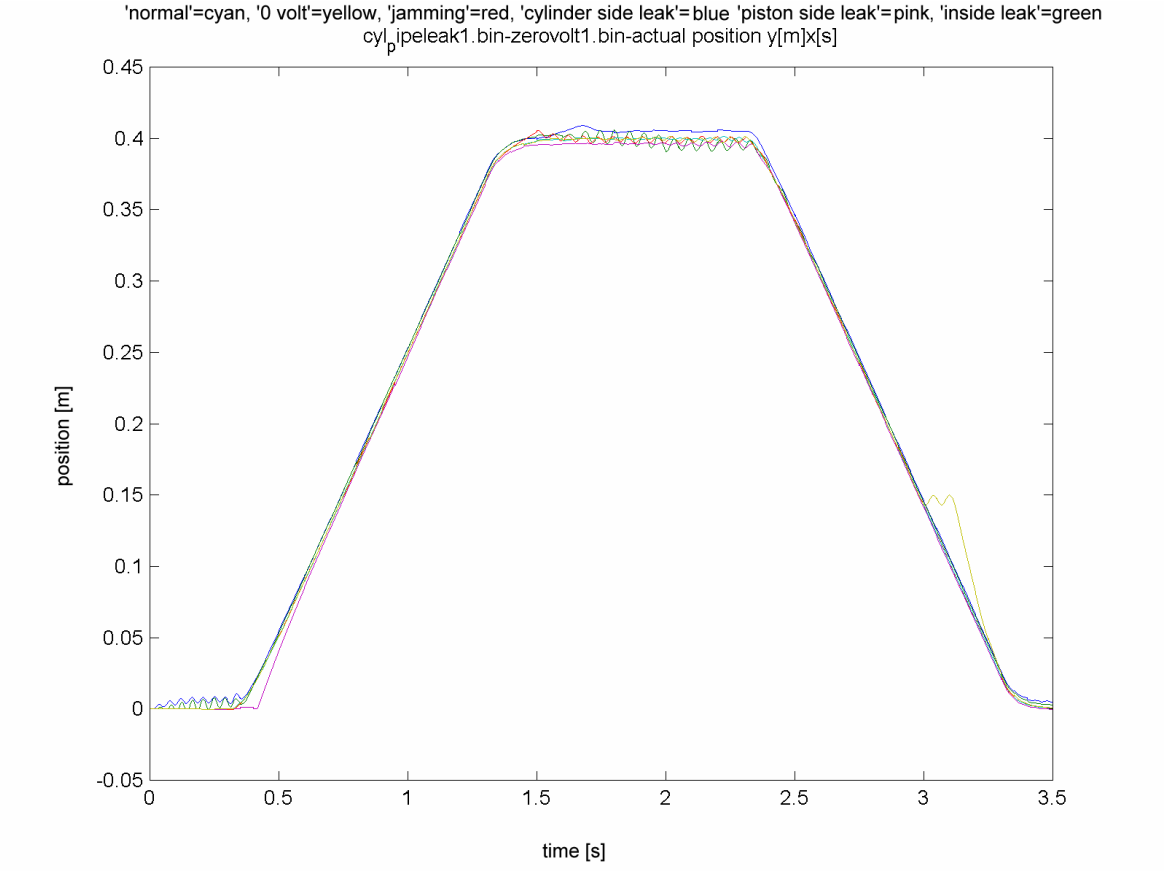

Figure 1. Position output (y) with different faults.

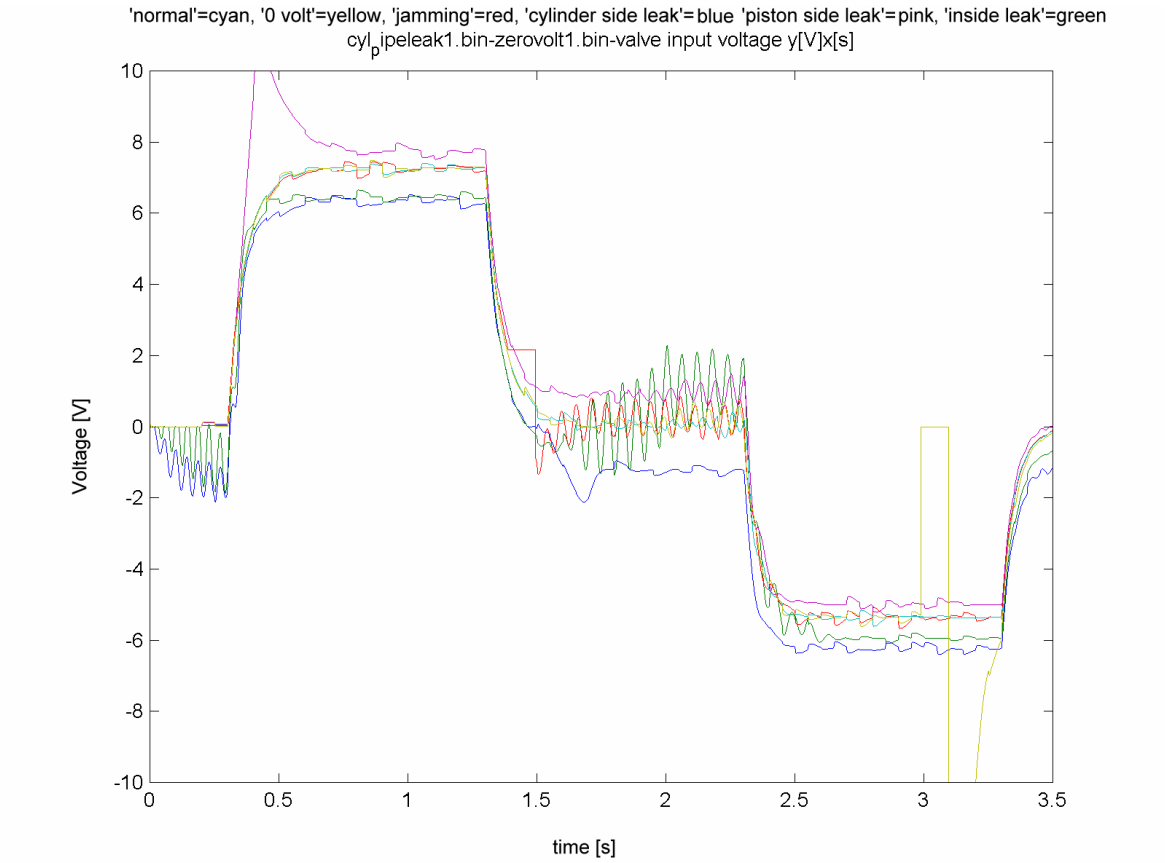

Figure 2. Control valve input voltage (U) with different faults.

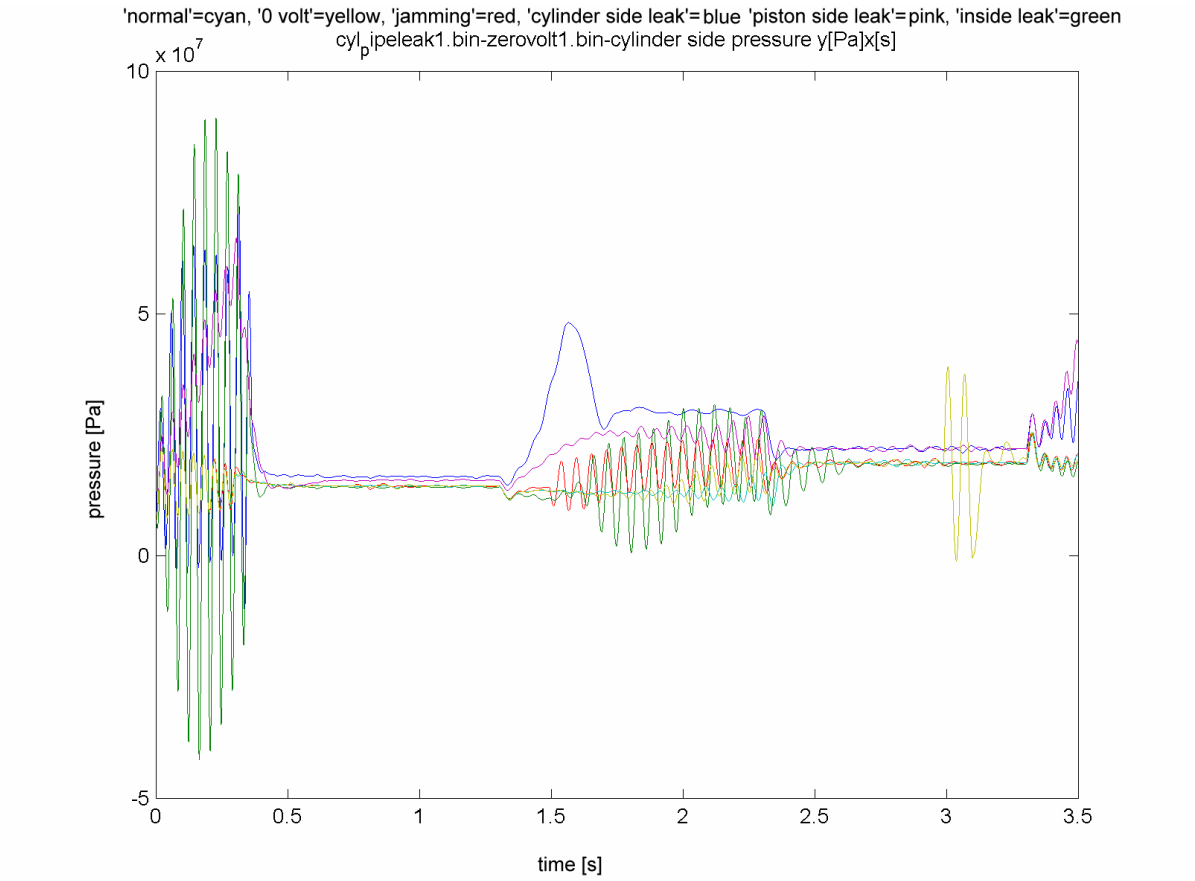

Figure 3. Cylinder side pressure output (p_2) with different faults.

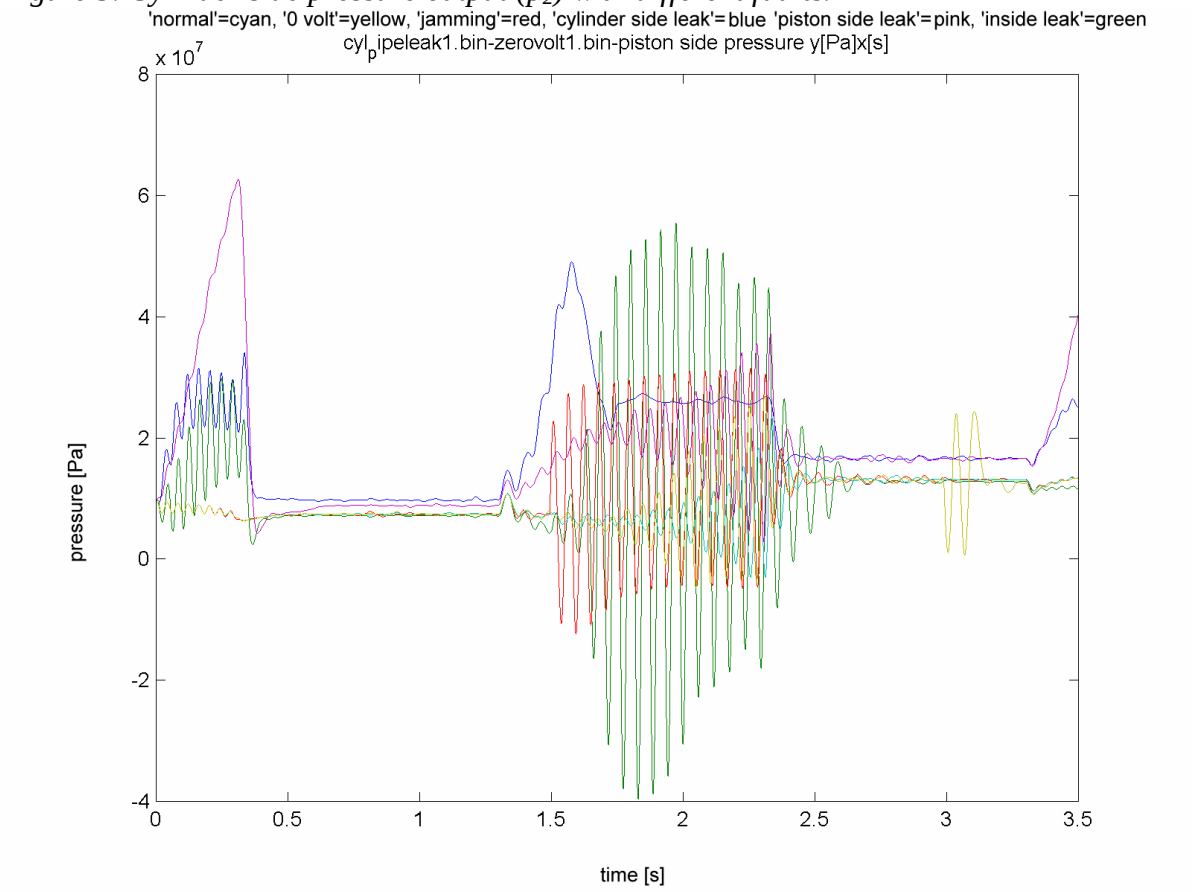

Figure 4. Piston side pressure output (p_3) with different faults.

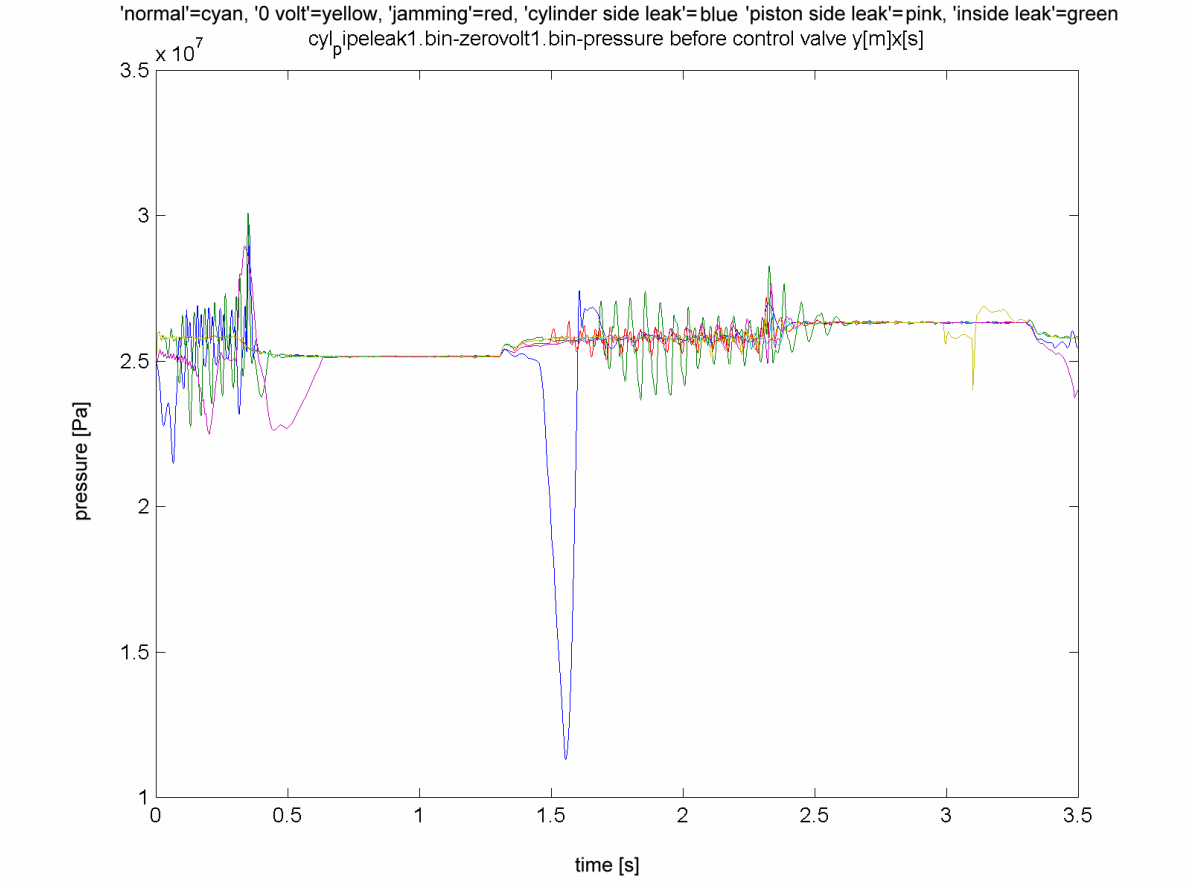

Figure 5. Pressure before control valve output (p_1) with different faults.

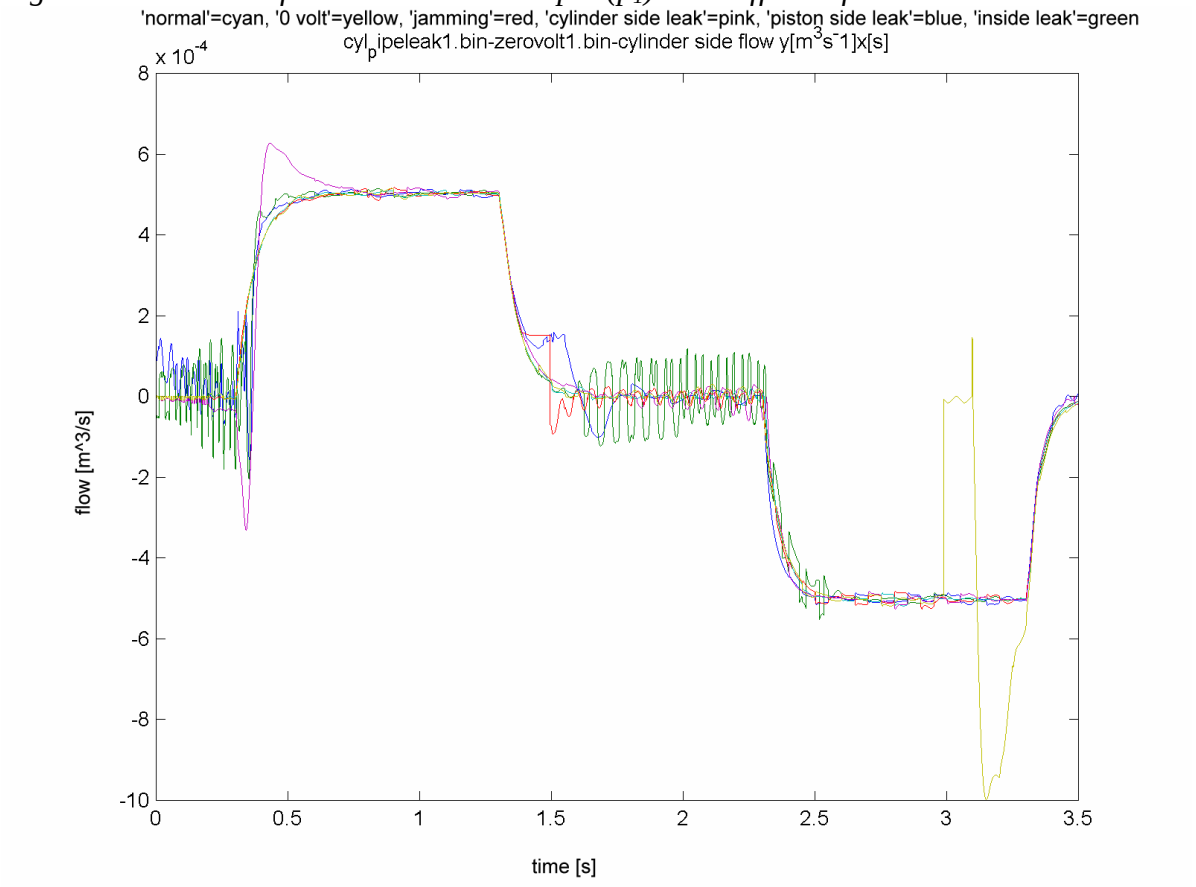

Figure 6. Cylinder side flow output (Q_A) with different faults.

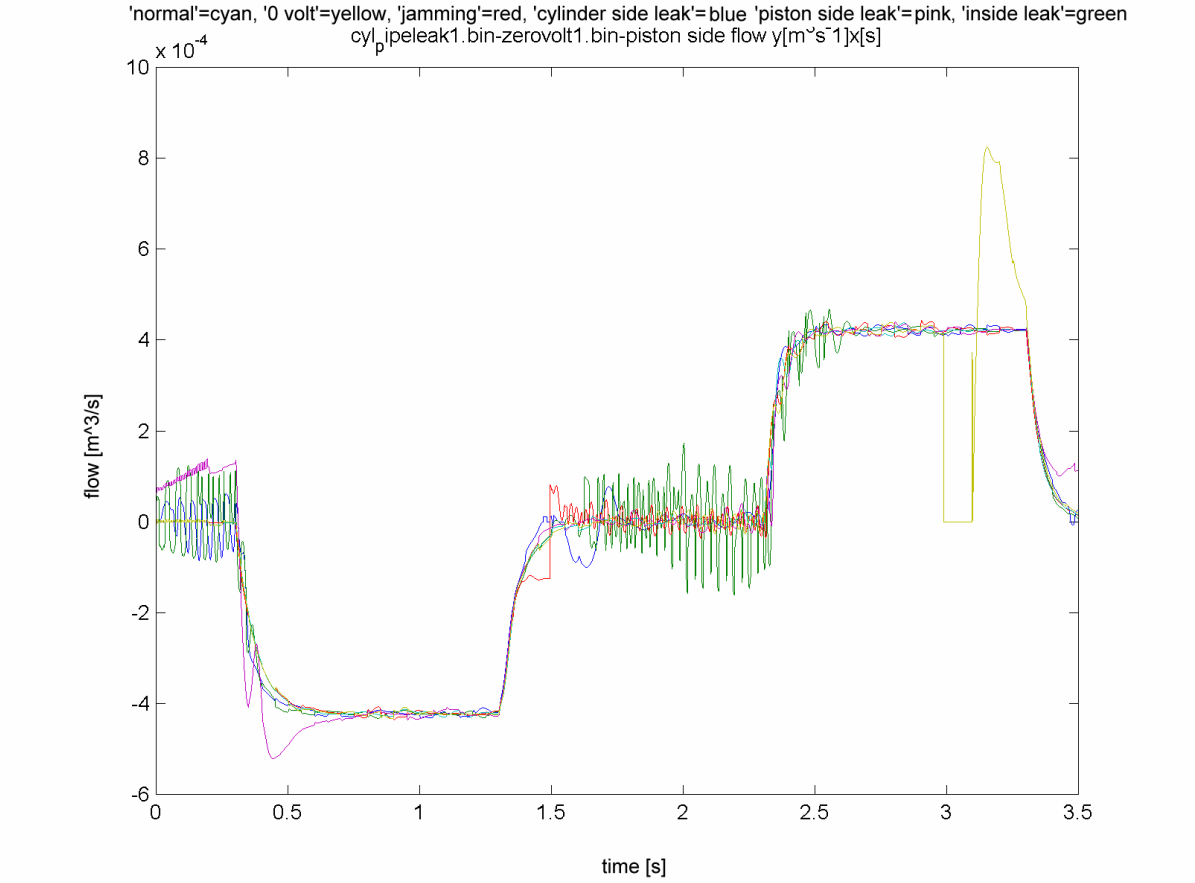

Figure 7. Piston side flow output (Q_B) with different faults.

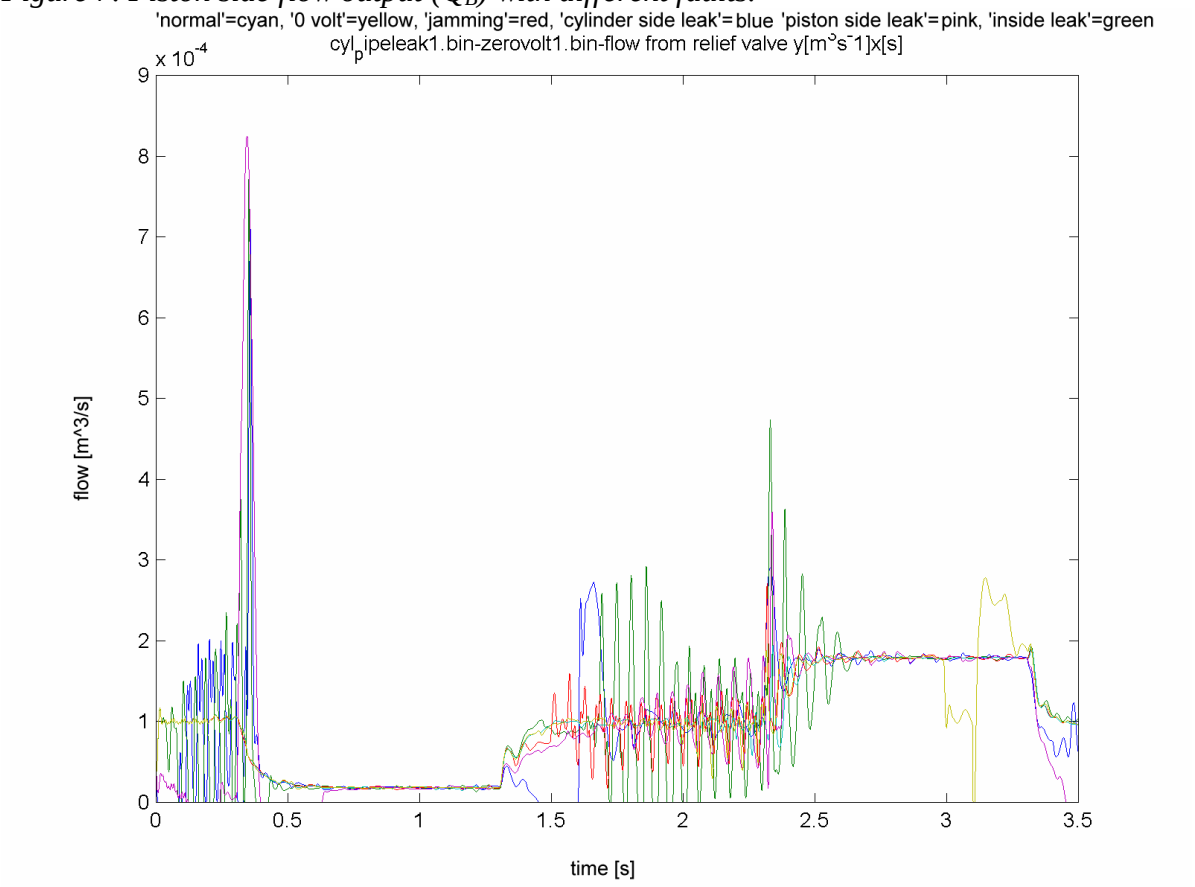

Figure 8. Flow from relief valve output (Q_{re}) with different faults.

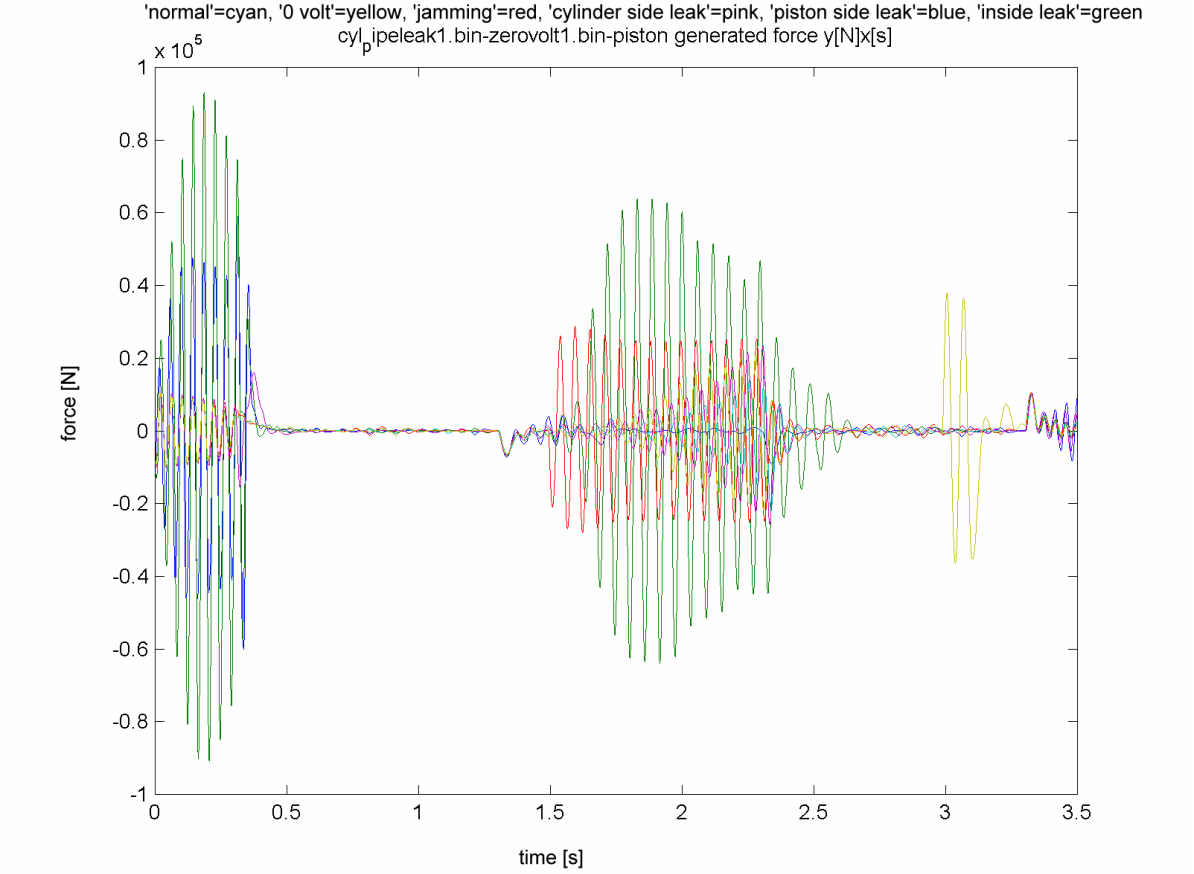

Figure 9. Supply force output (F_{su}) with different faults.

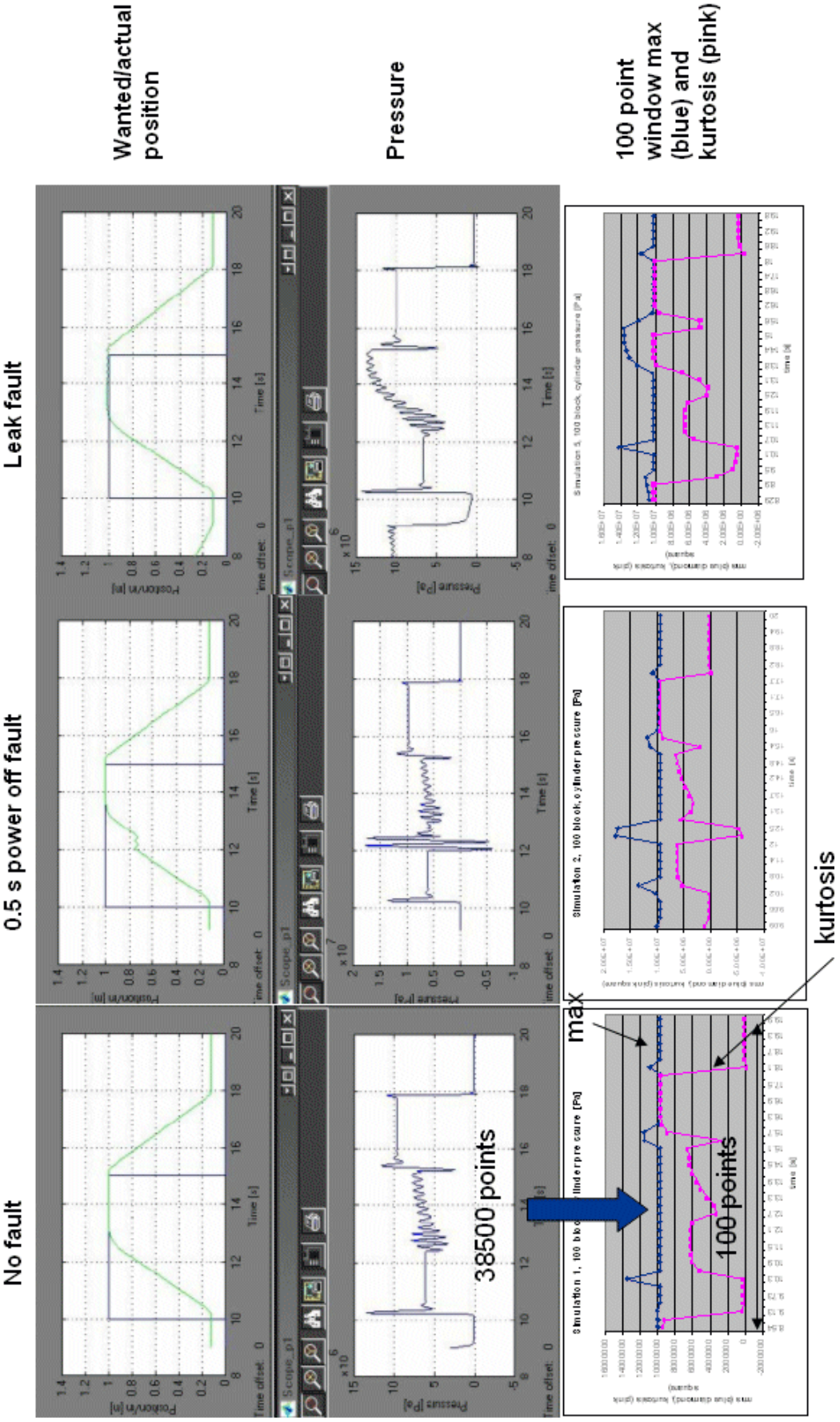

Figure 1. The calculation of statistical windows.

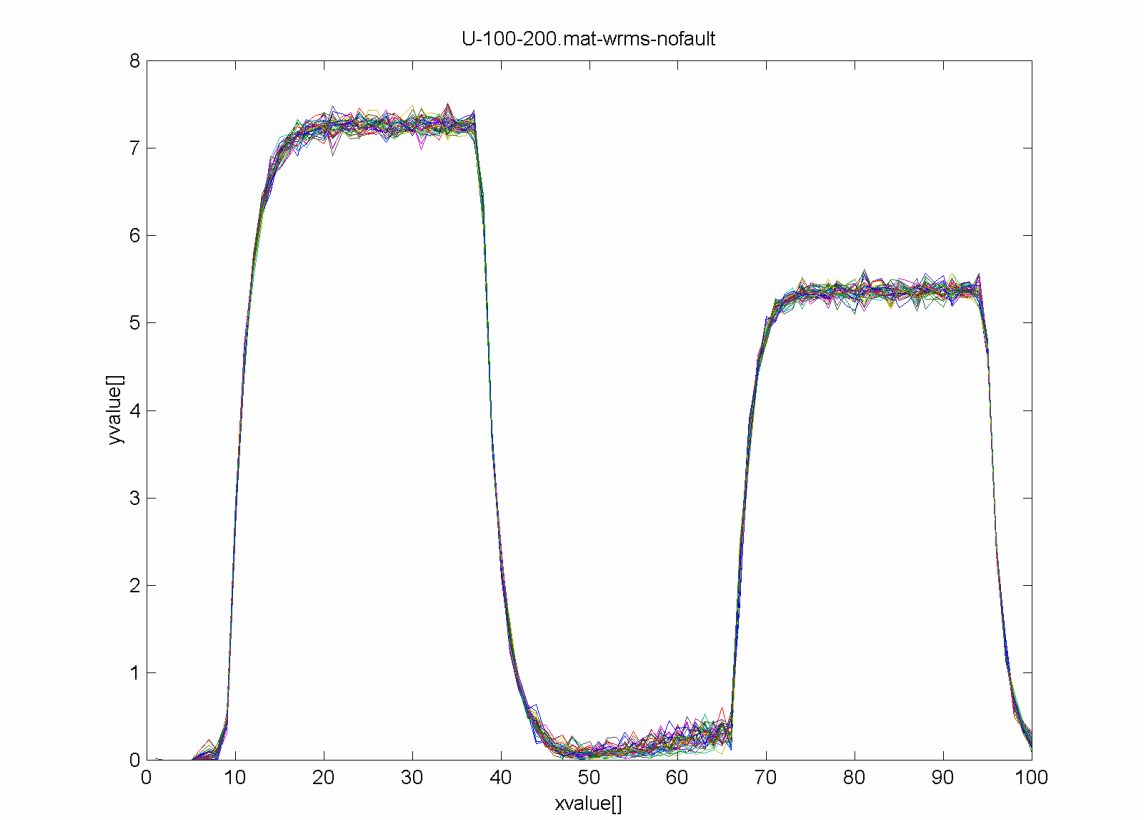

Figure 1. Model 2 100 point valve control voltage rms feature vectors for no fault-case.

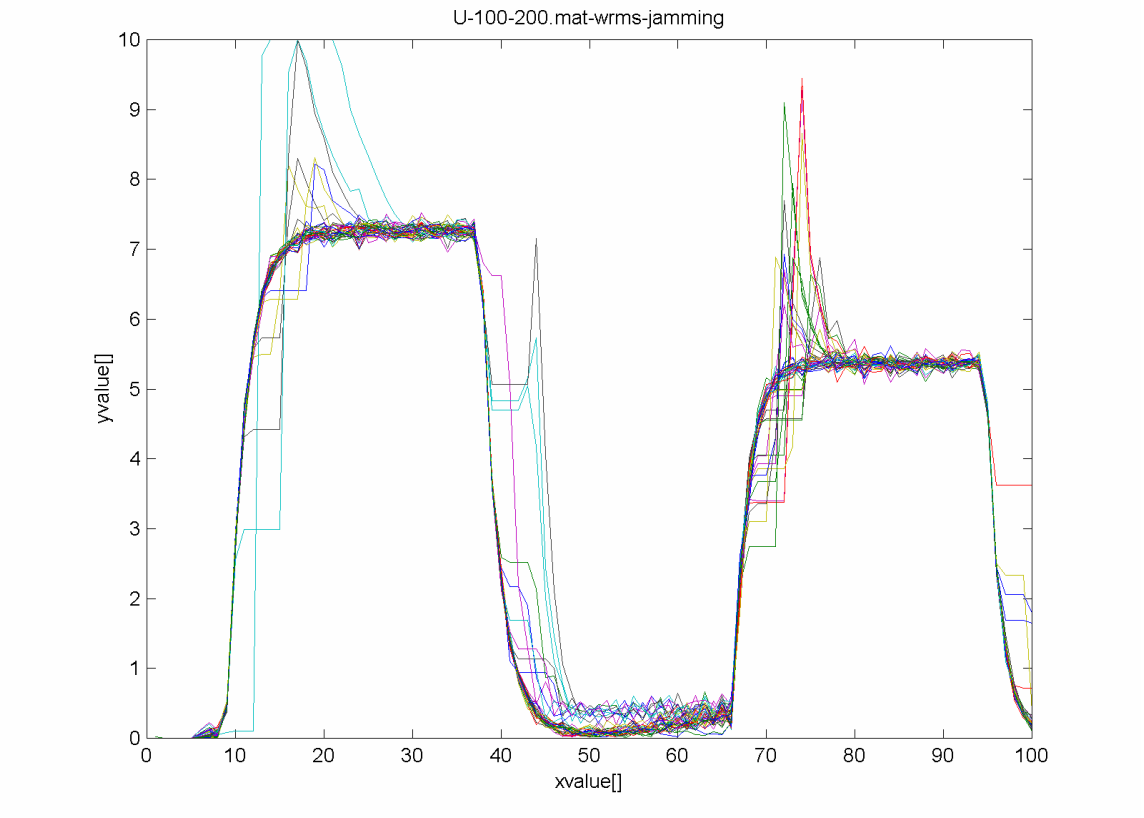

Figure 2. Model 2 100 point valve control voltage rms feature vectors for sticking fault-case.

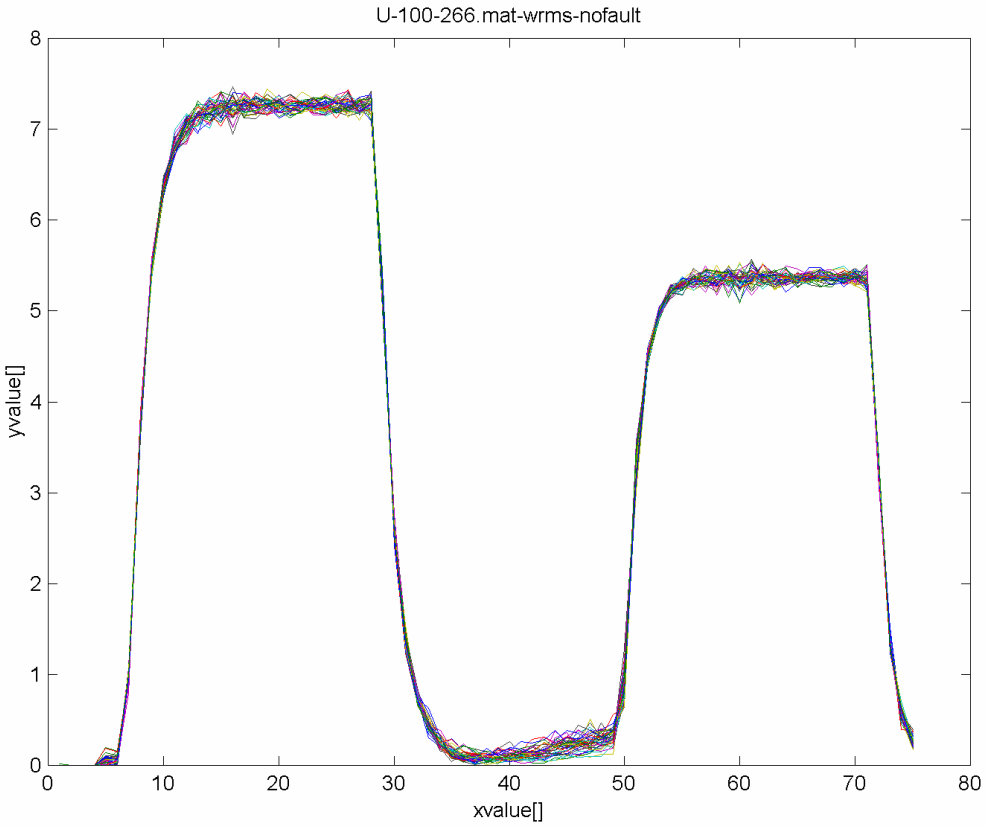

Figure 3. Model 2 75 point valve control voltage rms feature vectors for no fault-case.

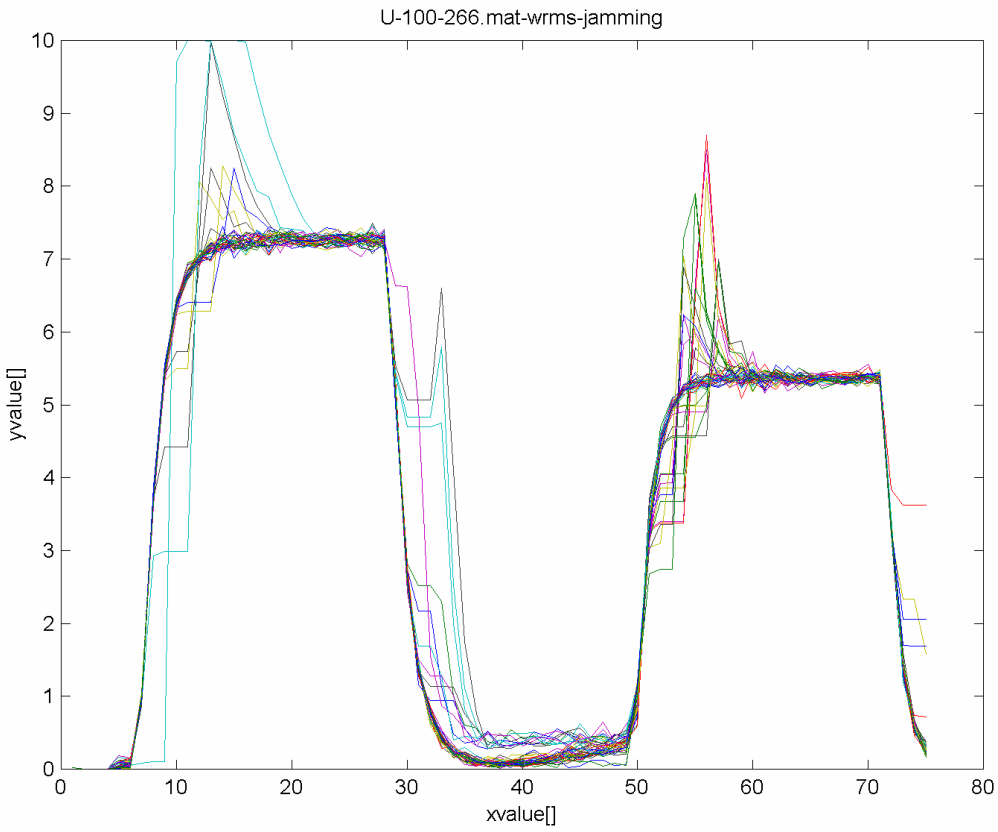

Figure 4. Model 2 75 point valve control voltage rms feature vectors for sticking fault-case.

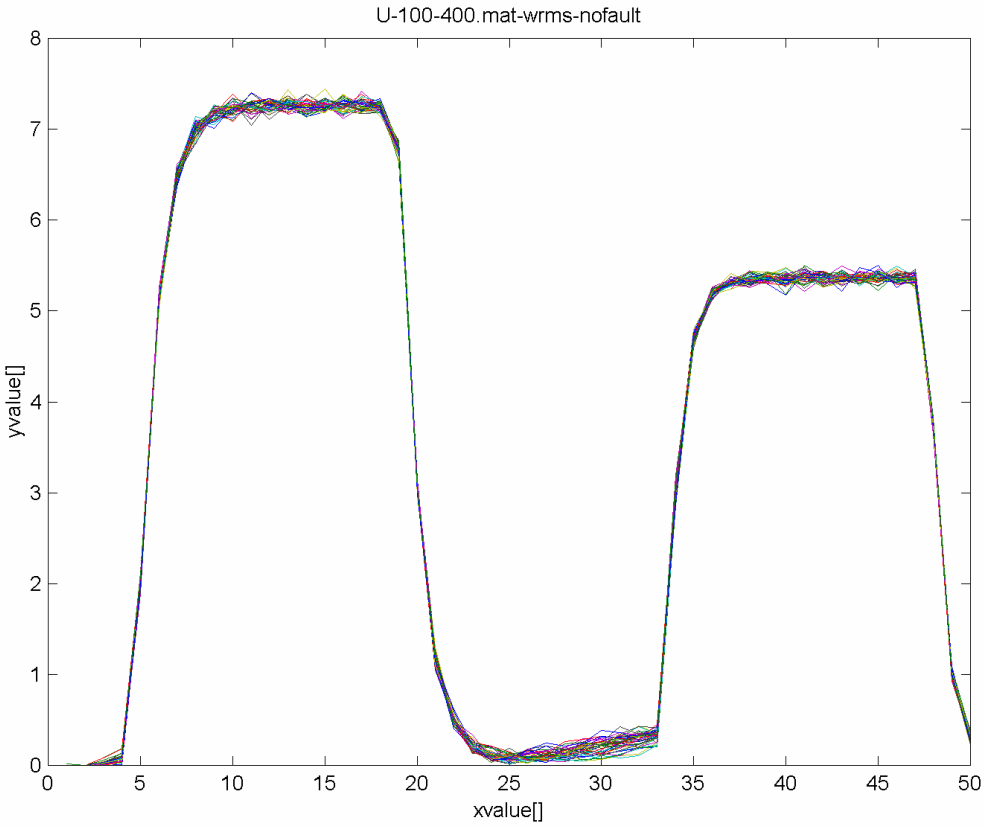

Figure 5. Model 2 50 point valve control voltage rms feature vectors for no fault-case.

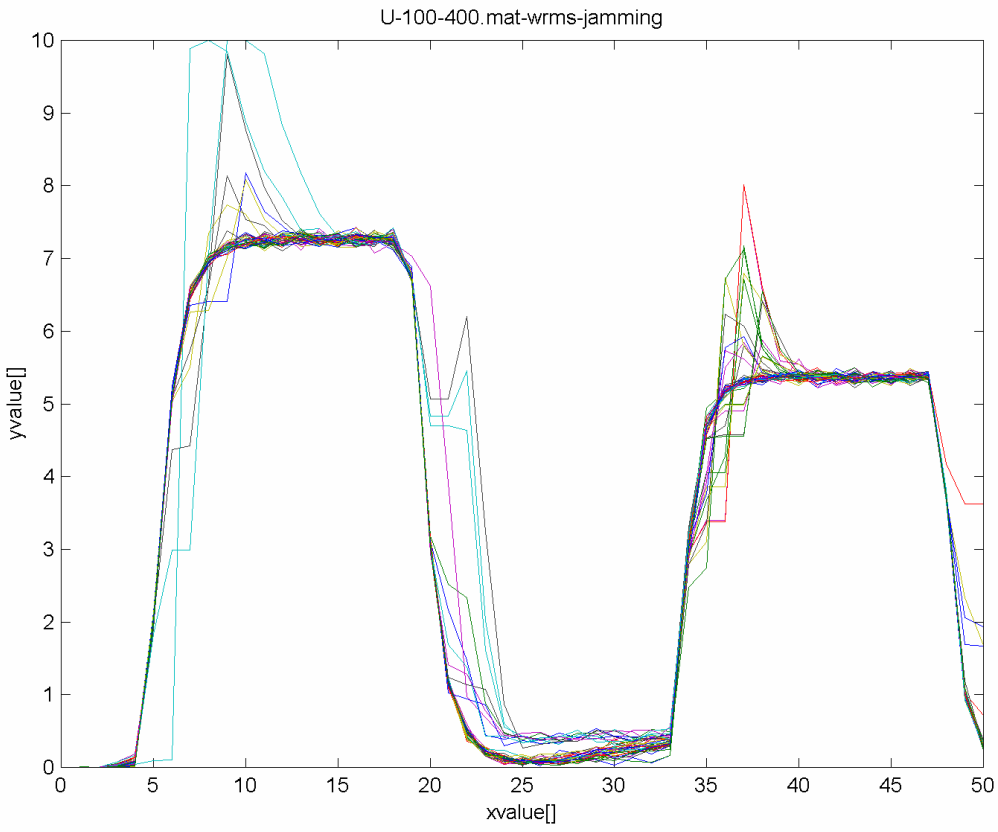

Figure 6. Model 2 50 point valve control voltage rms feature vectors for sticking fault-case.

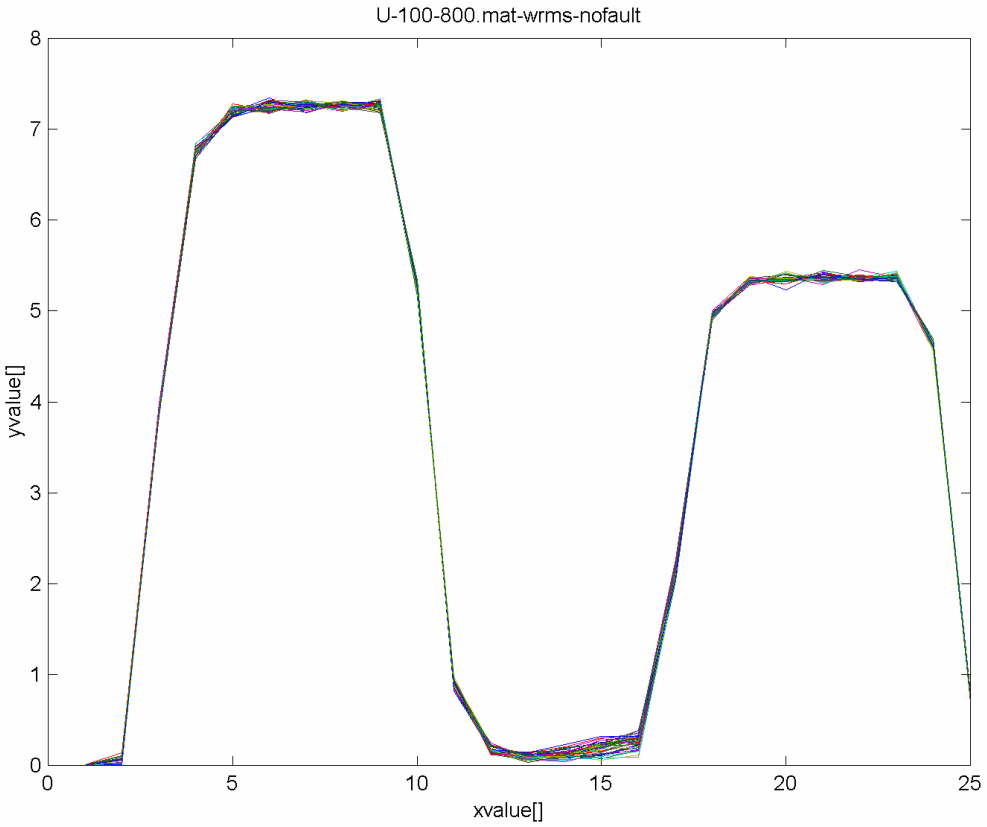

Figure 7. Model 2 25 point valve control voltage rms feature vectors for no fault-case.

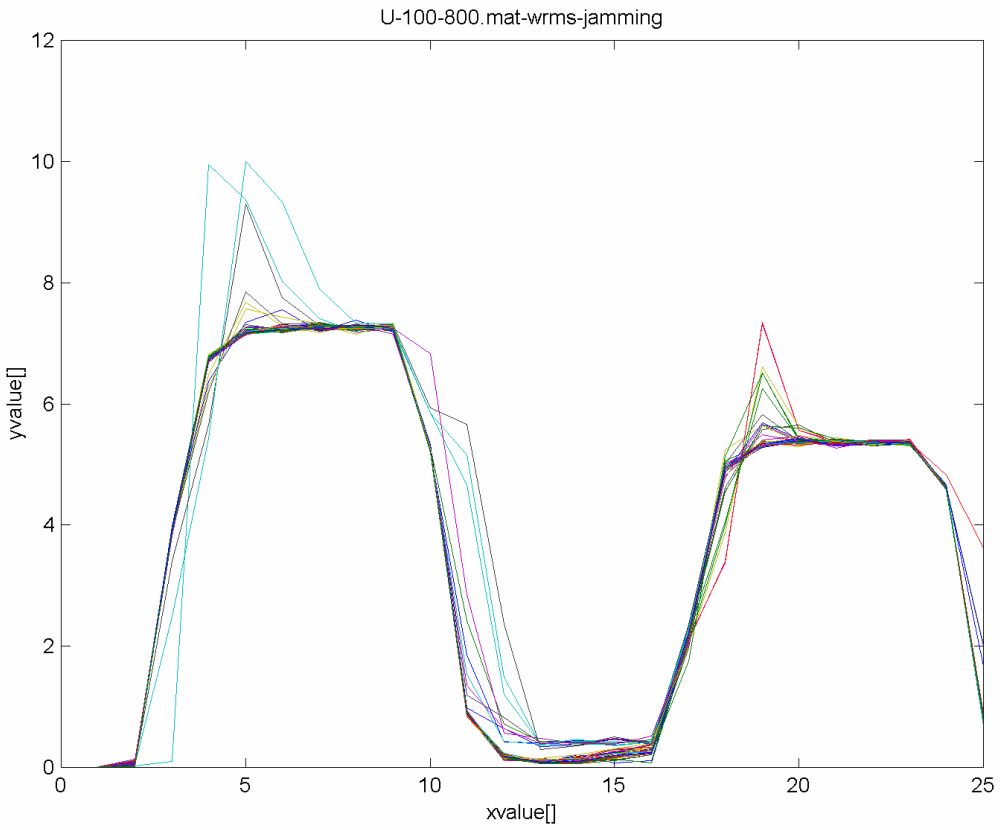

Figure 8. Model 2 25 point valve control voltage rms feature vectors for sticking fault-case.

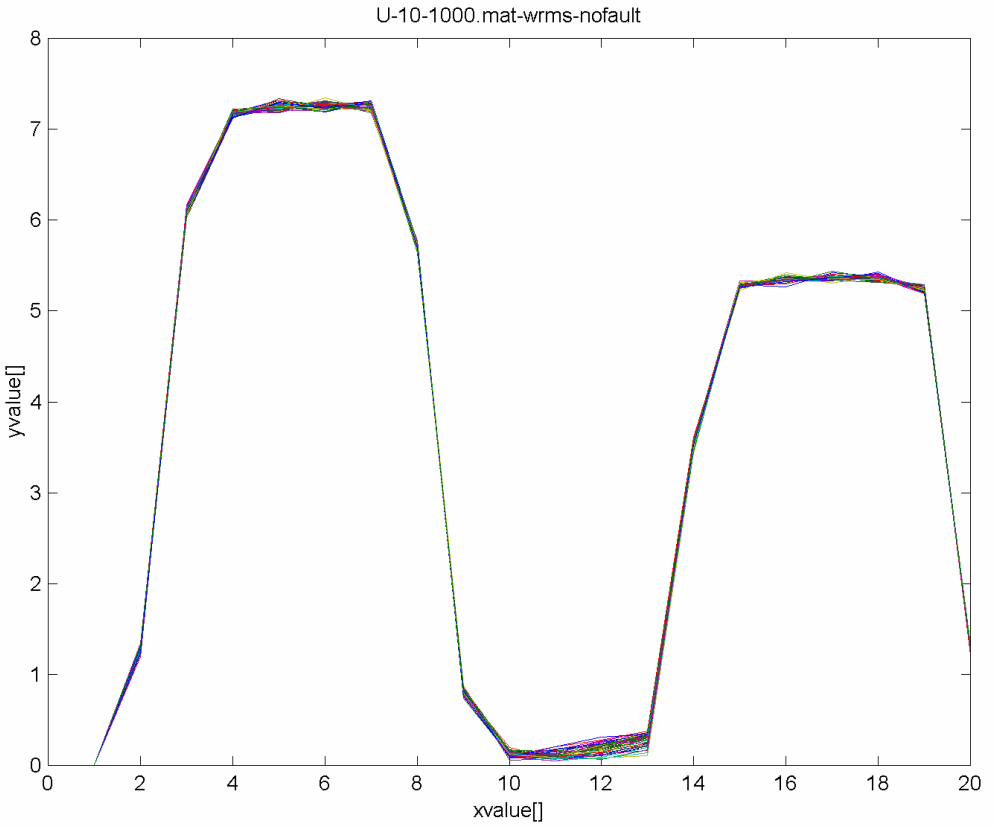

Figure 9. Model 2 20 point valve control voltage rms feature vectors for no fault-case.

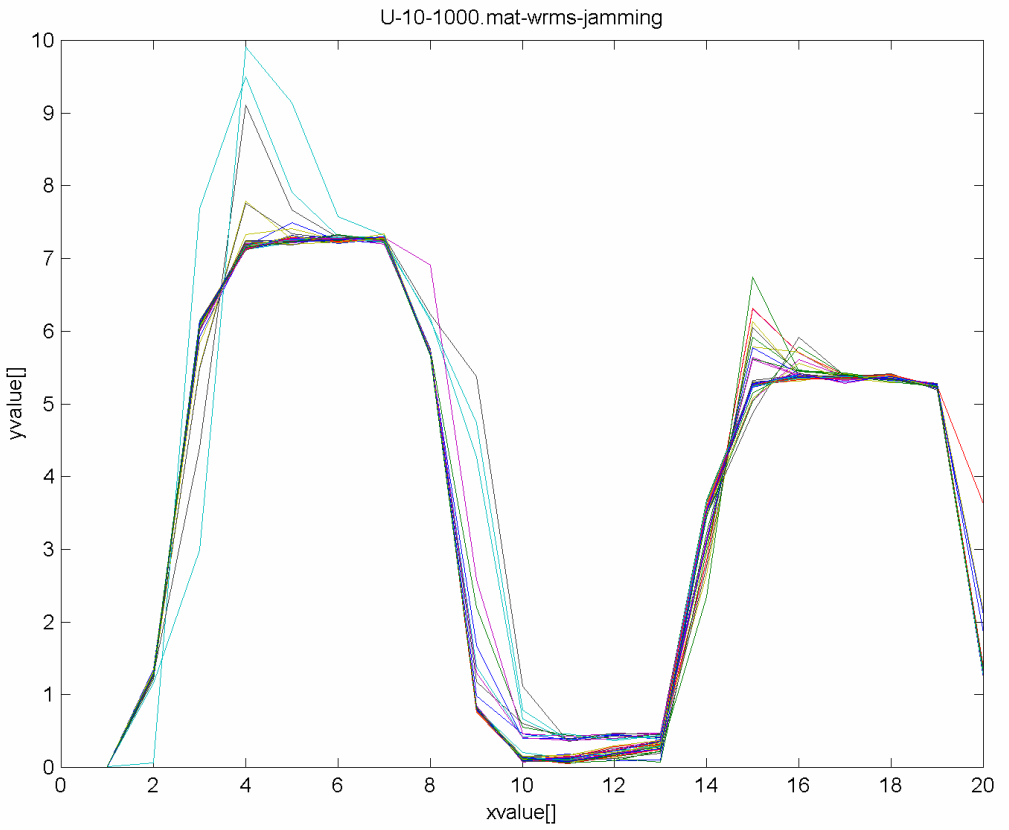

Figure 10. Model 2 20 point valve control voltage rms feature vectors for sticking fault-case.

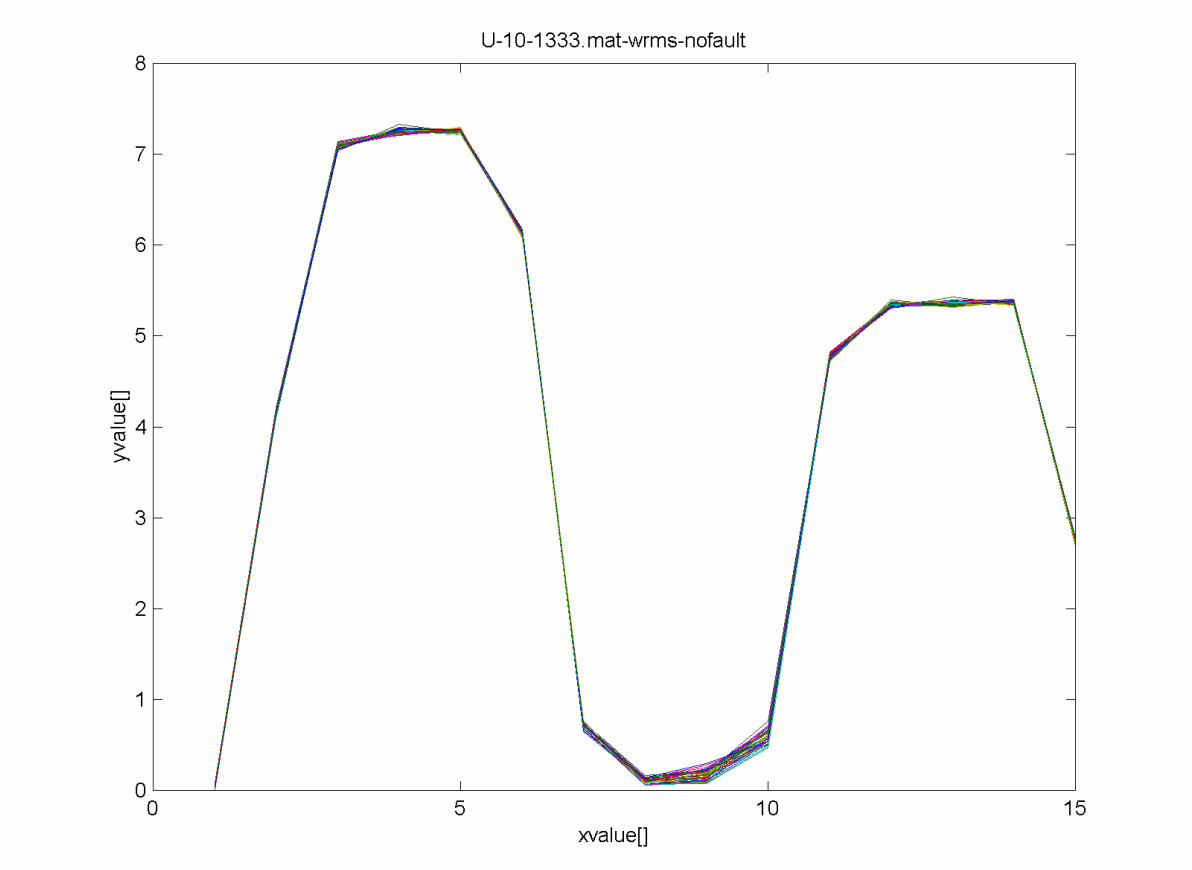

Figure 11. Model 2 15 point valve control voltage rms feature vectors for no fault-case.

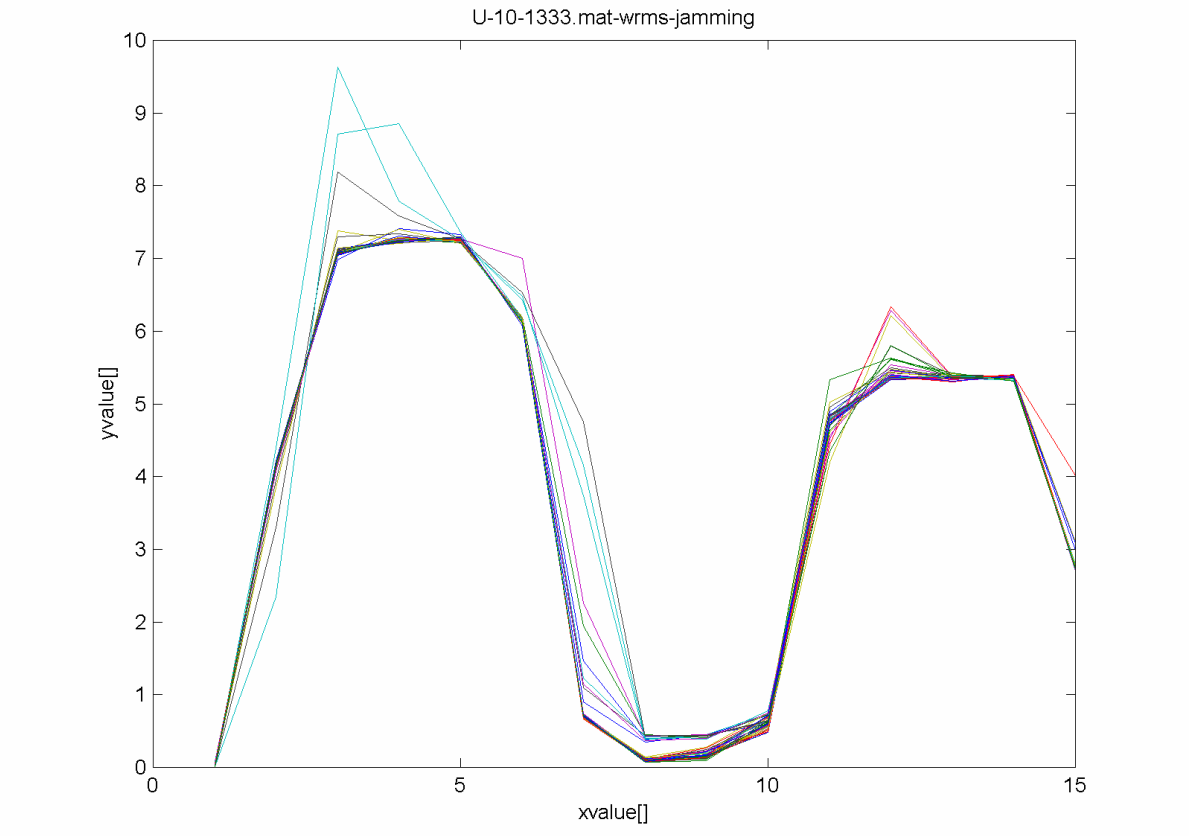

Figure 12. Model 2 15 point valve control voltage rms feature vectors for sticking fault-case.

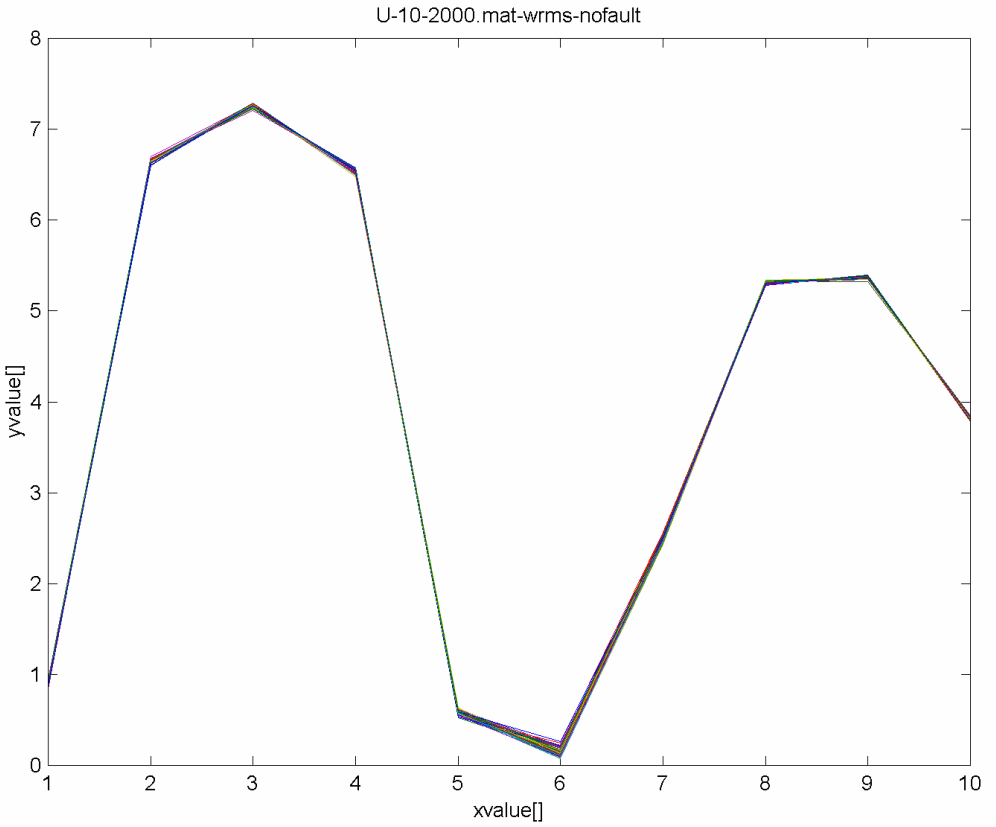

Figure 13. Model 2 10 point valve control voltage rms feature vectors for no fault-case.

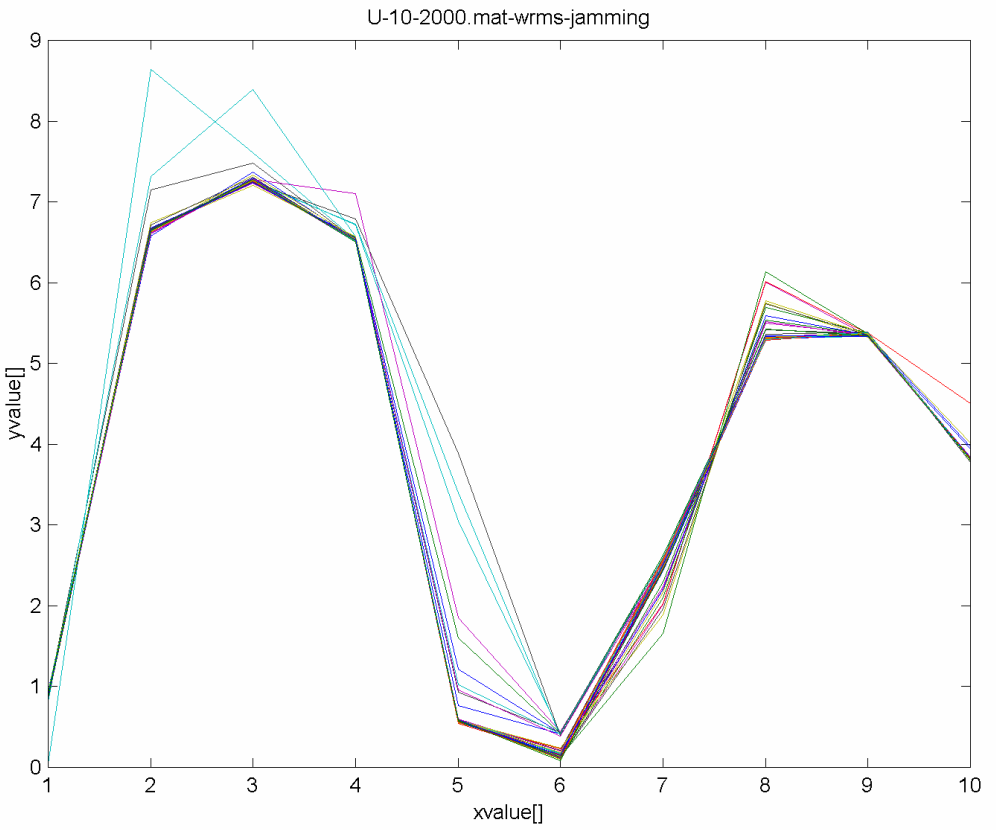

Figure 14. Model 2 10 point valve control voltage rms feature vectors for sticking fault-case.

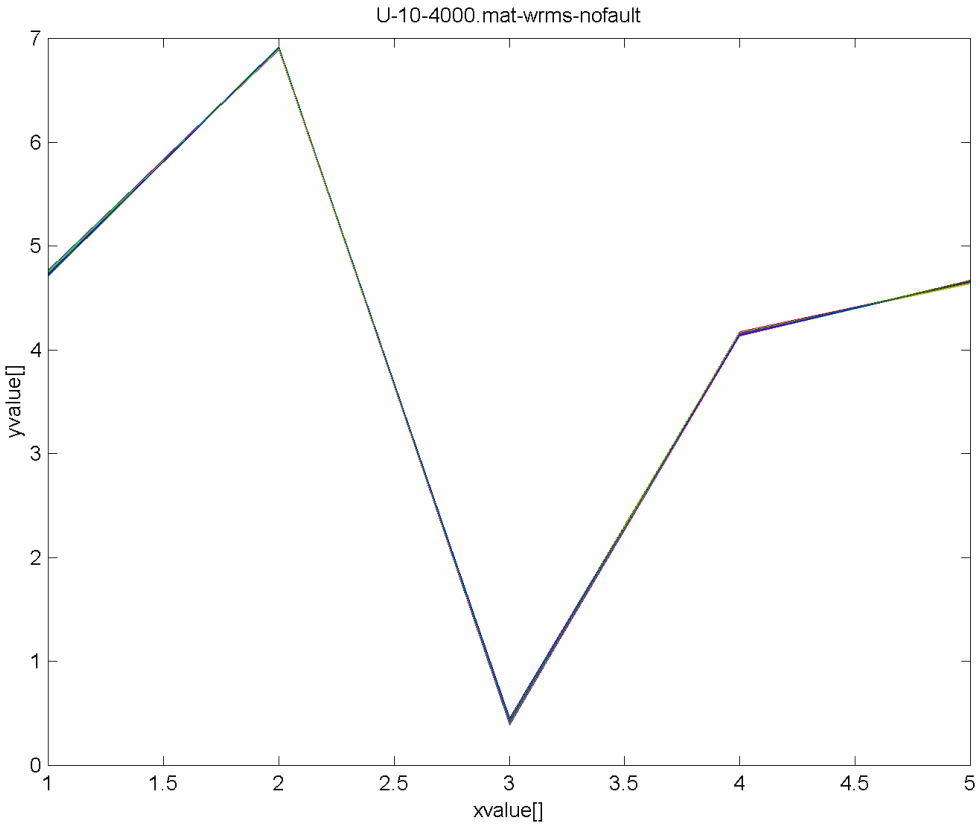

Figure 15. Model 2 5 point valve control voltage rms feature vectors for no fault-case.

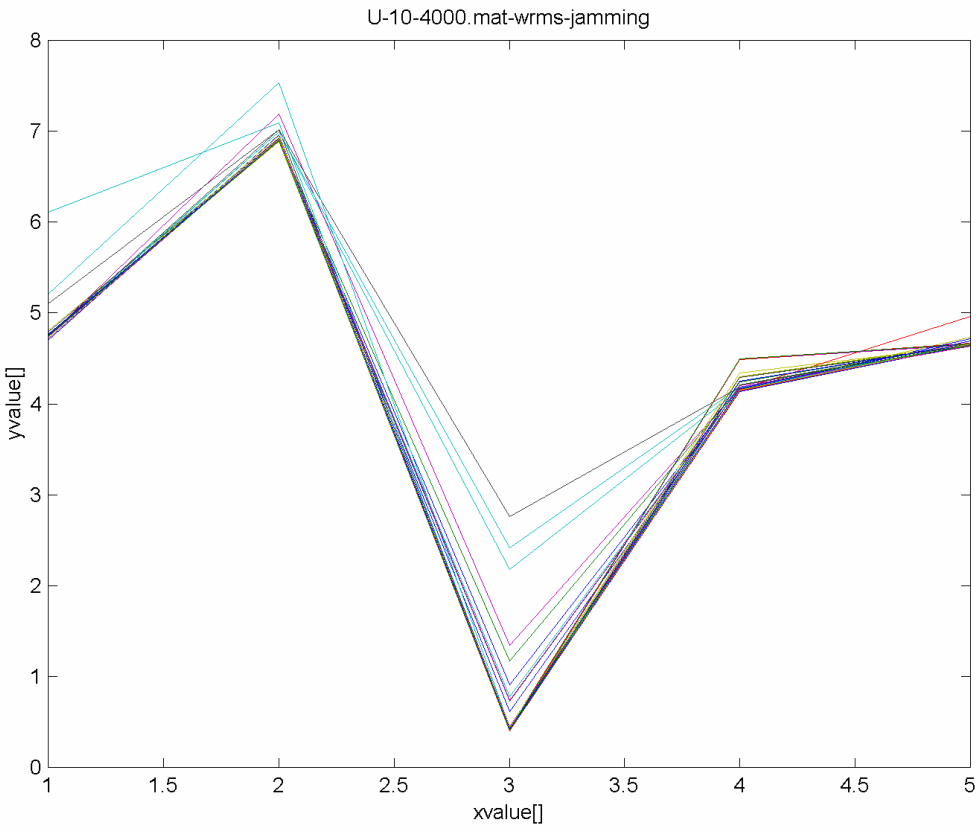

Figure 16. Model 2 5 point valve control voltage rms feature vectors for sticking fault-case.

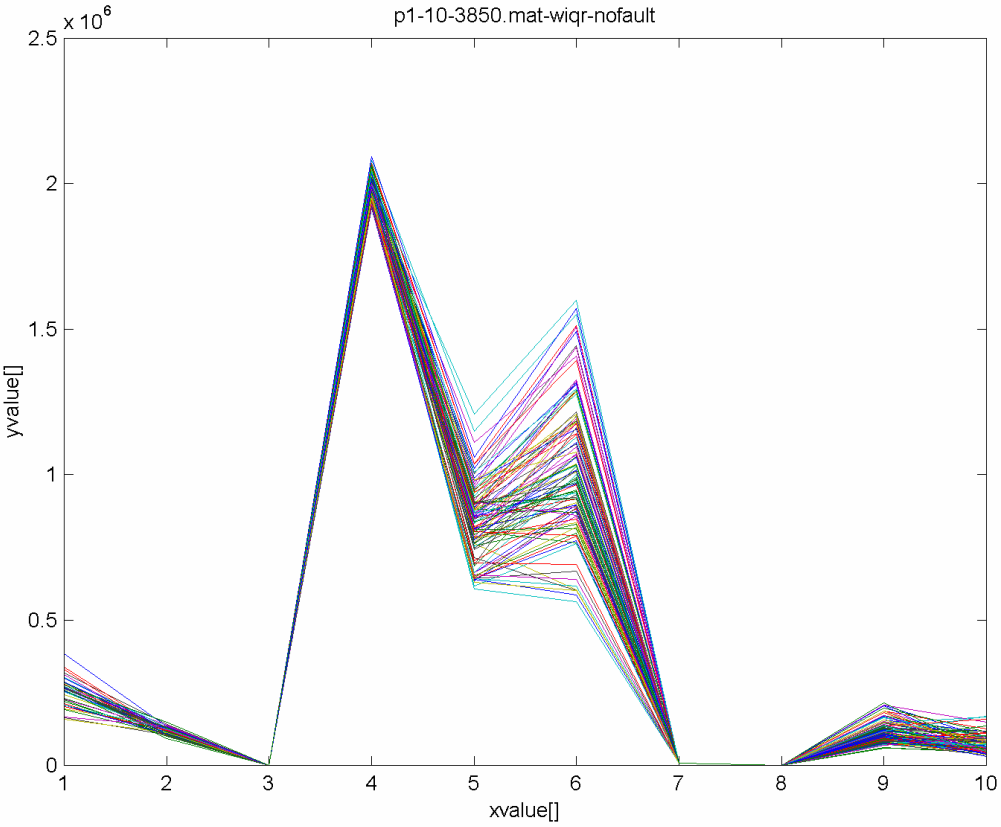

Figure 17. Model 1 10 point cylinder side pressure iqr feature vectors for no fault case.

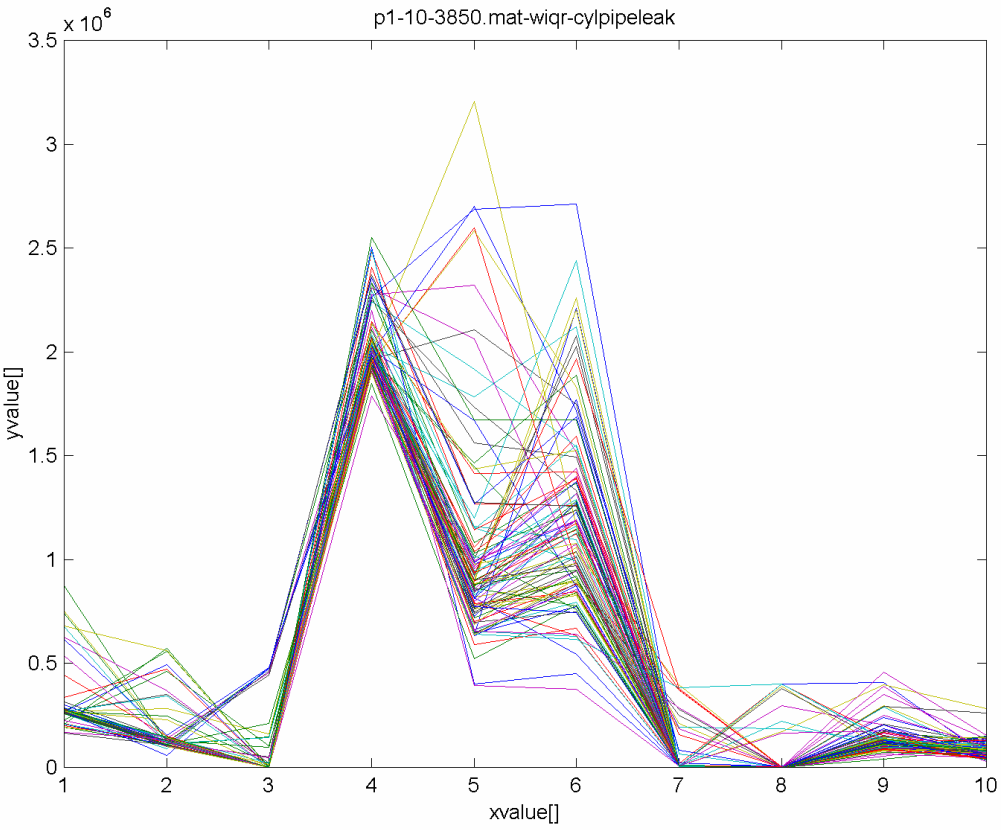

Figure 18. Model 1 10 point cylinder side pressure iqr feature vectors for cylinder side leak.

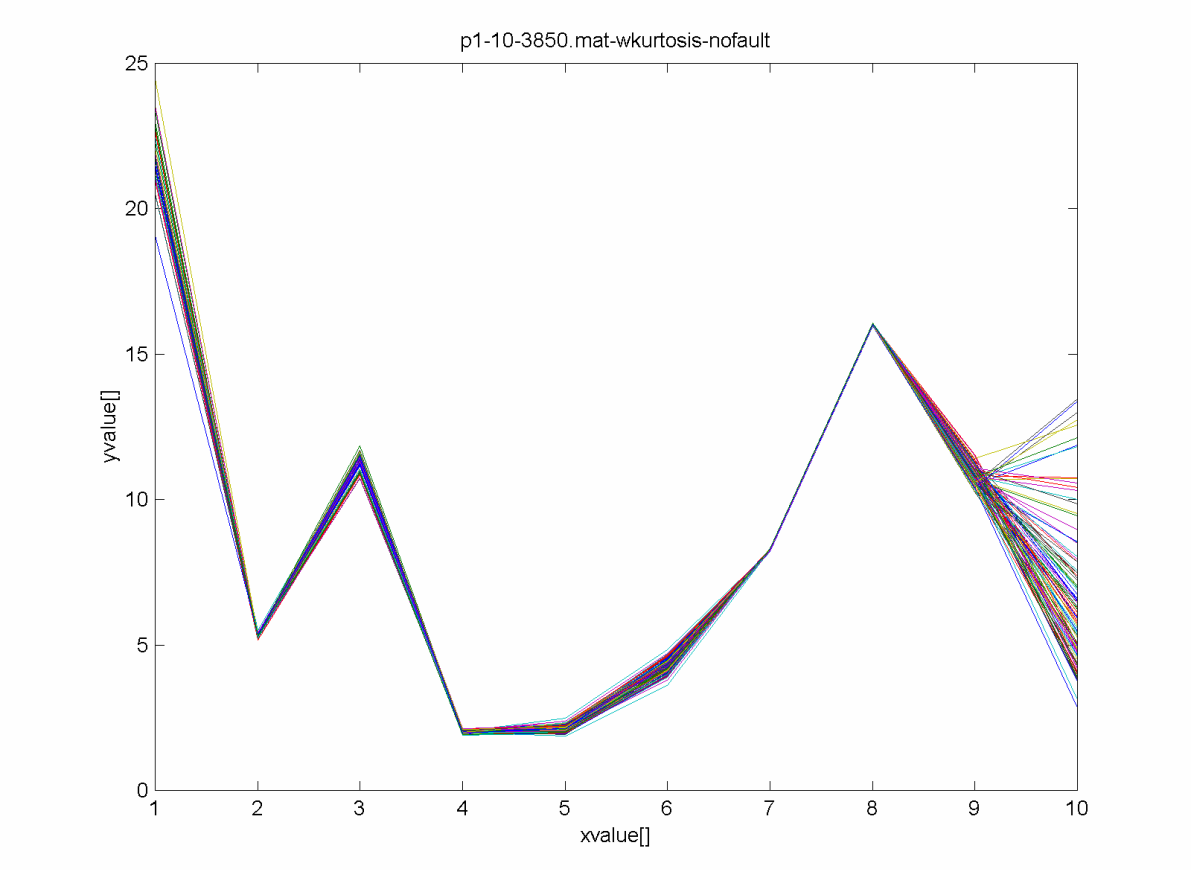

Figure 19. Model 1 10 point cylinder side pressure kurtosis feature vectors for no fault case.

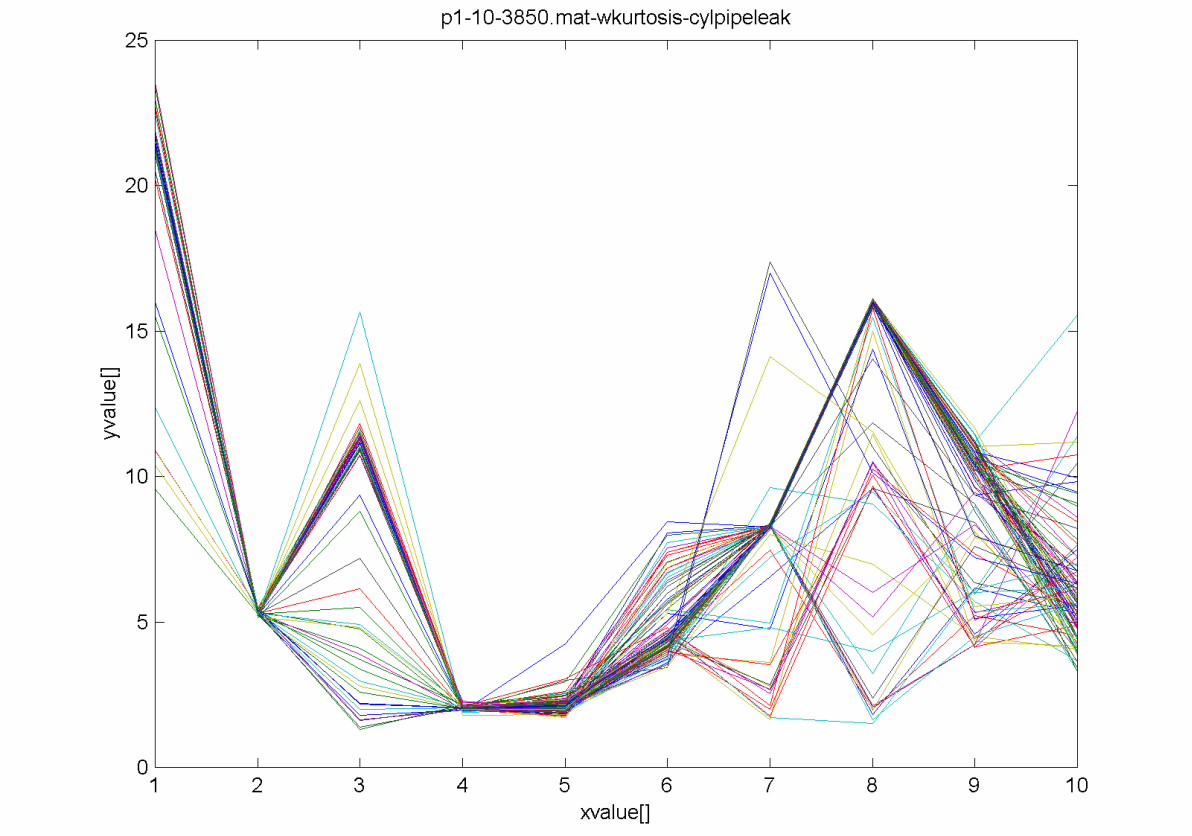

Figure 20. Model 1 10 point cylinder side pressure kurtosis feature vectors for cylinder side leak.

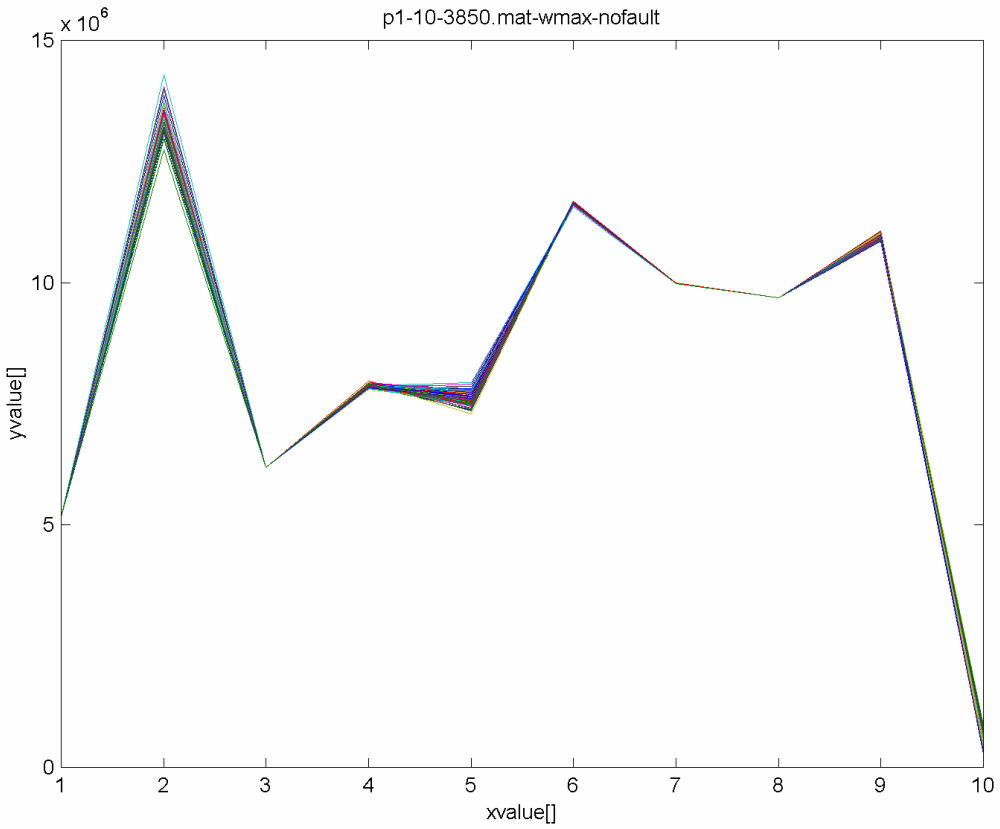

Figure 21. Model 1 10 point cylinder side pressure max feature vectors for no fault case.

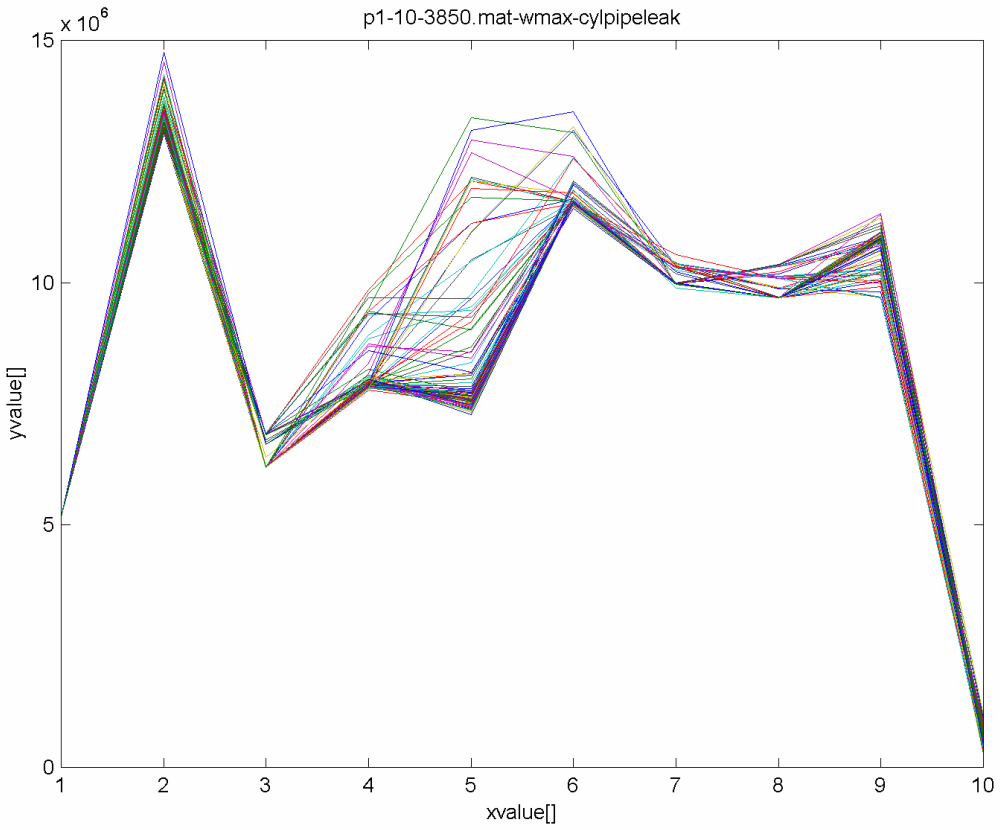

Figure 22. Model 1 10 point cylinder side pressure max feature vectors for cylinder side leak.

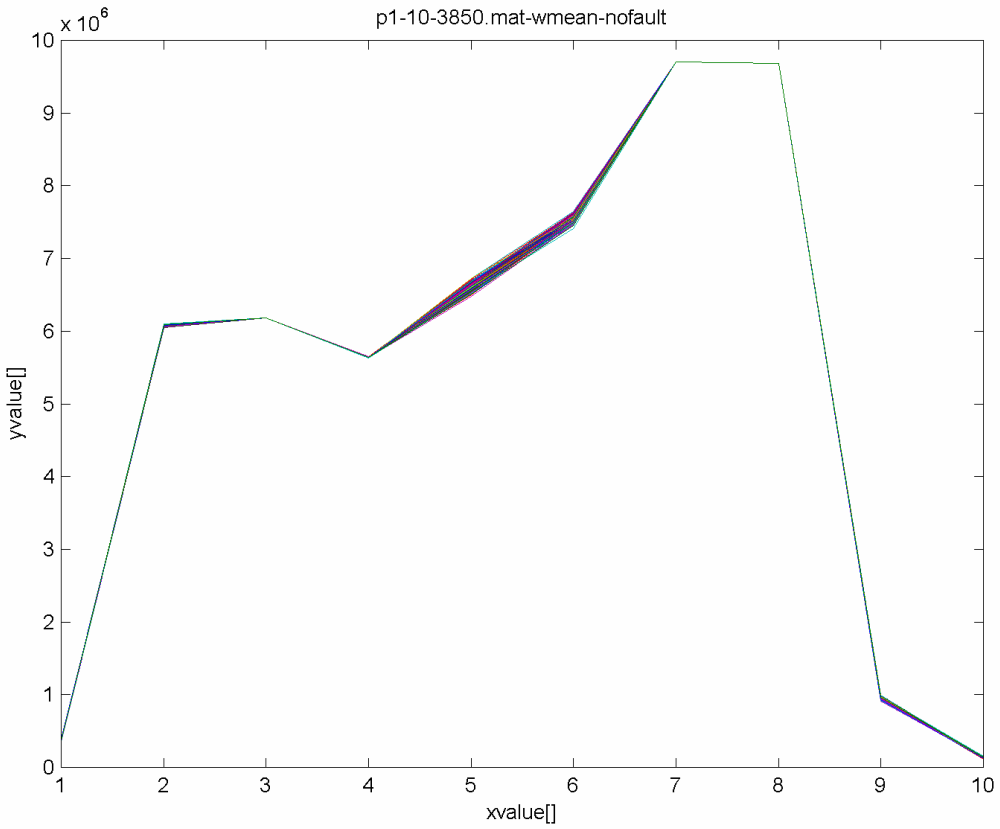

Figure 23. Model 1 10 point cylinder side pressure mean feature vectors for no fault case.

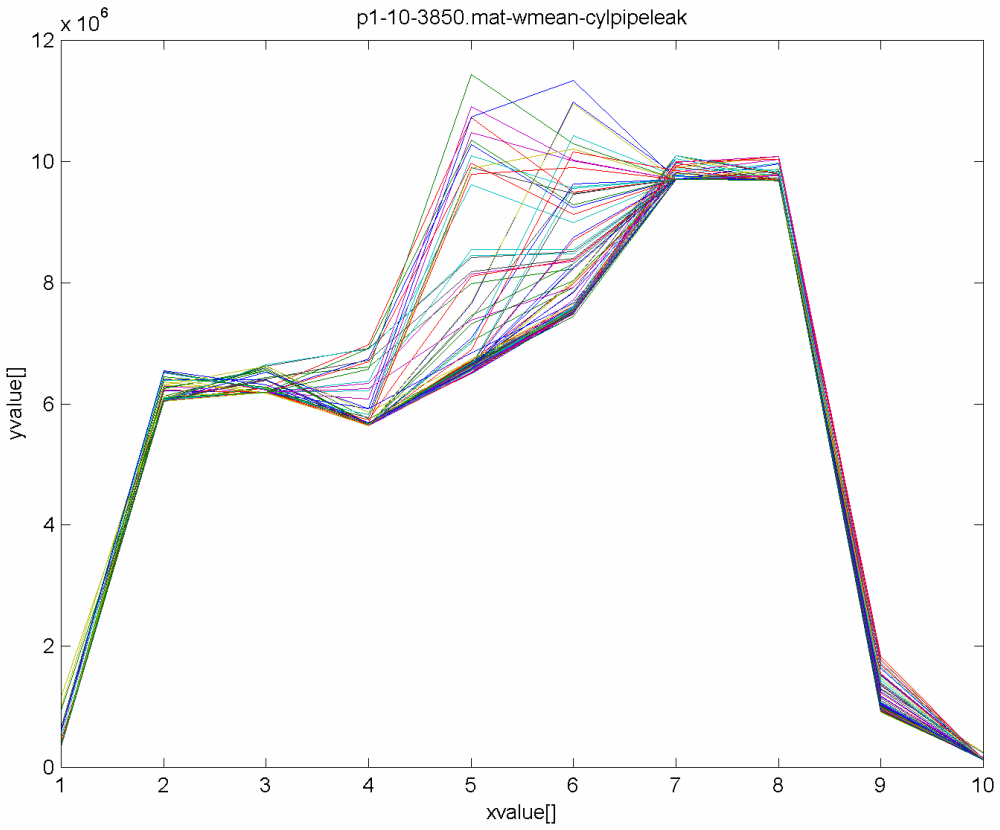

Figure 24. Model 1 10 point cylinder side pressure mean feature vectors for cylinder side leak.

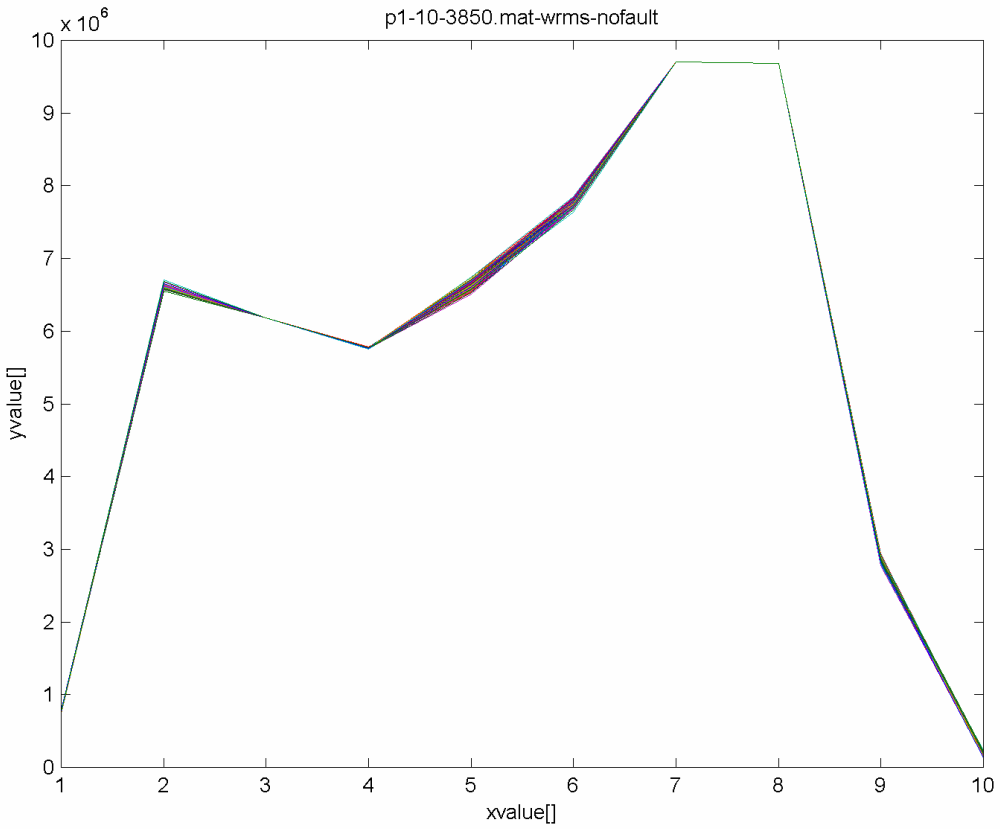

Figure 25. Model 1 10 point cylinder side pressure rms feature vectors for no fault case.

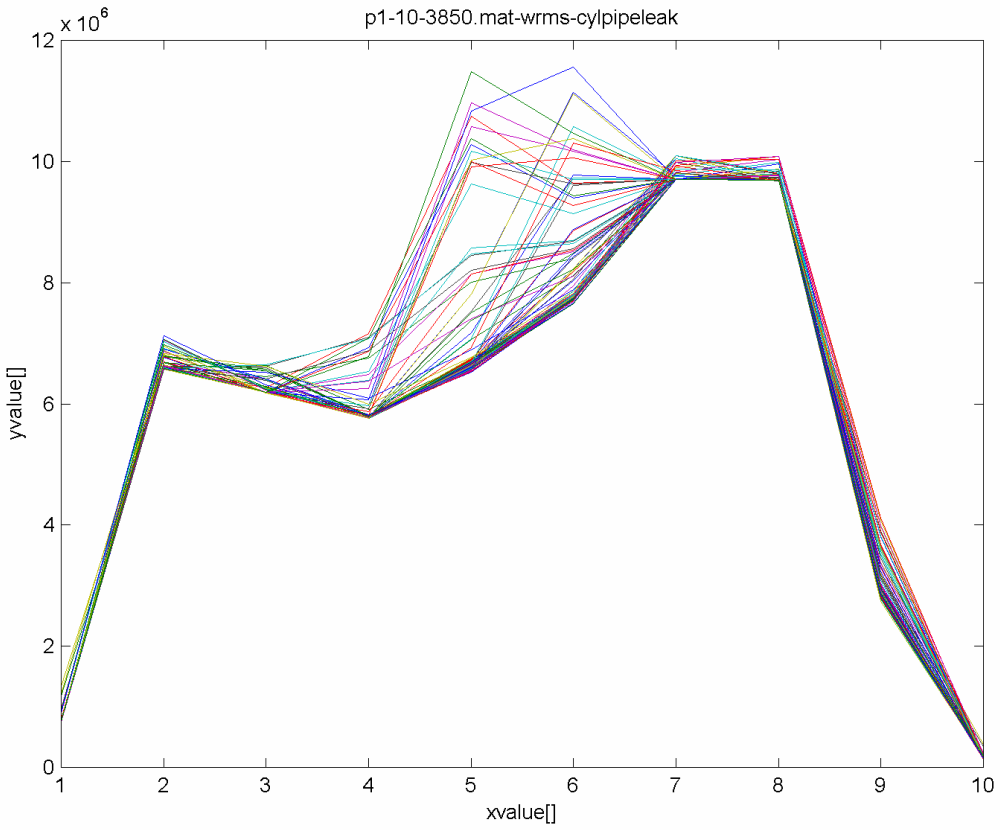

Figure 26. Model 1 10 point cylinder side pressure rms feature vectors for cylinder side leak.

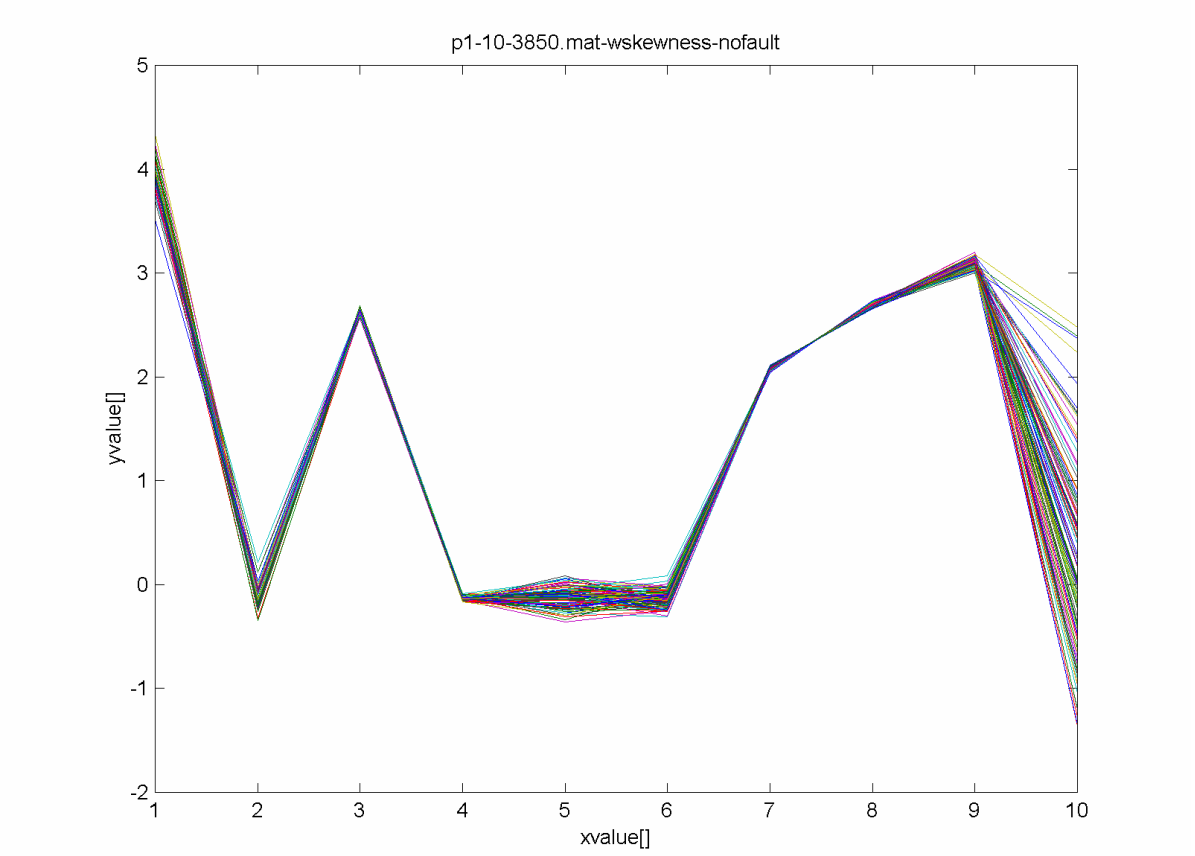

Figure 27. Model 1 10 point cylinder side pressure skewness feature vectors for no fault case.

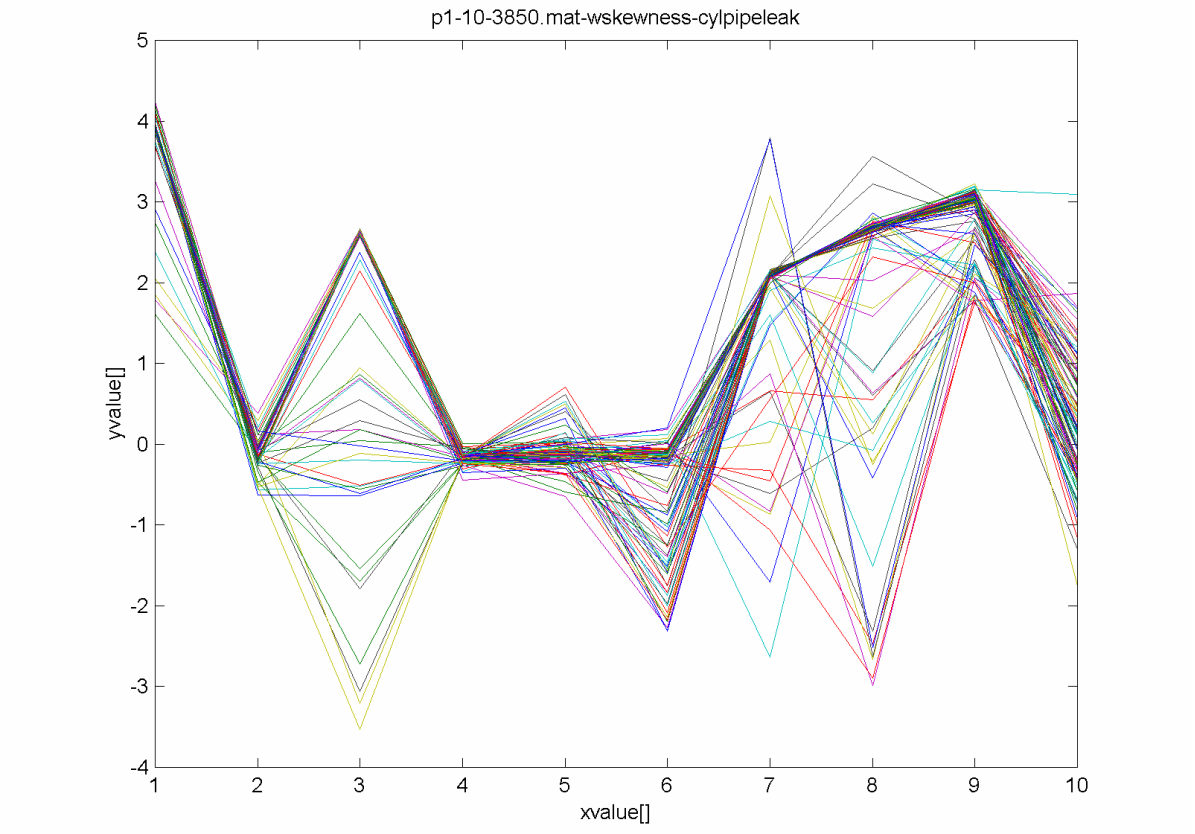

Figure 28. Model 1 10 point cylinder side pressure skewness feature vectors for cylinder side leak.

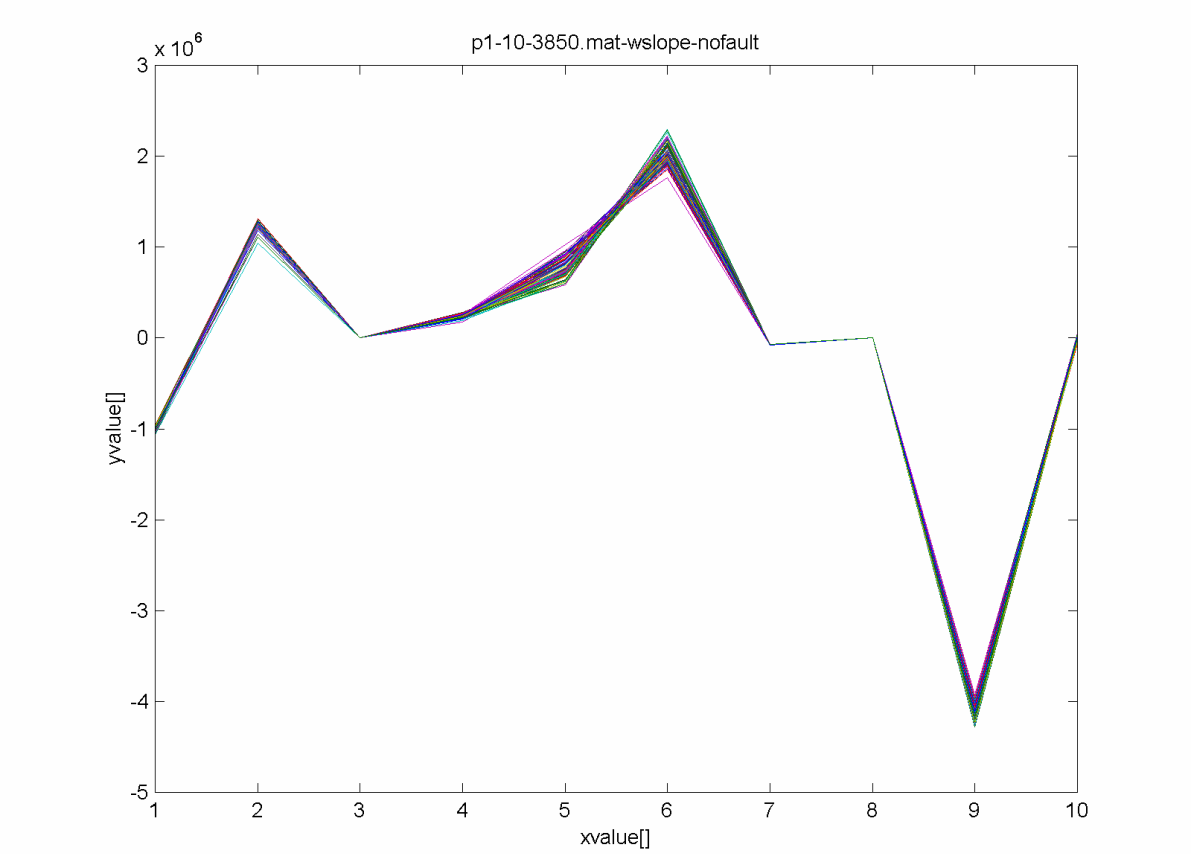

Figure 29. Model 1 10 point cylinder side pressure slope feature vectors for no fault case.

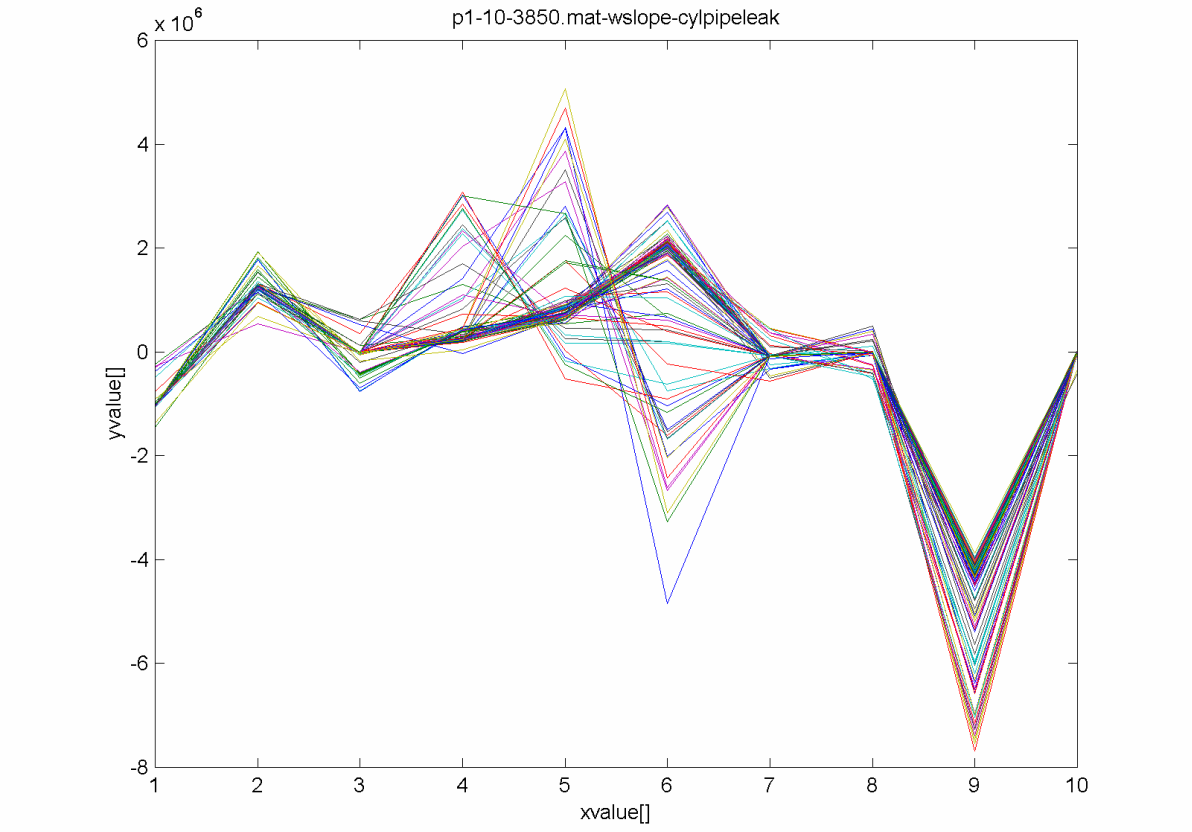

Figure 30. Model 1 10 point cylinder side pressure slope feature vectors for cylinder side leak.

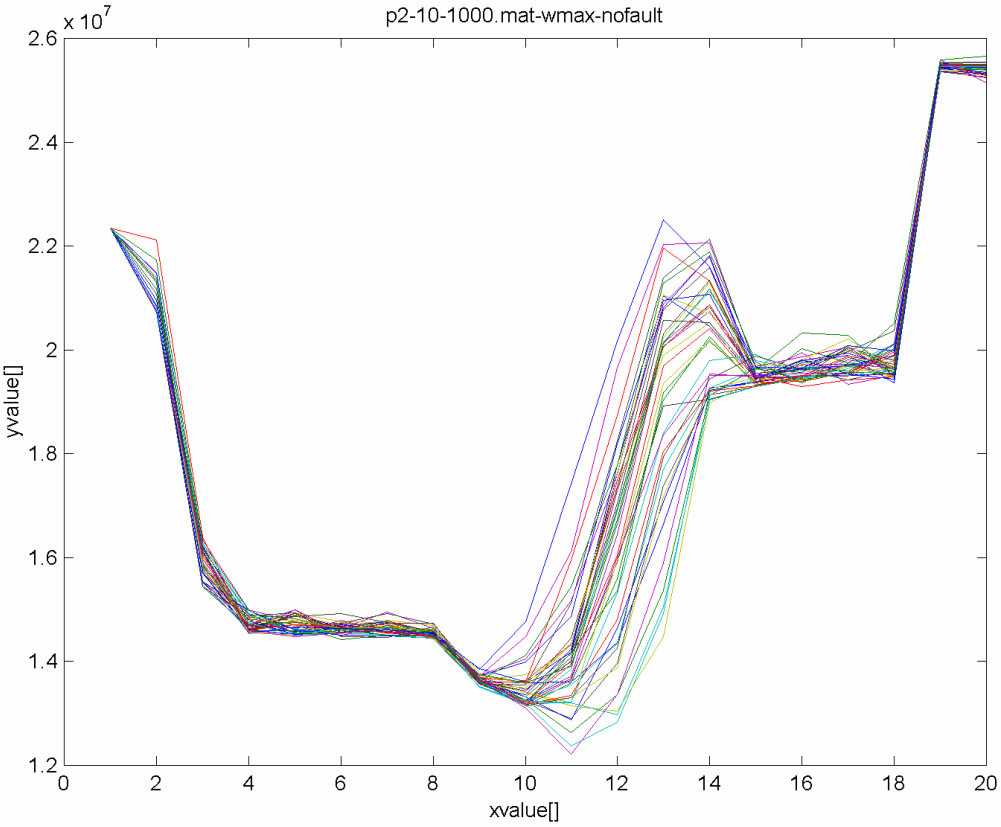

Figure 31. Model 2 20 point cylinder side pressure max feature vectors for no fault.

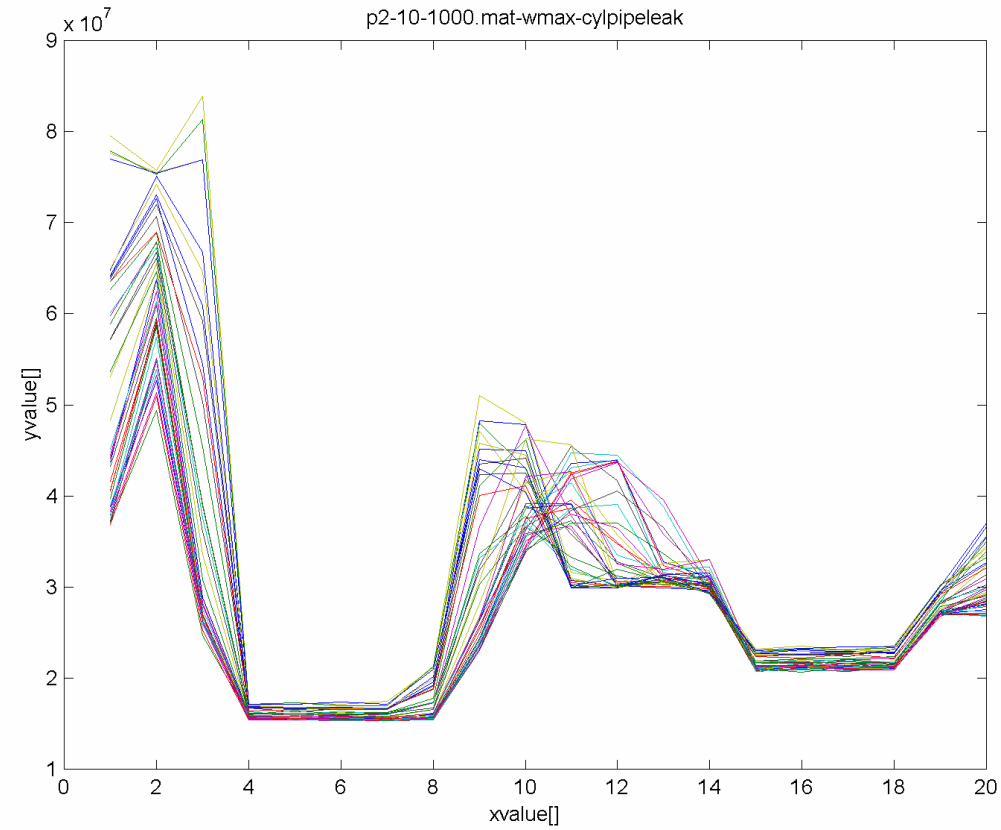

Figure 32. Model 2 20 point cylinder side pressure max feature vectors for cylinder side leak.

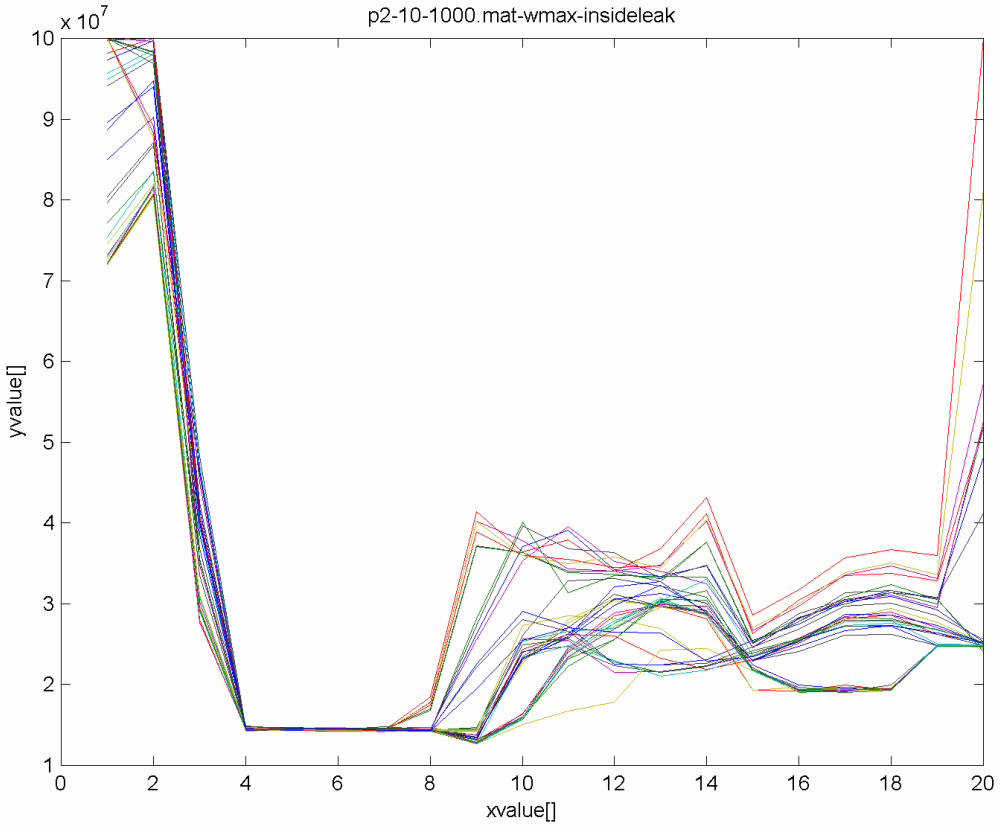

Figure 33. Model 2 20 point cylinder side pressure max feature vectors for inside leak.

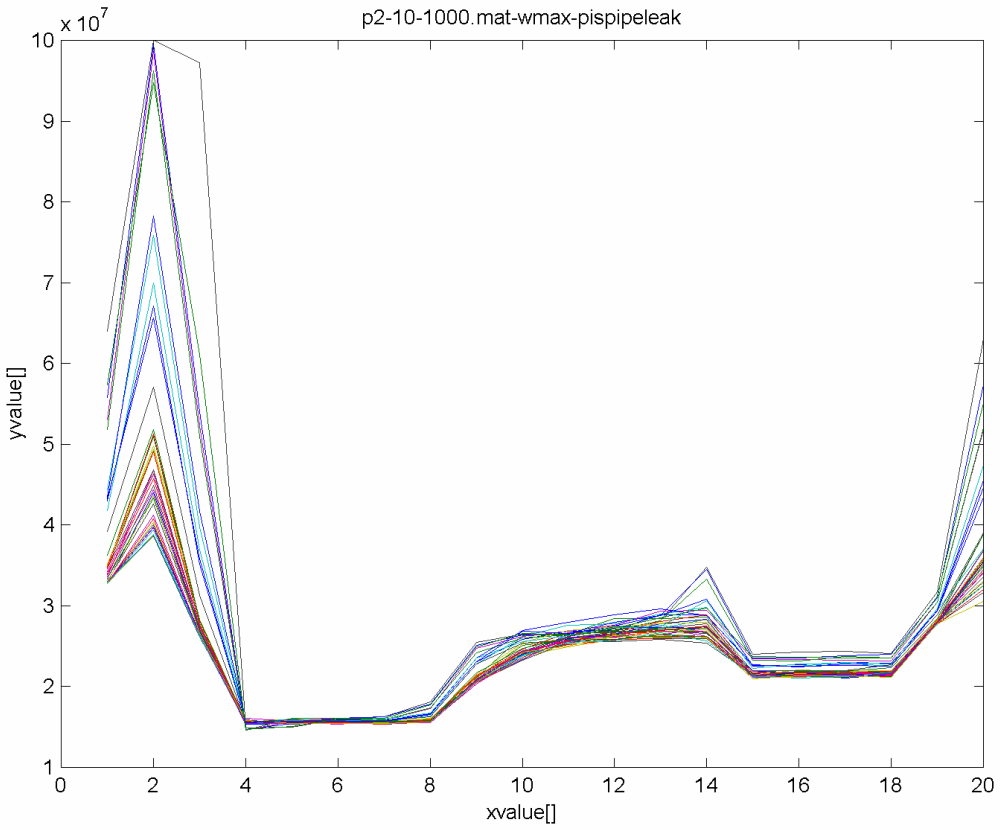

Figure 34. Model 2 20 point cylinder side pressure max feature vectors for piston side leak.

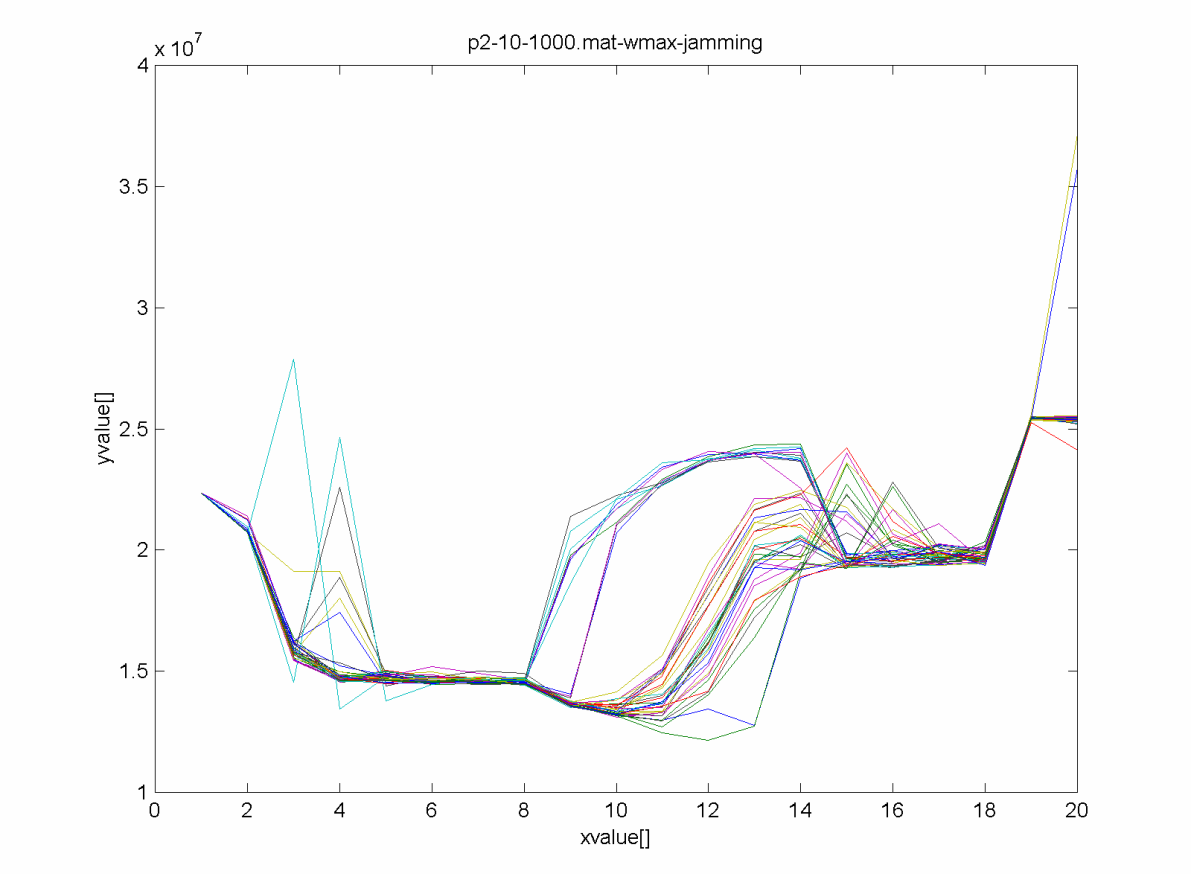

Figure 35. Model 2 20 point cylinder side pressure max feature vectors for sticking fault.

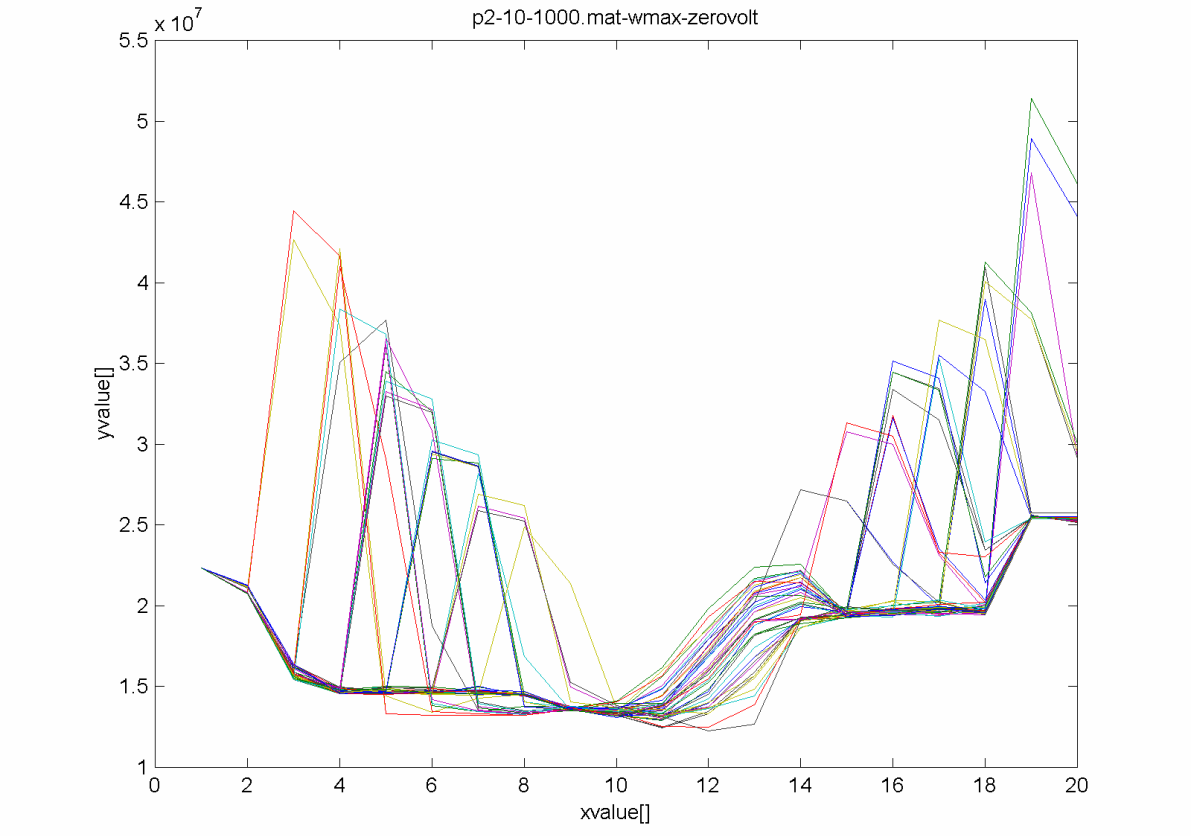

Figure 36. Model 2 20 point cylinder side pressure max feature vectors for zero volt fault.

Table 1. Model 1 cylinder side pressure classifiers error probabilities (the lower the value the better).

Error probability, 7 faults (1 no faults), 100 vectors per fault, 560 learn vectors, 140 test vectors									
wsize from 38500	100 points	75 points	50 points	25 points	20 points	15 points	10 points	5 points	avg 20,15,10,5
points									
linear	x	x	x	x	pres1_1925.mat	pres1_2566.mat	pres1_3850.mat	pres1_7700.mat	
iqr					0.6071	0.6786	0.6357	0.6143	0.633925
kurtosis					0.6214	0.5643	0.5357	0.5214	0.5607
max					0.4714	0.6	0.65	0.5643	0.571425
mean					0.4714	0.5643	0.5357	0.5357	0.526775
rms					0.5286	0.6214	0.5429	0.4571	0.5375
skewness					0.5214	0.6071	0.4643	0.5929	0.546425
slope					0.5857	0.5929	0.5286	0.6286	0.58395
									0.565814286
quadratic	x	x	x	x	pres1_1925.mat	pres1_2566.mat	pres1_3850.mat	pres1_7700.mat	
iqr					0.4	0.9714	0.4643	0.5571	0.5982
kurtosis					0.4929	0.4214	0.4214	0.45	0.446425
max					0.4786	0.5357	0.65	0.4857	0.5375
mean					0.3143	0.2929	0.4	0.4143	0.355375
rms					0.4071	0.4	0.3786	0.4429	0.40715
skewness					0.4357	0.5429	0.4643	0.4857	0.48215
slope					0.4571	0.3929	0.4143	0.4857	0.4375
									0.466328571
parzen	x	x	x	x	pres1_1925.mat	pres1_2566.mat	pres1_3850.mat	pres1_7700.mat	
iqr					0.6143	0.6	0.6143	0.6643	0.623225
kurtosis					0.7	0.6214	0.5357	0.55	0.601775
max					0.5214	0.5357	0.5	0.55	0.526775
mean					0.4786	0.4	0.5071	0.4643	0.4625
rms					0.5357	0.5214	0.4786	0.4643	0.5
skewness					0.5429	0.5786	0.5357	0.4786	0.53395
slope					0.5143	0.4857	0.4357	0.5571	0.4982
									0.535203571
NN2hidden	x	x	x	x	pres1_1925.mat	pres1_2566.mat	pres1_3850.mat	pres1_7700.mat	
iqr					0.5714	0.4929	0.6929	0.5643	0.580375
kurtosis					0.5786	0.6214	0.5714	0.5857	0.589275
max					0.5571	0.5786	0.55	0.6143	0.575
mean					0.5571	0.5857	0.6357	0.45	0.557125
rms					0.4571	0.5	0.5214	0.5071	0.4964
skewness					0.6714	0.6071	0.4929	0.5571	0.582125
slope					0.6786	0.4857	0.4929	0.5429	0.550025
									0.561475

Table 2. Model 2 valve control voltage classifiers error probabilities (the lower the value the better)

Error probability, 6 faults (1 no faults), 100 vectors per fault, 480 learn vectors, 120 test vectors														
wsize from 20000 points	100 points	75 points	50 points	25 points	20 points	15 points	10 points	5 points	avg all	avg 20,15,10,5				
linear	U-10-200.mat	U-10-266.mat	U-10-400.mat	U-10-800.mat	U-10-1000.mat	U-10-1333.mat	U-10-2000.mat	U-10-4000.mat						
iqr	0.1083	0.175	0.1167	0.325	0.1417	0.1417	0.1333	0.2417	0.172925	0.1646				
kurtosis	0.0917	0.2	0.3333	0.3417	0.1583	0.1833	0.3167	0.35	0.246875	0.252075				
max	0.05	0.0833	0.125	0.1333	0.0583	0.0917	0.0667	0.125	0.0916625	0.085425				
mean	0.1917	0.1	0.1083	0.2083	0.1	0.1167	0.0667	0.2	0.1364625	0.12085				
rms	0.15	0.1333	0.175	0.1333	0.1667	0.125	0.0833	0.1167	0.1354125	0.122925				
skewness	0.1333	0.225	0.1917	0.1583	0.175	0.225	0.1667	0.125	0.175	0.172925				
slope	0.15	0.1917	0.1583	0.2667	0.2083	0.1583	0.1667	0.2667	0.1958375	0.2				
									0.164882143	0.159828571				
quadratic	U-10-200.mat	U-10-266.mat	U-10-400.mat	U-10-800.mat	U-10-1000.mat	U-10-1333.mat	U-10-2000.mat	U-10-4000.mat						
iqr	0.2083	0.0583	0.0417	0.15	0.225	0.0417	0.0667	0.0833	0.109375	0.104175				
kurtosis	0.1167	0.1833	0.0917	0.2083	0.2	0.15	0.0833	0.225	0.1572875	0.164575				
max	0.0333	0.0667	0.0833	0.2667	0.05	0.025	0.4083	0.2833	0.152075	0.19165				
mean	0.0917	0.0417	0.05	0.1167	0.075	0.0583	0.0417	0.1083	0.072925	0.070825				
rms	0.05	0.0917	0.0333	0.175	0.05	0.025	0.05	0.1083	0.0729125	0.068325				
skewness	0.0667	0.0917	0.1583	0.075	0.0917	0.125	0.1167	0.1167	0.105225	0.112525				
slope	0.05	0.0583	0.05	0.1417	0.0417	0.025	0.0833	0.1333	0.0729125	0.070825				
									0.106101786	0.110414286				
parzen	U-10-200.mat	U-10-266.mat	U-10-400.mat	U-10-800.mat	U-10-1000.mat	U-10-1333.mat	U-10-2000.mat	U-10-4000.mat						
iqr	0.0583	0.0417	0.05	0.1167	0.1083	0.0833	0.075	0.0417	0.071875	0.077075				
kurtosis	0.0917	0.0917	0.1833	0.0833	0.15	0.1333	0.1583	0.1	0.12395	0.1354				
max	0.0333	0.0417	0.0333	0.0583	0.025	0.0167	0	0.0417	0.03125	0.02085				
mean	0.1583	0.0917	0.075	0.05	0.0583	0.0833	0.05	0.1083	0.0843625	0.074975				
rms	0.0833	0.075	0.0667	0.1083	0.0667	0.0667	0.0667	0.0833	0.0770875	0.07085				
skewness	0.0667	0.075	0.075	0.0583	0.0833	0.1167	0.0833	0.0417	0.075	0.08125				
slope	0.0833	0.0583	0.075	0.125	0.1	0.075	0.0583	0.15	0.0906125	0.095825				
									0.0791625	**0.079460714**				
NN2hidden	U-10-200.mat	U-10-266.mat	U-10-400.mat	U-10-800.mat	U-10-1000.mat	U-10-1333.mat	U-10-2000.mat	U-10-4000.mat						
iqr	0.0333	0.0583	0.1833	0.3833	0.1583	0.125	0.1833	0.3667	0.1864375	0.208325				
kurtosis	0.2333	0.175	0.2917	0.3	0.2333	0.2167	0.25	0.3333	0.2541625	0.258325				
max	0.0583	0.0583	0.0917	0.225	0.05	0.0917	0.0833	0.1	0.0947875	0.08125				
mean	0.3	0.175	0.15	0.25	0.125	0.2833	0.075	0.1917	0.19375	0.16875				
rms	0.075	0.15	0.1167	0.1417	0.1667	0.275	0.175	0.15	0.1562625	0.191675				
skewness	0.2833	0.1917	0.1667	0.3333	0.15	0.2	0.2833	0.3	0.2385375	0.233325				
slope	0.1417	0.1167	0.1167	0.2417	0.1583	0.1833	0.1917	0.3083	0.1823	0.2104				
									0.186605357	0.19315				

Table 3. Model 2 cylinder side pressure classifiers error probabilities (the lower the value the better)

Error probability, 6 faults (1 no faults), 100 vectors per fault, 480 learn vectors, 120 test vectors																					
wsize from 20000 points	100 points		75 points		50 points		25 points		20 points		15 points		10 points		5 points		awg 20,15,10,5	
linear	x		x		x		x		p2-10-1000.mat		p2-10-1333.mat		p2-10-2000.mat		p2-10-4000.mat			
iqr									0.0833		0.1167		0.0833		0.2333		0.12915	
kurtosis									0.1333		0.2667		0.25		0.4		0.2625	
max									0.05		0.0583		0.0833		0.1333		0.081225	
mean									0.125		0.1833		0.1333		0.1667		0.152075	
rms									0.075		0.15		0.0583		0.15		0.108325	
skewness									0.1417		0.1583		0.1917		0.1583		0.1625	
slope									0.1917		0.175		0.1333		0.2417		0.185425	
																	0.154457143	
quadratic	x		x		x		x		p2-10-1000.mat		p2-10-1333.mat		p2-10-2000.mat		p2-10-4000.mat			
iqr									0.1167		0.0583		0.0583		0.175		0.102075	
kurtosis									0.1333		0.1333		0.0917		0.175		0.133325	
max									0.0167		0.05		0.4083		0.275		0.1875	
mean									0.0583		0.0667		0.0417		0.1		0.066675	
rms									0.05		0.0333		0.025		0.15		0.064575	
skewness									0.0833		0.1		0.0833		0.0667		0.083325	
slope									0.0583		0.0833		0.05		0.1167		0.077075	
																	0.102078571	
parzen	x		x		x		x		p2-10-1000.mat		p2-10-1333.mat		p2-10-2000.mat		p2-10-4000.mat			
iqr									0.0583		0.0583		0.05		0.1083		0.068725	
kurtosis									0.1333		0.0833		0.1333		0.05		0.099975	
max									0.0583		0.0333		0.025		0.0333		0.037475	
mean									0.0833		0.1083		0.0667		0.0667		0.08125	
rms									0.0583		0.075		0.0417		0.1417		0.079175	
skewness									0.1		0.1		0.0917		0.0583		0.0875	
slope									0.0667		0.1167		0.0583		0.1083		0.0875	
																	0.077371429	
NN2hidden	x		x		x		x		p2-10-1000.mat		p2-10-1333.mat		p2-10-2000.mat		p2-10-4000.mat			
iqr									0.0917		0.0667		0.1583		0.2583		0.14375	
kurtosis									0.2		0.15		0.2917		0.3		0.235425	
max									0.25		0.05		0.1583		0.3917		0.2125	
mean									0.125		0.3		0.175		0.2083		0.202075	
rms									0.0417		0.1083		0.2583		0.1667		0.14375	
skewness									0.2417		0.1917		0.125		0.2917		0.212525	
slope									0.125		0.2917		0.1833		0.1583		0.189575	
																	0.191371429	

Table 4. Model 2 piston side pressure classifiers error probabilities (the lower the value the better)

Error probability, 6 faults (1 no faults), 100 vectors per fault, 480 learn vectors, 120 test vectors									
wsize from 20000 points	100 points	75 points	50 points	25 points	20 points	15 points	10 points	5 points	avg 20,15,10,5
linear	x	x	x	x	p3-10-1000.mat	p3-10-1333.mat	p3-10-2000.mat	p3-10-4000.mat	
iqr					0.1333	0.15	0.1167	0.1417	0.135425
kurtosis					0.1167	0.175	0.1583	0.2167	0.166675
max					0.0667	0.1417	0.0667	0.0833	0.0896
mean					0.0917	0.1333	0.1917	0.2417	0.1646
rms					0.1	0.1333	0.225	0.2083	0.16665
skewness					0.1167	0.1	0.1583	0.1667	0.135425
slope					0.1583	0.2083	0.075	0.2083	0.162475
									0.145835714
quadratic	x	x	x	x	p3-10-1000.mat	p3-10-1333.mat	p3-10-2000.mat	p3-10-4000.mat	
iqr					0.0667	0.0417	0.0333	0.05	0.047925
kurtosis					0.025	0.0917	0.0917	0.1167	0.081275
max					0.05	0.0417	0.0167	0.0417	0.037525
mean					0.0417	0.05	0.05	0.1167	0.0646
rms					0.0583	0.025	0.0083	0.075	0.04165
skewness					0.1583	0.0583	0.0833	0.0917	0.0979
slope					0.0417	0.05	0.0583	0.1333	0.070825
									0.0631
parzen	x	x	x	x	p3-10-1000.mat	p3-10-1333.mat	p3-10-2000.mat	p3-10-4000.mat	
iqr					0.0333	0.05	0.0833	0.0667	0.058325
kurtosis					0.0417	0.1333	0.1333	0.0833	0.0979
max					0.05	0.0083	0.0333	0.0417	0.033325
mean					0.1	0.0667	0.075	0.0833	0.08125
rms					0.075	0.0583	0.025	0.0917	0.0625
skewness					0.0917	0.1333	0.0917	0.05	0.091675
slope					0.0667	0.1167	0.05	0.1417	0.093775
									0.074107143
NN2hidden	x	x	x	x	p3-10-1000.mat	p3-10-1333.mat	p3-10-2000.mat	p3-10-4000.mat	
iqr					0.075	0.175	0.1417	0.125	0.129175
kurtosis					0.1083	0.1083	0.375	0.275	0.21665
max					0.0583	0.1333	0.0917	0.0667	0.0875
mean					0.2333	0.05	0.15	0.2583	0.1729
rms					0.1	0.125	0.275	0.3667	0.216675
skewness					0.2333	0.1667	0.275	0.2167	0.222925
slope					0.1167	0.2833	0.1583	0.2167	0.19375
									0.177082143